

***In vitro* evaluation of 2-methoxyestradiol-bis-sulphamate on
cell growth, morphology, cell cycle progression and its
possible induction of types of cell deaths in an oesophageal
carcinoma (SNO) cell line**

by

Thandi Vuyelwa Mqoco

24129080

Submitted in fulfillment of part of the requirements for the degree

Master of Science (Physiology)

in the Faculty of Health Sciences

University of Pretoria

2012

Declaration

I hereby declare that this dissertation, which is being submitted in fulfillment of part of the requirements for the degree Master of Science (Physiology) at the University of Pretoria, is my own work and it has not been submitted before at this or any other University.

Summary

Oesophageal squamous cell carcinoma is one of the most frequently occurring cancers in South Africa, with its highest incidence observed in South African black males. More efficient anticancer drugs are currently being researched with the aim of discovering new compounds that will aid in the treatment of cancer. 2-Methoxyestradiol (2ME2) is a naturally occurring estradiol metabolite currently undergoing human clinical trials. 2ME2 exerts antitumour, antiangiogenic and apoptotic effects both *in vitro* and *in vivo*. However, due to its limited bioavailability, analogues are being synthesized and tested in an attempt to improve this shortcoming. 2-Methoxyestradiol-bis-sulphamate (2-MeOE2bisMATE) is a bis-sulphamoylated derivative of 2ME2. 2-MeOE2bisMATE has antiproliferative effects both *in vitro* and *in vivo*. Although 2-MeOE2bisMATE is a potential anticancer drug the exact action mechanism of this compound is still unidentified.

In this study the *in vitro* effects of 2-MeOE2bisMATE on cell growth, morphology, cell cycle progression, as well as its potential to induce certain types of cell death and cytotoxicity in the oesophageal carcinoma (SNO) cell line were investigated.

Cell number determination studies revealed that 0.4 μ M of 2-MeOE2bisMATE significantly inhibited growth of SNO cells after 24 hours of exposure. Morphological studies demonstrated hallmarks of both apoptosis and autophagy such as chromatin condensation, membrane blebbing, apoptotic bodies and increased presence of autophagosomes. In addition, immunofluorescence indicated microtubule network disruption in 2-MeOE2bisMATE-treated cells when compared to vehicle-treated control cells. Fluorescent microscopy revealed that both apoptosis and autophagy were induced in SNO cells after 24 hours of exposure to 0.4 μ M 2-MeOE2bisMATE.

Cell cycle progression analysis revealed an increase in the number of cells in the G₂/M phase, as well as in the sub-G₁ fraction (indicating the presence of apoptosis) of 2-MeOE2bisMATE-treated cells. The annexin V-FITC assay verified the induction of apoptosis by 2-MeOE2bisMATE. An increase in the number of cells with reduced mitochondrial membrane potential and an increased caspase 6 activity were observed in

2-MeOE2bisMATE-treated cells. Autophagy induction was confirmed by flow cytometry using cyto-ID detection and the conjugated rabbit polyclonal anti-LC3B antibody assays.

This *in vitro* study demonstrated new insights to the action mechanism of 2-MeOE2bisMATE in oesophageal carcinoma (SNO) cells, since these activities have not been studied in oesophageal carcinoma cells up to date. Future studies are warranted to further determine which gene and protein expression changes are induced by 2-MeOE2bisMATE in SNO cells.

Keywords: oesophageal cancer, 2-methoxyestradiol-bis-sulphamate, cell cycle arrest, apoptosis, autophagy

Acknowledgements

- First and foremost I would like to thank the Almighty God for his unconditional love and for making it possible for me to obtain this degree. He deserves all the honour and the glory.
- I would like to express my gratitude and appreciation to my supervisor, Professor AM Joubert for her academic input, guidance, endless support and encouragement. Thank you for everything.
- I wish to thank Professor D van Papendorp, head of the Department of the Physiology for granting me the opportunity to conduct and complete my study in his department.
- A special thanks to Mrs. S Marais and Mr. A Stander for all of their assistance and technical expertise.
- I would like to thank Professor Vlegaar from the Department of Chemistry, University of Pretoria for synthesizing 2-MeOE2bisMATE, the compound which was used in this study.
- Thank you to the Electron Microscopy Unit of the University of Pretoria for the use of the transmission electron microscope and technical assistance.
- Thank you to the Department of Pharmacology University of Pretoria for the use of the flow cytometer.
- Thank you to Francinah and Ezekiel for maintenance of the laboratory.
- I wish to extend my gratitude to the National Research Foundation (NRF), Cancer Association of South Africa (AK246), the Medical Research Council (AG374, AK076), Postgraduate Mentor Bursary Programme (PGMP) and Research Committee

of the University of Pretoria (RESCOM) (Pretoria, South Africa) for providing financial assistance.

- A special thank you to Xolani Mhlanga for his support and assistance.

- Last but not least, I wish to thank my family for all of their everlasting love and support.

Research outputs:

Publications

- Mqoco T, Marais S, Joubert A. Influence of estradiol analogue on cell growth, morphology and death in oesophageal carcinoma cells. *Biocell* 2010;34(3):113-120.
- Thandi Mqoco, Sumari Marais, Dirk van Papendorp and Annie Joubert. 2-Methoxyestradiol-bis-sulphamate: a promising anticancer agent in an esophageal carcinoma (SNO) cell line. This manuscript was submitted to the *Biomedical Research Journal* on the 22nd February 2012 and it is currently under review.
- Tenille Steynberg, Michelle Visagie, Thandi Mqoco, Anu Idicula, Sean Moolman, Wim Richter, Anna Joubert. Qualitative assessment of smooth muscle cells grown on 2D and 3D polycaprolactone polymers via Scanning electron microscope. *Biomedical research journal* 2012;23(2):191-198.
- Sumari Marais, Thandi Mqoco, André Stander and Annie Joubert. The *in vitro* effects of a sulphamoylated derivative of 2-methoxyestradiol on cell number, morphology and alpha-tubulin disruption in cervical adenocarcinoma (HeLa) cells. *Biomedical research journal* 2012;23(2).

Conference proceedings

- Mqoco T, Marais S, Joubert A. Influence of 2-methoxyestradiol-bis-sulphamate on cell growth, morphology and its possible induction of cell death in esophageal carcinoma cells. *South African Journal of Science and Technology*.2010;29(4):212.

Conferences

- Mqoco T, Marais S, Joubert A. Influence of 2-methoxyestradiol-bis-sulphamate on cell growth, morphology and its possible induction of autophagy and apoptosis in SNO oesophageal carcinoma cells. Faculty Day, Faculty of Health Sciences, University of Pretoria, 2009.
- Mqoco T, Marais S, Joubert A. Influence of 2-methoxyestradiol-bis-sulphamate on cell growth, morphology and its possible induction of autophagy and apoptosis in

SNO oesophageal carcinoma cells. South African Academy of Sciences, Potchefstroom, 2009.

- Mqoco T, Marais S, Joubert A. Influence of 2-methoxyestradiol-bis-sulphamate on cell growth, morphology and its possible induction of autophagy and apoptosis in SNO oesophageal carcinoma cells. South African Society for Biochemistry and Molecular Biology (SASBMB) Congress, 2010.
- Mqoco T, Marais S, Joubert A. *In vitro* evaluation of 2-methoxyestradiol-bis-sulphamate on cell growth, morphology, cell cycle progression and possible induction of types of cell deaths in an oesophageal carcinoma (SNO) cell line. Faculty Day, Faculty of Health Sciences, University of Pretoria, 2010. I won third place in the poster presentations section.
- Mqoco T, Marais S, Joubert A. *In vitro* evaluation of 2-methoxyestradiol-bis-sulphamate on cell growth, morphology, cell cycle progression and possible induction of types of cell deaths in an oesophageal carcinoma (SNO) cell line. South African Academy of Sciences, 2010.
- Mqoco T, Marais S, Joubert A. *In vitro* evaluation of 2-methoxyestradiol-bis-sulphamate on cell growth, morphology, cell cycle progression and possible induction of types of cell deaths in an oesophageal carcinoma (SNO) cell line. South African Cell Death congress, Cape Town, 2011.
- Mqoco T, Marais S, Joubert A. 2-Methoxyestradiol-bis-sulphamate disrupts microtubule network, arrests cell cycle and induces apoptosis in an oesophageal carcinoma cell line. Faculty Day, Faculty of Health Sciences, University of Pretoria, 2011.

Table of contents

Declaration	1
Summary	2
Acknowledgements	4
Research outputs.....	6
List of abbreviations	14
List of figures	19
List of tables	22
Graphical representation of signaling pathways.....	23
Chapter 1: Literature review.....	24
1.1. Oesophageal cancer	24
1.2. Overview of cancer treatments	25
1.3. Overview of the cell cycle.....	27
1.3.1. Cell cycle phases.....	27
1.3.1.1. G ₁ phase.....	27
1.3.1.2. S phase.....	28
1.3.1.3. G ₂ phase.....	29
1.3.1.4. M phase.....	29
1.3.2. Cell cycle checkpoints.....	30

1.3.2.1. DNA checkpoint.....	30
1.3.2.2. Spindle checkpoint.....	31
1.4. Types of cell death.....	32
1.4.1. Apoptosis.....	33
1.4.1.1. Caspase-dependent signaling pathways.....	34
1.4.1.1.1. Extrinsic pathway.....	34
1.4.1.1.2. Intrinsic pathway.....	36
1.4.1.1.3. Endoplasmic Reticulum-mediated pathway.....	38
1.4.1.2. Caspase-independent pathway.....	38
1.4.2. Overview of autophagy.....	39
1.4.2.1. Macroautophagy.....	39
1.4.2.2. Microautophagy.....	41
1.4.2.3. Chaperone-mediated autophagy.....	41
1.5. Estrogens.....	43
1.5.1. Estrogens' metabolism.....	43
1.5.2. Overview of 2-methoxyestradiol.....	44
1.5.3. Overview of 2-methoxyestradiol-bis-sulphamate.....	46
Chapter 2: Research procedure.....	50
2.1. Type of study.....	50

2.2. Materials.....	50
2.2.1. Cell line.....	50
2.2.2. Compounds and reagents.....	50
2.3. General laboratory procedure.....	51
2.3.1. Preparation of general cell culture maintenance's reagents.....	51
2.3.2. General cell culture maintenance.....	51
2.3.3. General methods for experiments.....	52
2.4. Analytical experimental protocols.....	53
2.4.1. Cell growth and viability studies.....	53
2.4.1.1. Crystal violet staining.....	53
I) Materials.....	53
ii) Methods.....	53
2.4.1.2. Lactate dehydrogenase cytotoxic assay.....	54
I) Materials.....	54
ii) Methods.....	54
2.4.2. Morphology studies.....	55
2.4.2.1. Polarization-optical differential interference contrast.....	55
I) Methods.....	55
2.4.2.2. Light microscopy - haematoxylin & eosin staining.....	55

I) Materials.....	56
ii) Methods.....	56
2.4.2.3. Transmission electron microscopy.....	56
I) Materials.....	56
ii) Methods.....	56
2.4.2.4. Confocal-alpha (α)-tubulin assay.....	57
ii) Materials.....	57
iii) Methods.....	57
2.4.3. Determination of possible types of cell deaths.....	58
2.4.3.1. Fluorescent microscopy - triple staining technique.....	58
I) Materials.....	58
ii) Methods.....	58
2.4.3.2. Flow cytometry - cell cycle progression.....	59
I) Materials.....	59
ii) Methods.....	60
2.4.3.3. Flow cytometry - apoptosis detecting study (Annexin V-FITC).....	60
I) Materials.....	61
ii) Methods.....	61
2.4.3.4. Flow cytometry - mitocapture mitochondrial assay.....	61

I) Materials.....	62
ii) Methods.....	62
2.4.3.5. Spectrophotometry- caspase 6 & 8 calorimetric assays.....	62
I) Materials.....	62
ii) Methods.....	63
2.4.3.6 Flow cytometry - autophagy detection: anti-LC3B.....	63
I) Materials.....	63
ii) Methods.....	64
2.4.3.7. Flow cytometry - cyto-ID autophagy detection assay.....	64
I) Materials.....	64
ii) Methods.....	64
2.5. Logistics.....	65
2.4. Statistical analysis.....	65
Chapter 3: Results.....	66
3.1. Cell growth and viability studies.....	66
3.1.1. Crystal violet staining	66
3.1.2. Lactate dehydrogenase cytotoxic assay.....	71
3.2. Morphology studies.....	72
3.2.1. Polarization-optical differential interference contrast.....	72

3.2.2. Light microscopy - haematoxylin & eosin staining	73
3.2.3. Transmission electron microscope.....	76
3.2.4. Confocal-alpha (α)-tubulin assay.....	78
3.3. Determination of possible types of cell death.....	80
3.3.1. Fluorescent microscopy - triple staining technique.....	80
3.3.2. Flow cytometry - cell cycle progression.....	81
3.3.3. Flow cytometry - apoptosis detecting study (Annexin V-FITC).....	84
3.3.4. Flow cytometry - mitocapture mitochondrial assay.....	85
3.3.5. Spectrophotometry- caspase 6 & 8 calorimetric assays.....	86
3.3.6 Flow cytometry - autophagy detection: anti-LC3B.....	88
3.3.7. Flow cytometry - cyto-ID autophagy detection assay.....	88
Chapter 4: Discussion.....	90
Chapter 5: Conclusion.....	97
References.....	98

List of abbreviations

2ME2	2-Methoxyestradiol
2-MeOE2bisMATE	2-Methoxyestradiol-bis-sulphamate
AIF	Apoptosis Inducing Factor
ANOVA	Analysis of variance
AO	Acridine orange
Apaf-1	Apoptotic protease activating factor-1
APC/C	Anaphase promoting complex/cyclosome
Apo2L	Apoptosis antigen 2 ligand
Apo3L	Apoptosis antigen 3 ligand
Atg	Autophagy related genes
ATM	Ataxia-telangiectasia-mutated
Bcl-2	B-cell lymphoma protein 2
Bub	Budding uninhibited by benomyl
C	Control optical density
CAK	CDK-activating kinase
Caspase	Cysteine-dependent aspartate-specific protease
CARD	Caspase recruiting domain
Cdc	Cell division cycle
Cdc6	Cell division cycle 6
Cdc25B	Cell division cycle 25B
Cdc25C	Cell division cycle 25C
CDK	Cyclin-dependent kinase
CDK1	Cyclin-dependent kinase 1
CDK2	Cyclin-dependent kinase 2
CDK4	Cyclin-dependent kinase 4

CDK6	Cyclin-dependent kinase 6
Cdt1	Cdc-10 dependent transcript
cIAP1	Cellular inhibitor of apoptotic protein1
cIAP2	Cellular inhibitor of apoptotic protein2
CKI	CDK inhibitor
CMA	Chaperone-mediated autophagy
COMT	Catechol- <i>O</i> -methyltransferase
Cyt <i>c</i>	Cytochrome <i>c</i>
CYP450	Cytochrome P450
DAPI	4',6-Diamidino-2-Phenylindole
DD	Death domain
DED	Death effector domain
DIABLO	Direct IAP binding protein with low PI
DISC	Death-inducing signaling complex
DMEM	Dulbecco's modified Eagle's medium
DMSO	Dimethyl sulphoxide
DNA	Deoxyribonucleic acid
DR	Death receptor
DR3	Death receptor 3
DR4	Death receptor 4
DR5	Death receptor 5
DTT	Dithiothreitol
E2F	Elongation factor 2
Endo G	Endonuclease G
ER	Endoplasmic reticulum
FACS	Fluorescence activated cell sorter

FADD	Fas-associated death domain
FasL	Fatty acid synthetase ligand
FCS	Fetal calf serum
FITC	Fluorescein isothiocyanate
GI ₅₀	50% growth inhibition
GM	Growth medium
H&E	Haematoxylin & eosin
HO	Hoechst 33342
HPV	Human papilloma virus
Hsc 70	Heat shock cognate 70 kDa
Hsp 90	Heat shock protein 90 kDa
IAP	Inhibitor of Apoptosis Proteins
ICAD	Inhibitor of CAD
Jnk1	Jun N-terminal kinase 1
LAMP-2A	Lysosomal membrane protein type 2A
LC3	Light chain 3
LDH	Lactate dehydrogenase
Mad2	Mitotic arrest deficient 2
MCM	Minichromosome maintenance
mTOR	Mammalian target of rapamycin
mTORC1	Mammalian target of rapamycin complex 1
mTORC2	Mammalian target of rapamycin complex 2
MOMP	Mitochondrial membrane permeabilization
MPF	Maturation-promoting factor
PBS	Phosphate buffered saline
PCD	Programmed cell death

PE	Phosphatidylethanolamine
PI	Propidium iodide
PlasDIC	Polarization-optical differential interference contrast
Pre-RC	Pre-replicative complex
PS	Phosphatidylserine
Rb	Retinoblastoma protein
RIP1	Receptor interacting protein 1
RNA	Ribonucleic acid
ROS	Reactive oxygen species
SCF	Skp1/cullin/F-box protein
SD	Standard deviation
Smac	Second mitochondria-derived activator of caspase
STS	Steroid sulphatase
T	Optical density of the test well after drug exposure
TEM	Transmission electron microscopy
TLRs	Toll-like receptors
TLR3	Toll-like receptor 3
TLR4	Toll-like receptor 4
TNF	Tumor necrosis factor
TNFR1	Tumor necrosis factor receptor 1
To	Optical density at time zero
TRADD	TNF receptor-associated death domain
TRAIL-R	TNF-related apoptosis inducing ligand receptor
UPR	Unfolded-protein response
VEGF	Vascular endothelial growth factor
ORC	Origin recognition complex

XIAP

X chromosome-linked inhibitor of apoptosis protein

List of figures

Figure 1.1. Receptor-ligand mediated pathway.....	35
Figure 1.2. Mitochondrial mediated pathway.....	37
Figure 1.3. Microautophagy pathway.....	41
Figure 1.4. Chaperone-mediated autophagy pathway.....	42
Figure 1.5. Synthesis of 2-MeOE2bisMATE.....	47
Figure 3.1. SNO cell numbers expressed as a % of cells relative to cells propagated in growth medium only.....	68
Figure 3.2. Growth inhibitory effects of 2-MeOE2bisMATE (0.2-1 μ M) on SNO cells after 24 hours of exposure.....	68
Figure 3.3. Effects of 2-MeOE2bisMATE (0.2-1.0 μ M) on the proliferation of SNO cell after 48 hours of exposure.....	69
Figure 3.4. Growth inhibitory effects of 0.2-1 μ M of 2-MeOE2bisMATE on SNO cells after 48 hours of exposure.....	69
Figure 3.5. Crystal violet staining results following 72 hours of exposure of the 2-MeOE2bisMATE to SNO cell line.....	70
Figure 3.6. Growth inhibitory values of SNO cells after 72 hours of exposure.....	70
Figure 3.7. Analysis of LDH release in SNO cells treated with vehicle or 2-MeOE2bisMATE after 24 hours of exposure.....	71
Figure 3.8. PlasDIC images of SNO cells propagated in growth medium and vehicle-treated controls after an exposure period of 24 hours.....	72

Figure 3.9. PlasDIC images of SNO cells 0.4µM 2-MeOE2bisMATE-treated cells and actinomycin D-treated cells after 24 hours of exposure.....73

Figure 3.10. PlasDIC images of SNO cells with induced starvation after 24 hours of exposure.....73

Figure 3.11. Haematoxylin and eosin staining of SNO cells propagated in growth medium after 24 hours (40X and 100X magnification).....74

Figure 3.12. Haematoxylin and eosin staining of vehicle-treated cells after 24 hours of exposure (40X and 100X magnification).....74

Figure 3.13. Haematoxylin and eosin staining of SNO cells exposed to 0.4µM 2-MeOE2bisMATE following 24 hours of exposure (40X and 100X magnification).....75

Figure 3.14. Haematoxylin and eosin staining of actinomycin D-treated cells at 40X (A) and 100X (B) after 24 hours of treatment.....75

Figure 3.15. Haematoxylin and eosin staining of starved cells at 40X and 100X following 24 hours of treatment.....76

Figure 3.16. Transmission electron microscopy of SNO cells propagated in growth medium and vehicle-treated control (6000x magnification)77

Figure 3.17. Transmission electron microscopy images of SNO cells treated with 0.4µM 2-MeOE2bisMATE (6000x magnification)77

Figure 3.18. Transmission electron microscopy images of tamoxifen-treated and actinomycin D-treated cells after 24 hours (6000x magnification)78

Figure 3.19. Immunofluorescence using anti-α-tubulin antibodies and DAPI in cells propagated in the growth medium and in vehicle-treated cells.....79

Figure 3.20. Immunofluorescence using anti-α-tubulin antibodies and DAPI in cells treated with 0.4µM 2-MeOE2bis-MATE.....79

Figure 3.21. Triple-stained SNO cells propagated in growth medium and vehicle-treated control cells.....80

Figure 3.22. Triple-stained images of 0.4µM 2-MeOE2bisMATE-treated cells, actinomycin D-treated cells and starved cells.....81

Figure 3.23. Triple-stained images of 0.4µM 2-MeOE2bisMATE-treated cells, actinomycin D-treated cells and starved cells.....81

Figure 3.24. Cell cycle distribution histograms of cells propagated in the growth medium and of vehicle-treated cells after 24 hours.....82

Figure 3.25. Cell cycle distribution histogram following 24 hours exposure to 0.4µM 2-MeOE2bisMATE and actinomycin D.....82

Figure 3.26. Percentage of cells in sub-G₁, G₁, S & G₂/M phases.....83

Figure 3.27. Detection of apoptosis induction of cells propagated in the growth medium and of vehicle-treated cells.....84

Figure 3.28. Detection of apoptosis induction of 0.4µM 2-MeOE2bisMATE-treated SNO cells and actinomycin D-treated cells.....85

Figure 3.29. Histogram of 2-MeOE2bisMATE-treated cells overlaid on vehicle-treated control cells after 24 hours exposure.....86

Figure 3.30. Caspase 6 activity ratios of 0.4µM 2-MeOEbisMATE-treated and actinomycin D-treated cells compared to vehicle-treated cells following 24 hours.....87

Figure 3.31. Caspase 8 activity ratios of 0.4µM 2-MeOEbisMATE-treated and actinomycin D-treated cells compared to vehicle-treated cells.....87

Figure 3.32. LC3 Histogram of mean fluorescence intensity of 2-MeOE2bisMATE-treated cells overlaid on the vehicle-treated control cells in SNO cells.....88

Figure 3.33. Cyto-ID Histogram of 2-MeOE2bisMATE-treated cells overlaid on the vehicle-treated control cells in SNO cells after 24 hours of exposure.....89

Figure 4.1. Proposed mechanism of 2-MeOE2bisMATE in SNO cells.....96

List of tables

Table 1.1. Groups of anticancer agents currently used for chemotherapy...26

Table 3.1. Percentage of cells in sub-G₁, G₁, S & G₂/M phases.....83

Graphical representation of biochemical pathways

All graphical figures of biochemical pathways were designed by TV Mqoco using Microsoft PowerPoint 2007 (2006 Microsoft Corporation, United States of America) and saved as tiff images.

Chapter 1

Literature review

1.1. Oesophageal cancer

Oesophageal cancer is classified as one of the 10 most common cancers in the world [1-4]. There are two main subtypes of oesophageal cancer; adenocarcinoma and squamous cell carcinoma [1, 3, 4]. Adenocarcinoma usually occurs in the lower part of the oesophagus, near the stomach, and it is more prevalent in developed countries [3-5]. In contrast, oesophageal squamous cell carcinoma usually occurs in the upper and mid sections of the oesophagus, but it can also be found at any other location along the oesophagus and it is more common in developing countries [3-5].

In South Africa, squamous oesophageal cancer is considered to be more prevalent amongst black males, with the highest incidence being observed in the Transkei region [2, 6, 7]. The genetic, as well as the environmental factors that may be linked to the squamous oesophageal cancer still remain unclear. Several genes that are mainly associated with the regulation of cell proliferation, cell division or apoptosis have been found and they are believed to play a role in the development and progression of oesophageal cancer. The fundamental mechanism(s) by which this disease develops remain unidentified [1, 7]. In addition, there are some environmental factors that have been identified as possible contributors to the development of oesophageal squamous cell carcinoma in South Africa [2, 6, 8, 9]. The consumption of maize that is infected with fungal toxins produced by the *Fusarium* species as well as the lack of dietary intake of riboflavin, niacin, vitamin C, zinc, calcium and magnesium have been identified as some of the major contributors to this type of cancer [2, 7-10]. Other risk factors include smoking and alcohol abuse, as well as infections with deoxyribonucleic acid (DNA) viruses such as the human papilloma virus (HPV) [1, 4, 8]. In a study by Wang *et al.* (2010) a high prevalence of HPV L1 in oesophageal cancer cell samples was observed [11].

Squamous cell carcinoma of the oesophagus presents a major health problem. It is usually identified in its late stages because its development is asymptomatic [4, 12]. The 5-year

survival of patients who have been diagnosed with the disease is about 5-10%, therefore better diagnostic and therapeutic approaches are required, so as to reduce the elevated mortality figures that are associated with this disease [1, 4, 12].

1.2. Overview of cancer treatments

There are many different types of treatments that are used to combat cancer. The three main types of treatments are surgery, radiation therapy, and chemotherapy [13]. The selection of treatment depends on various factors e.g. the type and the stage of the cancer, as well as the health status of the patient [13, 14]. Surgery is used to prevent, diagnose, stage and cure cancers [14, 15]. Although it offers the greatest possibility to cure various benign tumours, the main shortcoming with this type of cancer treatment is that it is unsuccessful in treating metastasizing tumours [14].

Radiation therapy uses high energy waves that disrupt genes which control cell growth and division, ultimately leading to killing of the rapidly dividing cells [14, 16]. Radiation therapy can be used in conjunction with the other types of treatments. Although radiation therapy is intended to kill cancerous cells, it also affects dividing cells of normal tissues [16]. Surgery and radiation therapy are generally used to treat cancers that are localized within a specific organ or tissue, whereas chemotherapy is used in both localized and metastasizing of cancers [14].

In chemotherapy drugs are used to destroy cancer cells [17]. It is at times used together with the other 2 types of cancer treatments [14, 17]. Chemotherapy works by reducing the growth and/or killing of rapidly dividing cells. Such drugs have the potential to harm healthy cells that divide rapidly, such as those that form the lining of the digestive tract mucosa and those that are responsible for hair growth [17, 18]. Thus, current research is focusing on improving the specificity and therapeutic efficacy of chemotherapeutic agents, so that only cancerous cells will be affected. There are several anticancer agents currently used for chemotherapy, these agents can be divided into several categories based on their targets (Table 1.1).

Table 1.1. Groups of agents currently used in chemotherapy.

Group	Target	End result
Mitosis inhibitors	Tubulin/ microtubule systems	Cell cycle arrest in M phase, leading to cell death
Antimetabolites	DNA and Ribonucleic acid (RNA)	Cell cycle arrest
Alkalators	DNA	Damage to the DNA
Platinum-based	DNA	Breaks in the DNA chain

Among the group of mitosis inhibitors are microtubule-targeting compounds, which inhibit normal progression of mitosis by inhibiting the normal functioning of the microtubules [19, 20]. There are various compounds which have been identified as microtubule-targeting compounds; these include paclitaxel, epothilones, 2ME2 and podophyllotoxin [19, 20]. These compounds are grouped into two groups depending on their binding site on the microtubules [19]. Disruption of the normal functioning of the mitotic spindle results to mitotic arrest and subsequent induction of cell death [19-22]. Although these compounds have a high efficacy as chemotherapeutic drugs, they have various side effects which include toxicity to rapidly dividing normal cells [22]. Thus, research is in progress to identify more selective microtubule-targeting agents.

The balance between cell growth and proliferation, as well as cell death is of utmost importance in the growth and maintenance of multicellular organisms. Since these two processes have been implicated in the development of cancer, they will be discussed below.

1.3. Overview of the cell cycle

The cell cycle is a mechanism by which eukaryotic cells grow and proliferate [23]. During the cell cycle, a cell copies its DNA and then separates into two daughter cells [24, 25]. The cell cycle consists of four phases which occur in sequence, namely, gap₁ (G₁), synthesis (S), gap₂ (G₂) and mitotic (M) phase [23, 26, 27]. During G₁ and G₂ phases the cell ensures that all is ready for the process of DNA replication and of cell division, respectively [23, 25, 27]. During the S phase, DNA duplication takes place. The G₁, S and G₂ phases are collectively referred to as interphase [23, 27]. The M phase is the process of nuclear and cytoplasm division and it can be subdivided into prophase, metaphase, anaphase and telophase [23, 26, 27].

The progression from one phase of the cell cycle to the next is mainly controlled by a family of serine/threonine protein kinases called cyclin-dependent kinases (CDKs) [23, 27]. CDKs are present in an inactive form throughout the cell cycle within cells which have the potential to divide, but only become activated at specific points of the cell cycle [23, 27]. In mammalian cells, nine CDKs have been identified thus far, of these; the ones that required during the different phases of the cell cycle are as follows: CDK4 and CDK6 are active during the G₁ phase; CDK2 is active during the G₁ phase and S phase, with CDK1 active in both the G₂ and M phases [24, 27]. For their specific activation, CDKs require association with their specific regulatory subunits known as cyclin [24-26]. When activated, CDKs phosphorylate selected proteins required at specific stages of the cell cycle [23, 25, 26].

Cyclins are proteins whose synthesis is dependent on whether or not they are required at the specific phase of the cell cycle [28-31]. The activities of the CDKs can also be regulated by phosphorylation/dephosphorylation events as well as by CDK-inhibitors (CKI) [23, 24]. Phosphorylation of CDKs can either lead to their activation or their deactivation depending on the CDK amino acid residue that is phosphorylated [23, 24].

1.3.1. Cell cycle phases

1.3.1.1. G₁ phase

The G₁ phase is a period in which a cell decides whether it has received the necessary growth signals to proceed to the S phase [24, 32]. During this phase the cell receives signals from

both extracellular and intracellular environments. If the cell has not received the appropriate signals, it will not pass through a point known as restriction point (R-point), it will either temporally stop or it will exit the cell cycle and enter the phase known as the quiescence phase [24, 33, 34]. In early G₁ phase, the levels of D-type cyclins' increase due to appropriate growth signals and they bind with and activate CDK4 and CDK6 [33, 34]. Following their complete activation (i.e. after cyclin binding and phosphorylation by CDK-activating kinase (CAK)) cyclin D-CDK4/6 complexes phosphorylate the retinoblastoma protein (pRb). Rb is a tumor-suppressor protein, which when unphosphorylated binds to the elongation factor 2 (E2F). E2F controls transcription of several genes implicated in DNA synthesis and in cell cycle progression [24, 33, 34]. Cyclin E is another cyclin which is induced during the G₁ phase [29, 33]. Cyclin E binds with CDK2 to form a cyclin E-CDK2 complex. Cyclin E-CDK2 participate in keeping Rb in the hyper phosphorylated state and are important for transition from G₁ to S phase [24, 29].

The activities of CDK4/6 and CDK2 can be regulated by CKIs. Two groups of CKIs have been defined. The first group, the INK4, consist of p15^{INK4b}, p16^{INK4a}, p18^{INK4c} and p19^{INK4d} [29, 34]. These proteins function only at the G₁ phase, they form complexes with CDK4/6 before they bind to cyclin D [23, 24, 29, 34]. The second group of inhibitors, the Cip/Kip family consist of p21^{Waf1, Cip1, Sdi1}, p27^{kip1}, and p57^{Kip2} [23, 29]. Contrasting to the INK4 proteins, the Cip/Kip proteins serve as CKI in all phases of the cell cycle [23, 29, 34]. Deregulation of the Rb-cyclinD1-CDK4- p16^{INK4a} pathway has been shown to occur in lung tumours [35].

1.3.1.2. S phase

DNA replication, which is duplication of the genome, occurs during the S phase of the cell cycle [24]. During the late M to early G₁ phases of the cell cycle, the pre-replicative complex (pre-RC) binds onto the origin recognition complex (ORC) that is bound to chromatin [36, 38]. The ORC proteins form a six-membered complex that determines the site of initiation (i.e. site on the chromosome at which DNA replication begins) on the genome [38]. When ORC is bound to the replication sites it recruits other factors collectively referred to as pre-RC. The pre-RC consists of cell division cycle 6 (Cdc)6, cdc-10 dependent transcript (Cdt1)

and the minichromosome maintenance (MCM) protein complex [36-39]. MCM is a complex of 2-7 related proteins, whose function is to unwind DNA ahead of each replication fork [24].

At the beginning of the S phase, cyclin A levels increase and bind with CDK2. Cyclin A-CDK2 complex phosphorylate components of the DNA replication machinery, leading to the activation of a pre-RC thereby promoting the initiation of DNA replication [24].

1.3.1.3. G₂ phase

During the G₂ phase cells assess whether all the genetic material and cellular structures are correctly duplicated and they get ready to undergo mitosis [23, 39, 40]. This phase chiefly involves cyclin A-CDK1 complex [29]. Cyclin A-CDK1 complex promotes progression into the M phase. Nevertheless, cyclin B has also been shown to slowly increase in this phase and it binds to CDK1. The cyclin B-CDK1 complex is also known as the maturation-promoting factor (MPF) [24]. Cyclin B-CDK1 complex is however held inactive by remaining in the cytoplasm and by inhibitory phosphorylation at its Thr14 and Tyr15 amino acid residues by wee1 and myt1 protein kinases [23, 25, 33]. At the end of the G₂ phase, when the cell is ready to go into mitosis, the cyclin B-CDK1 complex is activated by phosphorylation at its Thr161 amino acid residue by phosphatases, Cdc25B and Cdc25C and it is transported into the nucleus [23, 33].

1.3.1.4. M phase

In the M phase of the cell cycle the chromosomes are pulled from the equator towards poles of the cell and cytoplasmic cleavage also takes place. Briefly, in the initial phase of the M phase, which is prophase, chromosomes condense and the microtubules start to form [26, 41, 42]. In metaphase chromosomes ascribe to the mitotic spindle and line up on the metaphase plate amongst the two centrosomes [26, 42]. After metaphase, the cell then enters anaphase, a phase where sister chromatids move to opposite poles [26, 41, 42]. In the last phase, which is telophase, the chromosomes reach the poles of the cell, a new nuclear membrane forms and the chromosomal decondensation begins [41, 42]. Then cytokinesis follows, in which the cytoplasm separates resulting in two daughter cells [41, 42].

Microtubules are one of the components that make up the cytoskeleton and are made up of alpha (α) and beta (β) tubulin heterodimers [43, 44]. They have several functions in the cells including maintenance of the cell's shape and morphology [44, 45]. During interphase, microtubules form part of the cellular transport mechanism of organelles and vesicles. However, when cells enter mitosis the microtubules are reorganized into mitotic spindle fibers which are required for the separation of chromosomes [46]. Microtubules are highly dynamic structures that constantly elongate and shorten, a process termed dynamic instability [46]. This behavior is regulated by various different proteins that bind to the microtubules.

In mitosis, microtubule dynamics increase, the formation and tension of kinetochore microtubules is important for proper attachment, separation, and segregation of chromosomes [43]. The kinetochore is a multiprotein complex that attaches the chromatids to microtubules which are connected to a spindle pole. The kinetochore generates forces that drive chromosome movement and delay the beginning of anaphase up to when chromosomes are properly attached to the mitotic spindle fibers [47].

Entry into mitosis is induced by increased activity of cyclin B-CDK1 complex [24, 29]. Activated cyclin B-CDK1 complex phosphorylates numerous proteins essential for the M phase [24]. Cyclin B-CDK1 complex activates the anaphase-promoting complex/ cyclosome (APC/C) which is an ubiquitin-protein ligase that regulates sister chromatid separation and exit from mitosis by targeting key proteins for degradation [24, 48]. APC/C promotes anaphase by degrading securin, the inhibitor of separase. Separase is a protease which cleaves cohesion, a protein that bind sister chromatids at the kinetochore thus preventing their separation [24, 41]. APC/C also targets cyclins A and B for degradation, the degradation of cyclin B leads to the end of the M phase [24, 33].

1.3.2. Cell cycle checkpoints

1.3.2.1. DNA checkpoint

During the cell cycle, damage to the DNA can lead to the activation of signaling cascade known as DNA checkpoints [33, 49]. The activated DNA checkpoints activate mechanisms which either repair the damage or, if the damage cannot be repaired, induce cell death [49, 50]. The cell cycle DNA damage checkpoints occur in the G_1/S and in G_2/M transitions and

may arrest the cells in the S or M phase [25, 29]. The G_1/S and in G_2/M checkpoints prevent entry into S and M phases respectively [23, 50].

At the G_1/S checkpoint, p53 is required for cell cycle arrest. p53 is a tumour suppressor protein that is phosphorylated by protein kinases such as ataxia-telangiectasia mutated (ATM), ataxia and rad3 related (ATR) in response to DNA damage [29, 33, 51]. When p53 is activated it stimulates the transcription of various genes such as p21, Mdm2 and Bax [29]. p21 is one the Cip/Kip family members and as already mentioned, it blocks cyclin-CDK activities, this prevents replication of damaged DNA [29, 33]. Mdm2 is a negative regulator of p53; it inhibits p53 transcriptional activity and facilitates its ubiquitination [24, 37]. Overexpression of mdm2 has been shown to lead to enhanced tumorigenic potential [24]. If DNA damage cannot be repaired, p53 can induce cell death by activating apoptosis promoting genes such as Bax [29].

When DNA damage occurs in G_2/M , cells can initiate cell cycle arrest irrespective of whether or not p53 is present [29, 33]. Entry into mitosis is prevented by keeping CDK1 in its inactive form. This can be done by phosphorylation or by sequestration of components of the cyclin B-CDK1 complex. Two protein kinases that facilitate these processes are protein kinases Chk1 and Chk2, which are triggered when there is DNA damage [29]. Chk1 and Chk2 phosphorylate a phosphatase Cdc25, thus resulting in the inhibition of Cdc25 activity and its binding to 14-3-3 proteins [29, 33]. 14-3-3 protein keeps the phosphatase in the cytoplasm and stops the removal of the inhibitory phosphorylation on Thr14 and Tyr15 of CDK1, thereby maintaining cyclin B-CDK1 in an inactive form [29, 33].

1.3.2.2. Spindle checkpoint

The spindle assembly checkpoint inhibits the commencement of anaphase until all kinetochores are attached properly to the mitotic spindle [29, 33, 41]. The proteins that are activated during this checkpoint include the mitotic arrest deficient 2 (Mad2) and the budding uninhibited by benomyl (bub) proteins [29, 33]. Mad2 prevents transition from metaphase into anaphase by binding to kinetochores thus preventing activation of APC/C [24, 29, 33].

1.4. Types of cell death

To date, there are several types of cell death that have been identified, such as mitotic catastrophe, oncosis, necrosis, apoptosis and autophagy. In this dissertation, only the two types of programmed cell deaths i.e. apoptosis and autophagy will be discussed in detail since they have been shown to be closely related to anticancer therapy. Mitotic catastrophe is a cell death pathway that occurs during mitosis as a result of errors in the cell cycle checkpoints and cellular damage [52, 53]. It is associated with morphological features such as the presence of multinucleated and micronucleated cells, with all these characteristics occurring prior to cell death [53-55]. Therefore mitotic catastrophe guards cells against unnecessary aneuploidization [53].

Oncosis (i.e. swelling, Greek origin) is a passive form of cell death [56, 57]. Oncosis occurs due to severe cellular damage as a result of cytotoxicity or failure of plasma membrane ion channels [56, 58]. It is characterized by cellular and organelle swelling, membrane blebbing, as well as increased permeability of the plasma membrane, which leads to cell lysis [57-59]. The lysed cell releases signaling molecules which in the end induce inflammation [56, 58, 59].

Necrosis is a type of cell death that is commonly referred to as an accidental type of cell death [52, 53, 60, 61]. The morphological features of necrosis include an increase in cell volume, enlargement of cytoplasmic organelles, severe plasma membrane damage and loss of intracellular contents [53, 60]. Recent studies have however suggested that the necrotic cell death may be a regulated cell death mechanism [52, 61, 62]. Death domain receptors and toll-like receptors (TLR) such as TNFR1, TNF-related apoptosis inducing ligand receptor (TRAIL-R), TLR3 and TLR4 are suggested to be involved in necrosis [62-64]. These receptors recruit a specific kinase known as the receptor interacting protein 1 (RIP1) and its activation leads to the induction of necrosis [62, 63]. Various cellular processes have been implicated in necrotic cell death; however the exact mechanism is still uncertain [63].

Apoptosis and autophagy are referred to as programmed cell death types, because they are genetically controlled. Programmed cell death (PCD) has significant role in numerous

biological events in multicellular organisms such as homeostasis, morphogenesis and in getting rid of damaged cells [64, 65].

1.4.1. Apoptosis

Apoptosis is a cellular mechanism by which cells undergo death in response to signals originating from inside or outside the cell without eliciting an inflammation [66, 67]. Apoptosis plays a significant role in cell growth during development and in homeostasis [68, 69]. For example during embryogenesis, cells located in-between the toes and fingers undergo apoptosis, resulting in free digits [70]. Too much or too little of the apoptosis pathway can result in diseases such as cancer, autoimmune diseases and neurodegenerative disorders [71, 72].

Cells undergoing apoptosis can be recognized by the following morphological features: cell shrinkage, chromatin condensation, nuclear fragmentation, plasma membrane blebbing and formation of apoptotic bodies [66, 73, 74]. During apoptosis phosphatidylserine (a phospholipid found in the inner surface of the plasma membrane) becomes exposed on the outer surface of the plasma membrane, resulting in the recognition and elimination of the cell by macrophages, therefore causing no inflammatory response [66, 71, 75, 76]. The morphological characteristics observed on cells undergoing apoptosis are due to the activities of a family of intracellular cysteine proteases known as cysteine-dependent aspartate-specific proteases (caspases) [77-79]

Caspases are a group of proteases that cleave their substrates specifically after the aspartate residues on the substrates [71, 72, 80]. Caspases are synthesized in an inactive form termed procaspases, and they contain a prodomain followed by large and small subunits. During apoptosis, a procaspase is cleaved to produce small and large subunits, which are the active forms of the caspase enzymes [71, 79, 81, 82]. Caspases can be categorized into two groups; the initiator caspases (which are involved in the starting the proteolytic cascade) and the effector caspases (involved in most of the cleavages that disassemble the cell). The initiator caspases includes caspase 2, 4, 8, 9 and 10 while the effector caspases includes caspases 3, 6 and 7 [71, 81].

Apoptosis can be activated by pathways that are dependent on caspases or by those independent on caspases. Three mechanisms are known to be involved in the caspase-dependent apoptotic process: extrinsic pathway (receptor-ligand mediated mechanism), intrinsic pathway (mitochondrial mediated pathway) and endoplasmic reticulum (ER)-mediated pathway [59].

1.4.1.1. Caspase-dependent signaling pathways

1.4.1.1.1. Extrinsic pathway (receptor-ligand mediated apoptosis)

The extrinsic pathway involves the binding of specific ligands to cell surface receptors, known as death receptors (DRs). Death receptors are members of the tumor necrosis factor (TNF) receptor superfamily which have apoptosis inducing activities [67, 69, 82, 83]. The best described ligands and their matching death receptors comprise of FasL/FasR, TNF- α /TNFR1, Apo-3 ligand (Apo-3L)/DR3, Apo-2 ligand (Apo-2L)/DR4 and Apo-2L/DR5 [69, 82]. Signaling of the apoptotic signal is facilitated by a cytoplasmic domain of the death receptors called the death domain (DD) [69, 83, 84]. After binding of a ligand to receptor, the DD of the receptor recruits adaptor proteins such as Fas-associated DD (FADD) or TNF receptor associated DD (TRADD) that also have a DD at their C-terminus and a second domain, called a death-effector domain (DED) at their N-terminus [83, 85]. The DED of the adaptor protein binds to the DED of an inactive initiator caspase (procaspase 8/10) forming a complex termed the death-inducing signaling complex (DISC), which leads to the activation and release of an active initiator caspase [69, 83, 84, 86, 87]. The activated initiator caspase then activates a series of effector caspases (caspase 3/6/7) resulting in the cleavage of caspase substrates (e.g. structural and proapoptotic proteins), which in the end leads to apoptosis (Figure 1.1) [83, 88]. The active initiator caspase can in addition cleave a B-cell lymphoma protein 2 (Bcl-2) family member termed Bid to truncated Bid (tBid), its active form. tBid promotes activation of the intrinsic pathway of apoptosis (Figure 1.1) [83, 87, 89, 90].

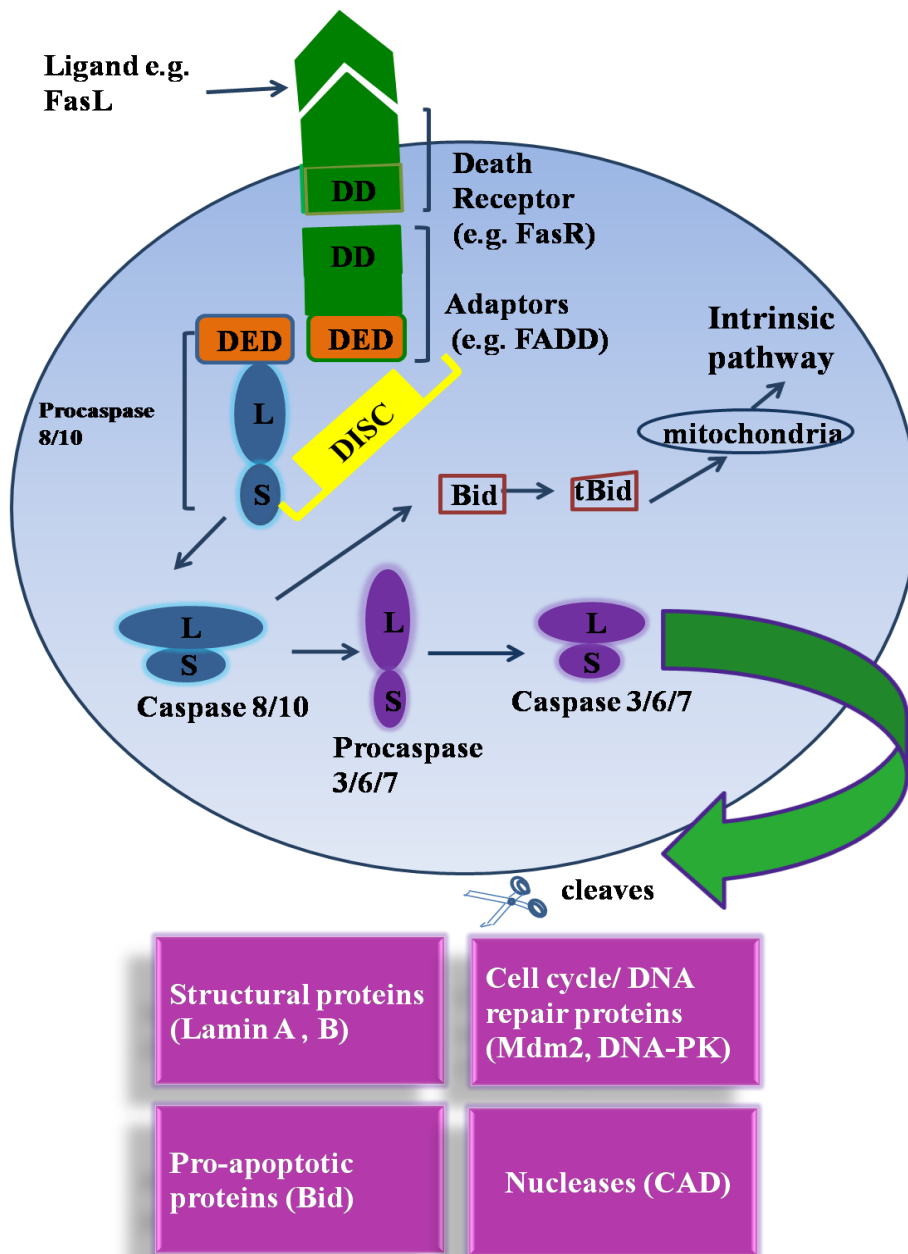


Figure 1.1. During the extrinsic pathway of apoptosis, the ligand (e.g. FasL) binds to the death receptor (e.g. FasR), which leads to the recruitment of adaptor proteins (e.g. FADD) and initiator procaspases (procaspase 8/10) via the death domain (DD) and the death-effector domain (DED), respectively. The resulting complex is known as the death inducing signaling complex (DISC). DISC formation leads to the activation of initiator caspase (caspase 8/10) which lead to the activation of effector caspases (caspase 3/6/7). Effector caspases (caspase 3/6/7) cleave various structural and proapoptotic proteins, leading to apoptosis. Activation of initiator caspase (caspase 8) can also result in the cleavage of the Bid to generate its active form tBid, which promotes induction of the intrinsic pathway.

1.4.1.1.2. Intrinsic pathway (mitochondrial-mediated apoptosis)

In the intrinsic pathway of apoptosis, the mitochondria play a central role in the transmission of death signals in response to the various forms of cellular stressors [83]. In this pathway, outer mitochondrial membrane permeabilization (MOMP) is produced by the formation of pores in the mitochondrial membrane. The formation of pores is controlled by Bcl-2 family of proteins [69, 83, 91]. These proteins can be categorized into two groups, namely, the anti-apoptotic proteins (Bcl-2, Bcl-x, Bcl-XL, Bcl-XS, Bcl-w and BAG) and the pro-apoptotic proteins (Bax, Bak, Bok, Bid, Bim, Bik, Noxa, Puma) [87, 91, 92]. Upon apoptosis induction, pro-apoptotic Bcl-2 proteins such as Bid translocates from the cytoplasm onto the outer mitochondrial membrane where they work together with other pro-apoptotic Bcl-2 proteins (e.g. Bax) to form a pore-like structure [83, 87]. This leads to the release of pro-apoptotic proteins such as cytochrome-*c* (Cyt *c*), second mitochondria-derived activator of caspase/direct IAP-binding protein with low pI (Smac/DIABLO), and serine protease HtrA2/Omi from the mitochondrial intermembrane space into the cytosol [85-87]. Cyt *c* together with ATP, binds to apoptotic protease-activating factor-1 (Apaf-1) forming the apoptosome complex [78, 83]. The apoptosome recruits procaspase 9 by the interaction of the caspase recruiting domain (CARD) of Apaf-1 with that of procaspase 9 which triggers the activation of the initiator caspase 9. Activated caspase 9 then initiates a caspase cascade involving effector caspases (e.g. caspase 3, caspase 7, and caspase 6), ultimately causing cell death (Figure 1.2.) [85-87]. Effector caspases are important mediators of events of the apoptosis since mice deficient in caspase 3 and 7 were resistant to apoptosis [73].

The Smac/DIABLO as well as the HtrA2/Omi promotes apoptosis by inhibiting the activity of apoptosis protein inhibitors (IAP) [82, 85, 87]. IAPs are proteins which attach to caspases thus inhibiting their activity and they have also been shown to promote the degradation of caspases [93-94]. In humans various family members of IAP have been identified which include the X chromosome-linked inhibitor of apoptosis protein (XIAP), cellular IAP1 (cIAP1), cIAP2, and survivin, amongst others [93-95].

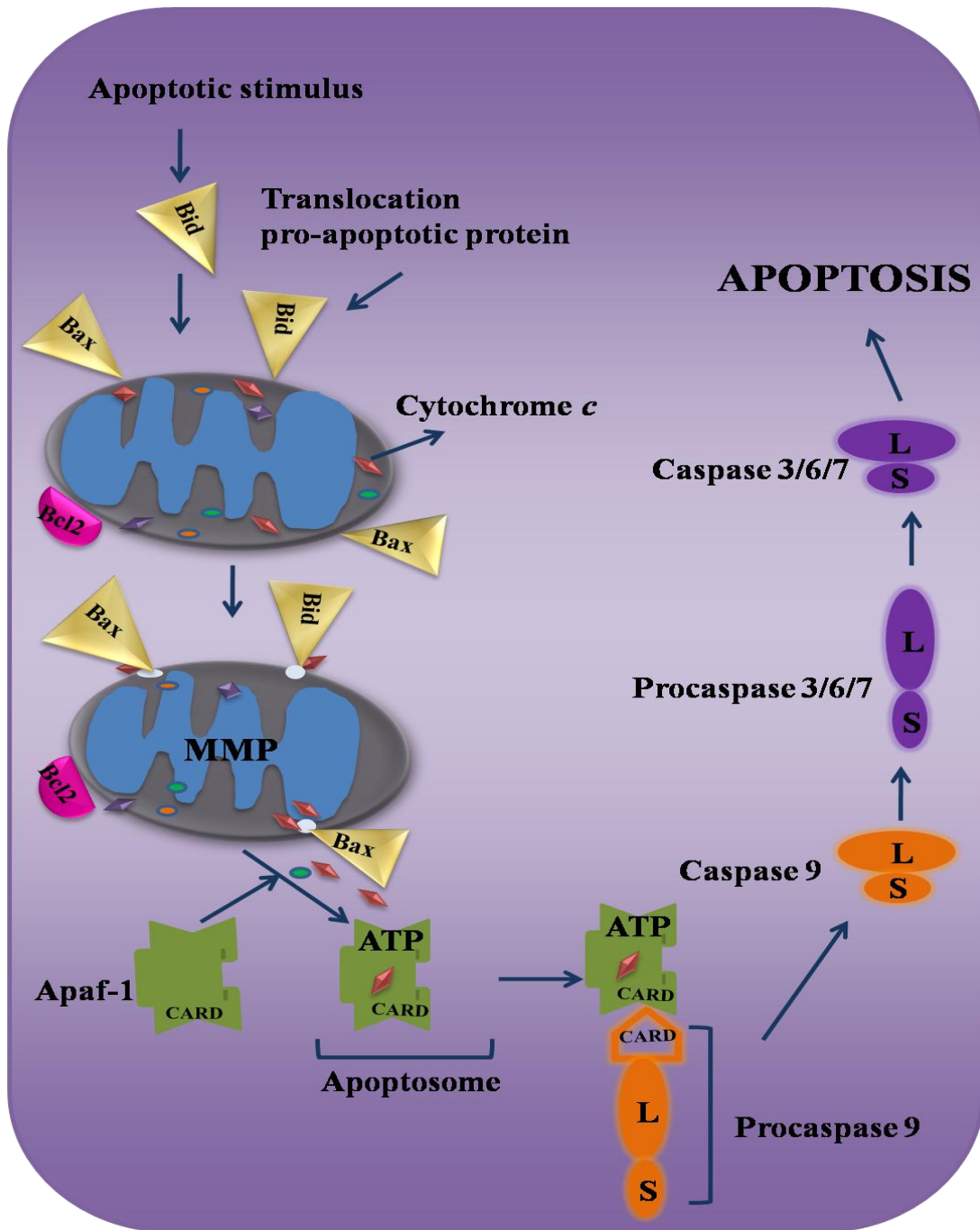


Figure 1.2. Mitochondrial mediated pathway. Upon apoptosis induction via the intrinsic pathway, pro-apoptotic Bcl-2 proteins such as Bid moves from the cytoplasm onto the outer mitochondrial membrane where it works together with other pro-apoptotic Bcl-2 proteins (e.g Bax) to form a pore-like structure. Cyt *c* becomes released into the cytosol and together with ATP binds to Apaf-1 forming the apoptosome complex. The apoptosome recruits procaspase 9 by the interaction of the CARD of Apaf-1 with that of procaspase 9 which activate the initiator caspase 9. Activated caspase 9 then recruits a caspase cascade involving effector caspases such as caspase 3, caspase 7, and caspase 6, ultimately resulting in apoptosis.

1.4.1.1.3. Endoplasmic reticulum-mediated apoptosis

ER mediated apoptosis is the third mechanism known to be involved in the caspase-dependent apoptotic process. The ER has multiple functions in the cell such as the synthesizing, and folding of membrane and secretory proteins as well as calcium storage [96-98]. The disruption of any of these functions may lead to the accumulation of misfolded proteins which can trigger ER stress [96, 98]. In an attempt to restore normal ER functioning, adaptive responses are activated. One of the ER stress responses is the unfolded-protein response (UPR) [96-98]. If UPR is however unable to counteract the accumulation of misfolded proteins then ER mediated apoptosis is activated. Apoptosis activated at the ER is proposed to involve two central pathways, a caspase- and a transcriptional-dependent pathway [97]. The caspase-dependent pathway induced by ER stress involves caspase 12 in murine and caspase 4 in humans. The activated caspase 12 activates caspase 9 which subsequently activates effector caspase 3 [96, 97]. It has been shown that Cyt *c* is not required for this type of apoptosis; meaning that caspase 12 directly triggers caspase 9 activation and subsequent apoptosis [96]. BH3-only class of proteins such as Bax/Bak has also been shown to take part in ER-mediated apoptosis. Bax and Bak can localize to the ER in response to ER stress, leading to calcium release and activation of murine caspase 12 [96, 98].

1.4.1.2. Caspase-independent pathway

Apoptosis can also be induced by caspase-independent death effector proteins such as the apoptosis-inducing factor (AIF), endonuclease G (Endo G), calpain, cathepsin and granzymes. Endo G and AIF are nucleases that are located in the mitochondrial intermembrane space [53, 99, 100]. During apoptosis, Endo G and AIF are released from the mitochondria into the nucleus where AIF causes chromatin condensation and DNA fragmentation while Endo G cleaves nuclear chromatin [53, 99]. Cathepsins D, B and L are proteases which are released from the lysosomes into the cytoplasm where they trigger apoptosis [53, 101]. These proteases can induce caspase-dependent or -independent apoptosis inclusive or exclusive of the contribution of the mitochondria [101]. Calpains are cytosolic calcium-activated cysteine proteases which activate apoptosis by cleaving pro-apoptotic or anti-apoptotic proteins like procaspase 12, Bcl-2, and Bax [102, 103]. Nakagawa *et al.* (2000)

showed that calpains may be responsible for cleaving Bcl-XL into a pro-apoptotic molecule [104]. Granzymes are a family of serine esterases which have been shown to induce apoptosis. They require perforin (pore forming proteins) in order to enter their target cells [105-107]. Granzymes induce apoptosis by various pathways including activating effector caspases or by cleaving the inhibitor of Caspase-Activated DNase (ICAD) resulting in DNA fragmentation [105, 106].

1.4.2. Overview of autophagy

Autophagy is a process whereby a cell degrades its intracellular components inside lysosomes [108]. It is one of the cell's two major pathways through which proteins are degraded and it is the only pathway known for degrading cellular organelles [109-111]. In normal cells, autophagy maintains cellular homeostasis by removing excessive proteins and damaged organelles [109]. Autophagy can be induced by various conditions such as starvation, growth factor withdrawal and stressors [109, 112, 113]. Generally, autophagy is a mechanism of survival for cells during periods of stress and starvation, but there are times where autophagy can progress to cell death. There are 3 major types of autophagy; macroautophagy, microautophagy and chaperone-mediated autophagy (CMA) [108, 112]. During macroautophagy, cytoplasmic contents are enclosed in a double-membrane vesicle, the autophagosome, which delivers them into the lysosome for degradation [113-116]. In microautophagy, the lysosomal membrane itself engulfs the cytoplasmic components, which leads to their degradation in the lumen [117, 118]. CMA is a lysosomal pathway that plays a part in the degradation of cytosolic proteins [112].

1.4.2.1. Macroautophagy

Macroautophagy (usually referred to as autophagy) begins with the formation of an isolation membrane which surrounds the cytoplasmic contents to be degraded. The isolation membrane then encloses to produce a double-membrane vesicle, the autophagosome, which transports the cytoplasmic components into the lysosome for degradation [109, 111, 113, 114]. In eukaryotic cells, nutrient starvation induces autophagy through inhibition of a major regulator of autophagy, known as mammalian target of rapamycin (mTOR) [110, 111, 115]. mTOR is a serine/threonine kinase that associates with numerous proteins to form 2 different signaling

complexes, mTOR complex 1 and 2 (mTORC1 and mTORC2) [115, 116]. The mTORC1 includes a regulatory associated protein of mTOR (RAPTOR), mLST8 and a proline-rich AKT substrate of 40 kDa (PRAS40) [117]. mTORC1 is implicated in autophagy induction during periods of starvation, while, the mTORC2 which contains rapamycin-insensitive companion of mTOR (RICTOR), mLST8, SIN1, and protor promotes the inhibition of autophagy by activating AKT kinase [117].

mTORC1 prevents autophagy induction by phosphorylating autophagy regulated gene 13 (Atg13) and uncoordinated 51-like kinase (ULK), which form part of the ULK-Atg13-FIP200 complex [118, 119]. During starvation, mTORC1 detaches from the ULK-Atg13-FIP200 complex, leading to the activation of ULKs, which then phosphorylates Atg13 as well as FIP200 [118, 119]. Jung *et al.* (2009) demonstrated that inhibition of mTOR in HEK293T cells by rapamycin or leucine deprivation lead to the dephosphorylation of ULK1, ULK 2 and Atg13, with subsequent autophagy induction [119]. RNAi-mediated knock down of ULK1 in cultured cells resulted in an inhibition of amino acid starvation-induced autophagy [120].

The formation of the isolation membrane requires the activity of Beclin 1-hVps34-hVps 15 complex [108, 118]. This complex is important for the recruitment of other Atg proteins that are important for the formation of the autophagosome and for producing phosphatidylinositol3-phosphate [121, 116]. Furthermore, autophagosome elongation, and expansion is regulated by two ubiquitin-like conjugation systems [120, 121]. The Atg5-Atg12 conjugate associates with Atg16L, and this complex then promotes the conversion of recruitment and conversion of LC3I to LC3II, which is required during the elongation step [112-114, 122]. In the second conjugation system, LC3I is conjugated to phosphatidylethanolamine (PE) to form LC3II by Atg7 and Atg3 [114]. LC3II is found on the inner and outer membrane of the autophagosome and it one of the methods used to monitor autophagy induction [112, 118, 119].

Autophagy can be repressed by the binding of the apoptosis-related proteins, Bcl2 or Bcl-XL, to Beclin 1. During starvation conditions, Jun N-terminal kinase 1 (Jnk1) promotes induction of autophagy by phosphorylating Bcl2 thus disturbing the interaction involving Beclin 1 and Bcl-2 [112, 113]. The interaction of Bcl2/Bcl-XL and Beclin is one of the molecular mechanisms of crosstalk between apoptosis and autophagy [123].

1.4.2.2. Microautophagy

During microautophagy, the lysosome engulfs the cytoplasmic components, which leads to their degradation in the lysosomal lumen [108, 121]. The process of microautophagy can be broken down into various steps which include: invagination of the lysosomal membrane, formation of autophagic tubes, formation and growth of autophagic vesicle, vesicle scission, and degradation of autophagic vesicles (Figure 1.3.) [124]. mTOR signaling pathways have also been shown to regulate microautophagy [124]. The fundamental mechanisms behind microautophagy are still not clearly defined and remain to be studied.

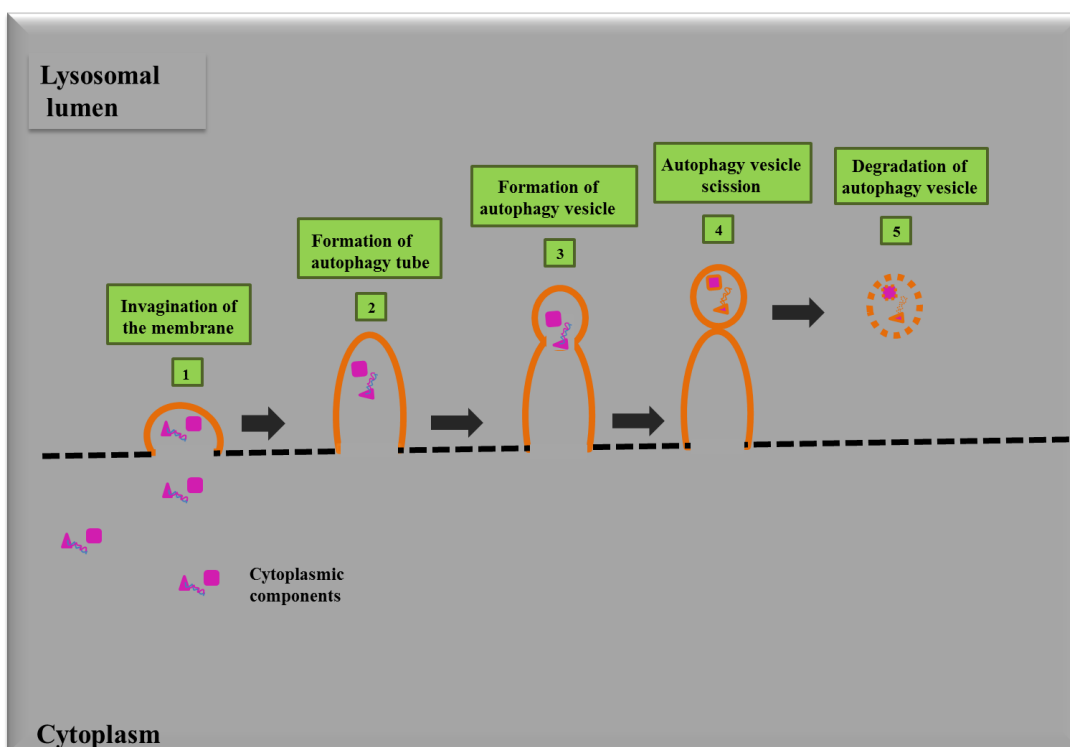


Figure 1.3. Schematic representation of microautophagy events.

1.4.2.3. Chaperone-mediated autophagy

CMA refers to a type of autophagy where soluble cytosolic proteins are selectively transported into the lysosome for degradation [125, 126]. CMA has been found to be activated under stressful conditions such as starvation and oxidative stress [127, 128]. Only proteins which have a target amino acid sequence related to the pentapeptide KFERQ (Lys-Phe-Glu-Arg-Gln) can be substrates for CMA [127, 128]. The CMA substrate proteins are

recognized by cytosolic chaperones (heat shock cognate 70 kDa (cys-hsc70)) together with their cochaperones. The cys-hsc70-cochaperone complex transports and binds the substrate protein to a lysosomal-associated membrane protein 2A (LAMP-2A) [125, 126,129]. Once the substrate is bound to the LAMP2A, it is unfolded by the cys-hsc70-cochaperone complex and it is then translocated across the lysosomal membrane by a lysosomal membrane chaperone (lys-hsc70) [125, 126, 129]. Agarraberes *et al.* (1997) demonstrated that blocking antibodies against lys-hsc70 prevented substrate translocation [130]. Once the unfolded substrate is in the lysosome lumen, it is degraded by proteases which are present in the lysosomal lumen (Figure 1.4) [125, 129].

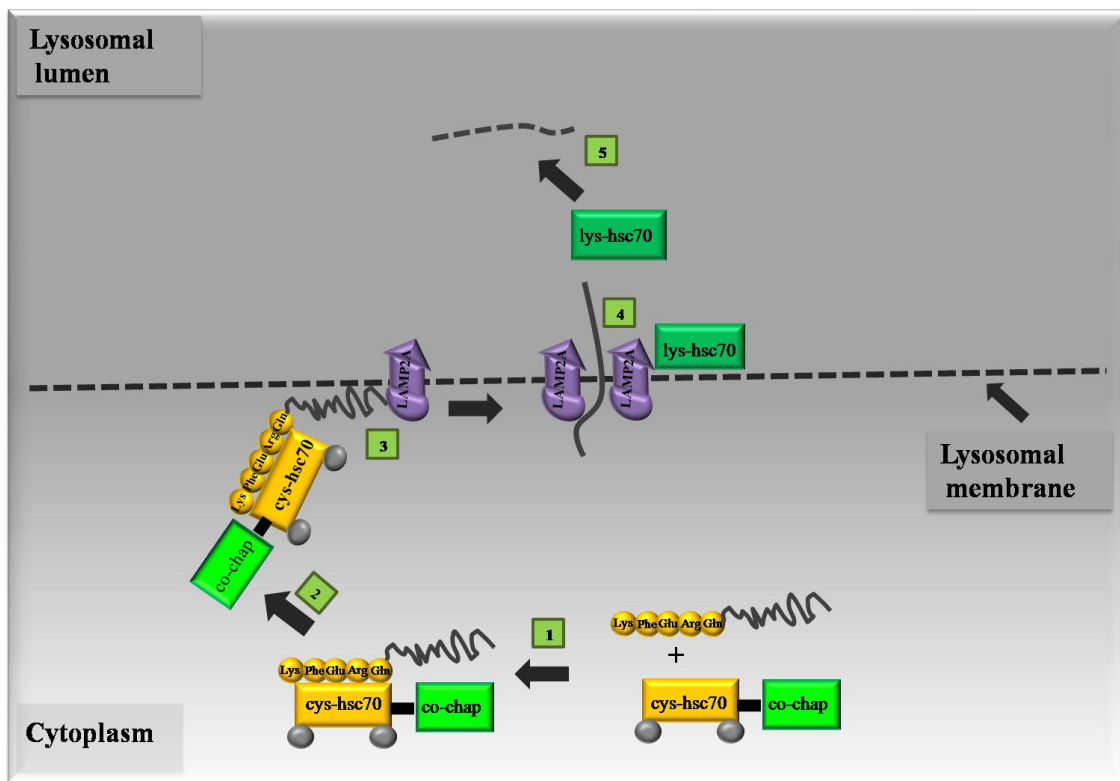


Figure 1.4. During CMA, proteins with a target amino acid sequence Lys-Phe-Glu-Arg-Gln (KFERQ) are recognized by cytosolic chaperone (cys-hsc70) together with their cochaperones (1). The cys-hsc70-cochaperone complex transports and binds the CMA substrate protein to LAMP-2A (2&3). Once the substrate is bound to the LAMP2A, it is unfolded by the cys-hsc70-cochaperone complex and it is then translocated across the lysosomal membrane by a lysosomal membrane chaperone (lys-hsc70) into the lysosomal lumen where it is degraded (4, 5).

1.5. Estrogens

1.5.1. Estrogen's metabolism

Estrogens are steroid hormones which are primarily produced and secreted by the ovaries. They are regarded as primary female sex hormones, since they promote the development and maintenance of female characteristics [131]. There are three major naturally occurring estrogens in females, namely, estrone, 17- β -estradiol, and estriol, with 17- β -estradiol being the most abundant estrogen in premenopausal woman [131, 132]. 17- β -estradiol has been implicated in carcinogenesis due to its ability to stimulate cell growth by means of binding to estrogen receptors. Additionally, 17- β -estradiol may play a role in carcinogenesis by formation of quinones and reactive oxygen species (ROS) by its products of oxidation, leading to DNA damage [132, 133].

Estrone and estradiol are substrates for phase I enzymes of the cytochrome P450 (CYP450) family, CYP1A1/1A2 and CYP3A4 [132-134]. 17- β -estradiol/estrone is mainly hydroxylated in the liver [135]. The formation of 2-hydroxyestrone, 2-hydroxyestradiol, 4-hydroxyestrone and 4-hydroxyestradiol metabolites result from the hydroxylation of the A-ring of 17- β -estradiol or estrone, while 16 α -hydroxyestrone, 16 α -hydroxyestradiol and estriol metabolites result from hydroxylation of the D-ring of 17- β -estradiol or estrone [133, 135]. 2-Hydroxyestradiol and 4-hydroxyestradiol metabolites have estrogenic and genotoxic properties, with 4-hydroxyestradiol being the most potent cell proliferator. Furthermore, 4-hydroxyestrone and 16 α -hydroxyestradiol are reported as being both estrogenic and carcinogenic [132].

2- and 4-Hydroxy metabolites are further converted to methoxylated metabolites namely; 2-methoxyestrone, 2-methoxyestradiol (2ME2), 4-methoxyestrone, 4-methoxyestradiol, as well as 2-hydroxyestrone 3-methyl ether, 2-hydroxyestradiol 3-methyl ether, 4-hydroxyestrone 3-methyl ether and 4-hydroxyestradiol 3-methyl ether by catechol *O*-methyltransferase (COMT) [133, 135].

Studies have shown that 2ME2, one of the metabolites of 17- β -estradiol has unique biological actions that are not the same as those of 17- β -estradiol and the catechol estrogens. 2ME2 has apoptosis-inducing properties in both transformed and malignant cells [136-139].

1.5.2. Overview of 2-methoxyestradiol

During the last few decades 2ME2 has been shown to be a promising anticancer drug. 2ME2 has the ability to inhibit the proliferation of various cell lines both *in vitro* and *in vivo* [138-142]. Studies on breast cancer (MCF-7) carcinoma cells and oesophageal (WHCO3) demonstrated that 2ME2 was an effective antiproliferative agent with inhibitory concentrations between 1 and 20mM [143, 144]. Xenograft experiments have demonstrated that oral administration of 2ME2 reduced growth of transplanted 3-methylcholanthrene-induced sarcoma (Meth-A) and mouse melanoma cell line (B16) by 66% and 85% in C3H mice respectively [139]. The antiproliferative activity of 2ME2 was found to be time- and concentration-dependent, as well as estrogen receptor independent [143, 145]. In a study conducted by LaVallee *et al.* (2002) 2ME2 was effective at inhibiting cell proliferation of estrogen-responsive (MCF7) and estrogen-independent (MDAMB- 435 and MDA-MB-231) cell lines [145].

In addition to its antiproliferative effects, 2ME2 has anti-angiogenic properties. Angiogenesis is a process by which new capillaries are made from pre-existing blood vessels; they are formed in and around tumors and they are essential for tumor growth and metastasis [146]. In cancer, angiogenesis promotes growth of cancerous cells. 2ME2 inhibits angiogenesis by disrupting endothelial tubulin dynamics which have an effect on the expression and activity of hypoxia inducible factor 1- α (HIF-1 α) and vascular endothelial growth factor (VEGF) [147, 148]. HIF-1 α is a subunit of HIF-1, a transcription factor which is normally activated during hypoxia to facilitate transcription of genes involved in angiogenesis, oxygen transport, glucose metabolism, growth factor signaling, apoptosis, invasion and metastasis [149]. VEGF is promotes growth of new blood vessels by stimulating endothelial cells which form the lining of the blood vessels' lumen and transport nutrients and oxygen to other tissues of blood vessels [150]. 2ME2 reduced tumour vasculature in mice injected subcutaneously with MethA sarcoma and B16 melanoma cells and subsequently treated with oral doses of 2ME2 [139]. There was a significant reduction in tumour growth of a human neuroblastoma

xenograft model in mice after 14 days of treatment with 2ME2. Anti-angiogenic effects, as well as apoptotic effects were also observed [150]. In a rat aorta *ex vivo* model, 2ME2 inhibited growth and sprouting of endothelial tubular formations [138].

2ME2 binds to the colchicine binding site on tubulin, causing cells to undergo mitotic arrest which subsequently leads to the induction of apoptosis [151-153]. In a study conducted by Stander *et al.* (2010) the exposure of breast cancer cells (MCF-7) to 2ME2 resulted in an increase in the number of cells in the G₂/M phase, as well as an increase in the number of cells in the sub-G₁ phase, indicating that apoptosis was induced in these cells [154]. Similarly Fukui and Zhu (2009) demonstrated that exposure of breast cancer cells (MDA-MB-435) to 2ME2 arrested cells in G₂/M phase and apoptosis occurred in a concentration- and time-dependent manner [142]. G₂/M arrests in addition to increased apoptosis in 2ME2-treated cells are believed to contribute predominantly to its strong antiproliferative effect in these cells [155].

In gastric carcinoma cell lines (SC-M1 and NUGC-3), 2ME2 appears to induce caspase 3 activation which leads to apoptosis via the caspase activation cascade, resulting in a G₂/M cell cycle arrest [148]. 2ME2 binds to the colchicine site of tubulin, thus inhibiting tubulin polymerization. In a study by Mukhopadhyay *et al.* (1997) the apoptotic cell death that was induced by 2ME2 was shown to be p53 mediated, as the functional activity of p53 increased after treatment with 2ME2 [156]. However, several other studies indicate that the induction of apoptosis by 2ME2 may be independent of p53 [157, 158]. 2ME2 treatment results in the up-regulation of death receptor 5 (DR5) expression both *in vitro* and *in vivo*. DR5 is involved in the extrinsic pathway of apoptosis [159]. The mechanism of action of 2ME2 seems to be cell line dependent.

Although, 2ME2 has been revealed to exert antiproliferative, antitumour and anti-angiogenic properties, human clinical trials for the treatment of breast cancer, prostate cancer and multiple myeloma have shown that high oral doses of 2ME2 (registered as Panzem[®] by Entremed, Inc. (Rockville, MD)) are needed per day in order to significantly reduce the growth of certain tumours [160-163]. In a study conducted by Ireson *et al.* (2004) 10mg/kg of 2ME2 was administered orally (*p.o.*) or intravenously (*i.v.*). Data from this study indicated that 2ME2 was below the limit of detection in plasma subsequent *p.o.* dosing and was rapidly

removed from the plasma following administration of a single *i.v.* dose, which suggests that the agent undergoes rapid biotransformation *in vivo* [164]. Studies have demonstrated that doses of 75 (oral) and 150 mg kg⁻¹day⁻¹ (intraperitoneal) of 2ME2 were required to reduce the growth of melanoma or myeloma tumours [141, 165].

In another clinical trial a dose of up to 6g/day of 2ME2 had to be used in an attempt to maintain the plasma concentration of 2ME2 in the range of 3-17ng/ml, which is the plasma concentration that is required for efficient antitumor activity of 2ME2 [160]. 2ME2 has low bioavailability and it is rapidly inactivation due to its metabolism by 17 β -hydroxysteroid dehydrogenase type 2 and by conjugation of both 3- and 17-hydroxyl moieties to form glucuronides. 17 β -hydroxysteroid dehydrogenase type 2 is an enzyme that is expressed in the gastrointestinal tract and the liver. This enzyme oxidizes 2ME2 to its inactive metabolite, 2ME1 [166-168]. A study conducted by Newman *et al.* (2006) showed that after just 48 hours, 95% of the added 2ME2 was metabolized to 2ME1. The latter confirms 2ME2's limited oral bioavailability [166].

In an attempt to address the problem of low solubility and bioavailability, new nanocrystal dispersion (NCD) formulation of 2ME2 has been developed [163, 169]. It has been demonstrated that a nanoparticulate dispersion of 2ME2 leads to higher plasma levels (about 3-4%) compared to the old 2ME2 formulation, however, the bioavailability still remains very low [168].

Thus, analogues of 2ME2 are currently being designed, synthesized and tested in an attempt to create compounds with improved anticancer potency and oral bioavailability.

1.5.3. Overview of 2-methoxyestradiol-bis-sulphamate

2-Methoxyestradiol-bis-sulphamate (2-MeOE2bisMATE) is a bis-sulphamoylated derivative of 2ME2, which is currently being researched as a potential anticancer drug. 2-MeOE2bisMATE (also known as STX140) was created by the addition of sulphamate groups at position 3 and position 17 of 2ME2 (Figure 1.5), and it was initially developed as an inhibitor of steroid sulphatase (STS), which is an enzyme that converts estrone sulphate to estrone [168]. Estrone can then be converted into a biologically active estrogen,

17- β -estradiol. 17- β -estradiol binds to estrogen receptors and it stimulates the growth of hormone-dependent tumours [168, 170, 171].

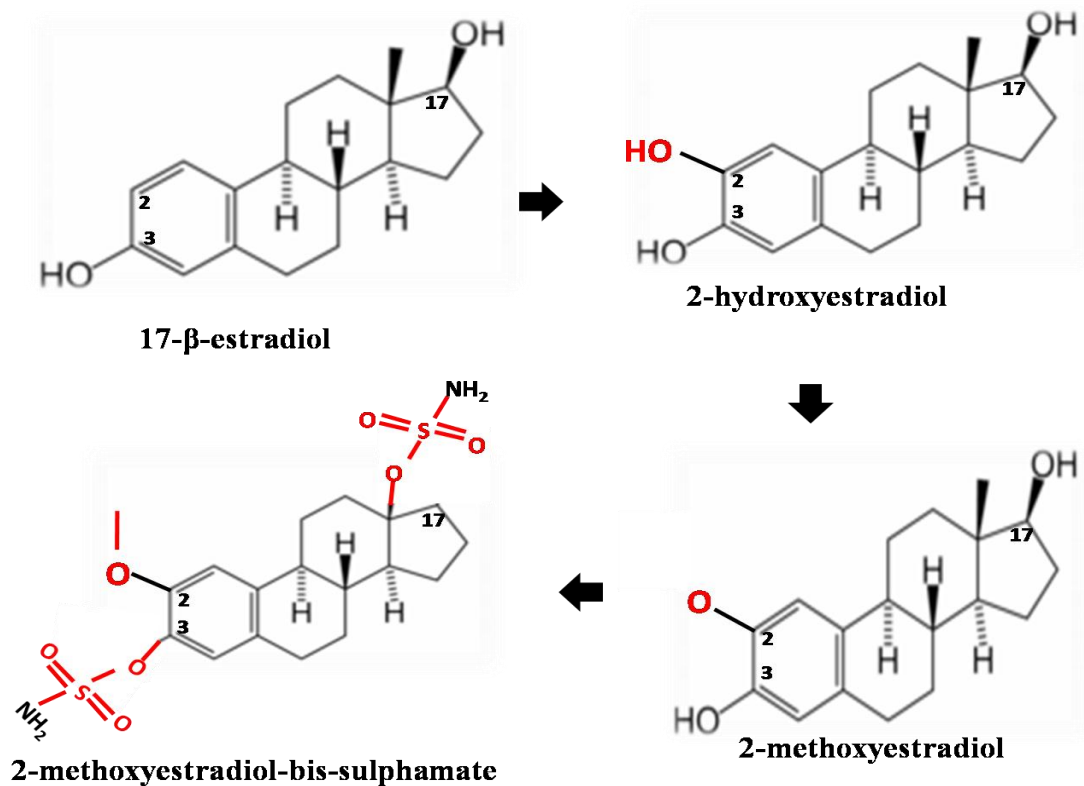


Figure 1.5. Schematic diagram illustrating the synthesis of 2-MeOE2bisMATE from 2ME2.

Recent *in vitro* studies from our laboratory and from other researchers, have found that 2-MeOE2bisMATE inhibits cell growth in cancer cell lines namely the human breast adenocarcinoma estrogen receptor positive cell line (MCF-7), human breast adenocarcinoma estrogen receptor negative cell line (MDA-MB-231), human umbilical vein endothelial cells (HUVEC), human prostate cancer cell line (PC3) and ovarian cancer cells [172-176].

In a study conducted by Newman *et al.* (2008), a concentration of 500nM of 2-MeOE2bisMATE inhibited the proliferation of drug resistant cells (MCF-7_{DOX}). MCF-7_{DOX} cells are known to be resistant to various metastatic breast cancer drugs such as taxol and doxorubicin [177]. Visagie *et al.* (2010, 2011) revealed that an exposure of breast cancer cells (MCF-7) population to 0.4 μ M of 2-MeOE2bisMATE for a period of 48 hours yielded a 47% growth reduction, while the same dose-time relationship yielded a 79% growth reduction in the nontumorigenic MCF-12A cell population. The tumorigenic MCF-7 cells were more

susceptible to 2-MeOE2bisMATE treatment compared to the normal MCF-12A cells [178, 179]. Some cell types were found to be more sensitive to 2-MeOE2bisMATE, suggesting differential signal transduction exerted by this compound.

2-MeOE2bisMATE has revealed improved biological activity and oral bioavailability when compared to 2ME2 [164, 177, 180, 181]. This characteristic is made possible by its ability to transit the liver without undergoing first pass metabolism. This is attributed to the ability of sulfamoylated derivatives to reversibly bind to carbonic anhydrase II (CAII) in erythrocytes after which they are then slowly released into the blood circulation system [174, 182-184].

Since the exact mechanism of action of 2-MeOE2bisMATE is still unknown and appears to be cell line dependent. The purpose of this *in vitro* study was to investigate effects of 2-MeOE2bisMATE in a South African oesophageal carcinoma cell line (SNO) by exploring its influence on cell growth, morphology, cell cycle progression and possible induction of types of cell deaths. These activities have not been studied previously in these cells.

1.6. Significance of this study

South Africa (mostly Transkei region) has the highest incidence of oesophageal squamous cell carcinoma. It is of great importance that effective chemotherapeutic compounds are discovered, which will be used to treat this form of cancer. Knowledge obtained from *in vitro* study will contribute to the understanding of the efficacy of 2-MeOE2bisMATE in inhibiting the growth of oesophageal carcinoma cells, and to understanding the mechanism of action of 2-MeOE2bisMATE in these cells, which is currently unknown. Understanding of *in vitro* molecular mechanisms of this compound will enable researchers to focus on affected cellular mechanisms and to identify active compounds with subsequent evaluation as possible candidates for use in anticancer therapy.

1.7. Specific aims of this study

- I. To conduct time- and dose-dependent studies using spectrophotometry to observe the viability of SNO cells after exposure to 2-MeOE2bisMATE.
- II. To investigate changes in cell morphology via polarization-optical differential interference contrast microscopy, light microscopy and transmission electron microscopy after exposure of SNO cells to 2-MeOE2bisMATE.
- III. To determine whether 2-MeOE2bisMATE disrupts tubulin function and structure in SNO cells.
- IV. To determine whether 2-MeOEBisMATE increases the activities of caspase 6 and 8 in SNO cells.
- V. To identify types of cell deaths that may be induced by 2-MeOE2bisMATE using fluorescence microscopy and flow cytometry to study its effects on cell cycle progression, mitochondrial membrane potential (mitotracker assay), apoptosis (annexin V) and autophagy markers (LC3 marker and Cyto-ID autophagy detection assays).

Chapter 2

Research procedure

2.1. Type of study

This research project is considered as a preclinical *in vitro* study; therefore it is not directly related to an *in vivo* study and cannot be extrapolated to an *in vivo* environment. The scientific information gained from this research will contribute to the action mechanism of this compound and will provide targets for future *in vivo* investigation.

2.2. Materials

2.2.1. Cell line

SNO oesophageal carcinoma cell line was purchased from the Highveld Biological Ltd. (Pty) (Sandringham, South Africa). The cells are described as non-keratinizing squamous epithelial cells.

2.2.2. Compound and reagents

In view of the fact that 2-MeOE2bisMATE is currently not commercially available, the compound was synthesized by Professor Vlegaar from the Department of Chemistry (University of Pretoria, Pretoria, South Africa). Dulbecco's Modified Eagle's Medium (DMEM), penicillin, streptomycin, fungizone and trypsin were bought from Highveld Biological (Pty) Ltd. (Sandringham, South Africa). Dimethyl sulphoxide (DMSO) and trypan blue were purchased from Sigma-Aldrich Co. (St Louis, United States of America). Heat-inactivated fetal calf serum (FCS), sterile cell culture flasks, and plates were obtained through Separations (Pty) Ltd. (Randburg, Johannesburg, South Africa). All other analytical grade chemicals were supplied by Sigma Chemical Co. (St. Louis, MO, United States of America).

2.3. General laboratory procedures

2.3.1. Preparations of general cell culture maintenance's reagents

I. DMEM complete

DMEM with glucose, sodium pyruvate and L-glutamine was supplemented with 10% fetal bovine serum, 100µg/l penicillin, 100µg/l streptomycin and 250µg/l fungizone.

II. Phosphate buffered saline (PBS)

A tenfold concentrated stock solution of PBS consisting of 80g/l NaCl, 2g/l KCl, 2g/l KH₂PO₄ and 11.5g/l Na₂PO₄ was prepared with the pH adjusted to 7.4. The solution was then stored in the refrigerator (4°C) in aliquots of 500ml. One times solution was made and then autoclaved (120°C, 15psi, 20 minutes) before being utilized.

III. Freeze medium

Freeze medium was made by adding 70% complete DMEM, 20% FCS and 10% DMSO. The solution was made in 50ml sterile tube and stored at 4°C.

2.3.2. General cell culture maintenance

I. Maintenance and subculturing

Cells were grown as monolayers in sterile 25cm² or 75cm² tissue culture flasks in a Forma Scientific water-jacketed incubator (Ohio, United States of America) at 37°C and 5% CO₂. Cells were maintained in 5ml of DMEM complete in 25cm² or in 8ml DMEM complete in 75cm² flasks. The growth medium was routinely replaced with fresh medium. When cells were confluent, they were dispersed by being trypsinized. This was done by removing the medium from the culture, the cells were washed twice with sterile PBS before a volume of 2ml of trypsin was added and the flask was placed at 37°C for 2-3 minutes (i.e. when cells appear round in shape). After incubation, the trypsin was removed and the cells were detached from the flask by gently hitting the flask. The cells were resuspended in fresh medium and divided into subcultures or used in experiments. All solutions were filtered

through a 0.22 μ m membrane filter and all procedures were conducted under aseptic conditions.

II. Preservation

When necessary, cells were frozen in cell culture freeze medium at a concentration of 5×10^6 cells per ml. The freeze medium was prepared as stated above. A 1ml cell suspension was transferred into 1.5ml vials and wrapped in cotton wool in a polystyrene foam box. This ensured that the vials cool at a rate of 1°C/min. The box was placed in a freezer (-70°C) for a day or two then the vials were stored in liquid nitrogen.

2.3.3. General methods for experiments

Experiments were conducted in 96-well tissue plates, 6-well plates or 25cm² cell culture flasks. For 96-well plates, cells were seeded at a density of 5 000 cells per well in 200 μ l medium. For 6-well plates, cells were seeded on heat-sterilized coverslips at a density of 350 000 cells per well in 3 ml medium. For 25 cm² cell culture flasks, cells were seeded at 1×10^6 or 500 000 cells in 5 ml of medium.

The number of cells was determined by making use of a haemocytometer. A cell suspension of 20 μ l was resuspended with 80 μ l PBS, 20 μ l of that solution was then mixed with 20 μ l trypan blue to give a concentration of cells with a dilution factor of 10. The trypan blue is a dye that penetrates through the cell membrane of cells whose cell membrane is not intact, thus viable cells will not take up the dye whereas nonviable cell will stain blue [185].

The number of cells per ml is determined by the following equation:

Cells/ml = average count of viable cells in the four corner squares of haemocytometer x dilution factor x 10^4

Stock solutions of 2-MeOE2bisMATE with a concentration of 2.0×10^{-3} M were prepared in dimethyl sulphoxide (DMSO) and stored at -20°C. Dose (0.2-1 μ M) and times (24, 48 and 72 hours) were chosen since previous studies in our laboratory and in the literature have shown that it is within this range that 2-MeOE2bisMATE is most efficient as an antiproliferative agent [174, 186].

Control samples included cells propagated in growth medium. Another control, vehicle-treated comprised of cells treated with the same volume of DMSO used to expose cells with 2-MeOE2bisMATE. The DMSO content of the final dilutions never exceeded 0.05% (v/v). Positive control for induction of apoptosis included cells exposed to actinomycin D (0.1µg/ml) and a positive control for induction of autophagy comprised of starved cells (cells which were propagated in a solution which contains both growth medium and PBS at a ratio of 1:2 respectively). Tamoxifen (at a final concentration of 20µM) was also used as a positive control for induction of autophagy.

2.4. Analytical experimental protocols

2.4.1. Cell number and viability assays

2.4.1.1. Crystal violet staining

Crystal violet staining is a triphenylmethane dye which is known as gentian violet. Crystal violet stains the DNA in the cells' nuclei. Gellies *et al.* (1989) showed that when crystal violet is solubilised in Triton-X100, the optical density of the solution obtained from spectrophotometry is linearly related to the quantity of viable cells [187]. In this study, crystal violet staining was used to study the effects of 2-MeOE2bisMATE on cell proliferation. Staining the cell nuclei with crystal violet dye allows for fast and reliable quantification of cell numbers, if the cells are grown in a monolayer culture [187, 188]. The absorbance of the dye measured at 570nm corresponds to cell quantities.

I. Materials

Glutaraldehyde, Crystal violet and Triton-X100 were purchased from Merck (Munich, Germany).

II. Methods

SNO cells were seeded at a cell density of 5 000 cells per well in 96-well tissue culture plates and incubated at 37°C for 24 hours to ensure attachment. The medium was discarded and cells were exposed to a dilution series ranging from 0.2-1µM of 2-MeOE2bisMATE including controls as previously described. As already mentioned, this concentration range

was chosen since previous studies have shown that it is within this range that 2-MeOE2bisMATE is most efficient as an antiproliferative agent [174, 186]. The experiment was terminated by the addition of 100µl of 1% glutaraldehyde in water for 15 minutes. Crystal violet (100µl) (1%, in water) was added to the wells and incubated for 30 minutes, after which the culture wells were immersed in running tap water for 15 minutes. The plates were left overnight to dry. Then 200µl of Triton-X100 (0.2% in water) was added to each well. Plates were incubated for 30 minutes and 100µl of the liquid content was transferred to 96-well plates. The absorbance of the samples was analyzed using an ELX800 Universal Microplate Reader (Bio- Tek Instruments, Inc., Analytical Diagnostic Products, Weltevreden, SA).

2.4.1.2. Lactate dehydrogenase cytotoxic assay

Lactate dehydrogenase (LDH) is a cytosolic enzyme which is present in all cell types and it is rapidly released into the cell culture medium upon cell death (late apoptosis or necrosis) by leaking through a damaged plasma membrane. The activity of the LDH in culture medium can be used as an indicator of cell membrane integrity and as measurement of the cytotoxicity of a drug. Absorbance is directly proportional to the concentration of LDH in the cell culture medium [189].

I. Materials

Lactate dehydrogenase assay kit was bought from BIOCOM biotech Pty (Ltd) (Clubview, South Africa).

II. Methods

Exponentially growing SNO cells were seeded in 96-well tissue culture plates at a cell density of 5 000 cells per well. Cells were incubated at 37°C for a period of 24 hours to allow for attachment. After incubation, the medium was discarded and cells were exposed to 2-MeOE2bisMATE, including previously defined controls respectively. After exposure, the plate was gently shaken and the supernatant was centrifuged at 600xg for 10 minutes. Thereafter, 10µl of the supernatant was transferred to an optically clear 96-well plate. Subsequently, 100µl of the LDH Reaction Mix was added to each well, mixed and incubated

for two hours at room temperature. The absorbance of all controls was measured with a plate reader equipped with a 450nm filter and a reference wavelength of 630nm. The absorbance of the samples was analyzed using an EL_x800 Universal Microplate Reader available from Bio-Tek Instruments Inc. (Vermont, United States of America).

2.4.2. Morphology studies

2.4.2.1. Polarization-optical differential interference contrast

I. Methods

Polarization-optical differential interference contrast (PlasDIC) is a new polarization-optical transmitted light differential interference contrast method. Unlike conventional DIC, linearly polarized light is only generated after the objective [190]. PlasDIC allows for high quality imaging of cells and thus morphological characteristics specific for types of cell death can be easily recognized. PlasDIC was used to observe morphological characteristics of SNO cells after they were exposed to 2-MeOE2bisMATE. These images were captured using the Zeiss Axiovert-40 microscope (Zeiss, Göttingen, Germany).

2.4.2.2. Light microscopy - haematoxylin & eosin staining

Light microscopy was used to reveal morphological changes of the nuclear and cytoplasmic components of SNO cells that may be affected by 2-MeOE2bisMATE. Haematoxylin is a dye that stains the nucleic acids of the cells a blue-purple colour. Eosin stains the cytoplasm of the cells a red colour [191]. Morphological changes such as the appearance of apoptotic bodies and membrane blebbing can be viewed by means of a light microscope. Haematoxylin and eosin staining results provided both qualitative and quantitative (mitotic indices) data. Mitotic indices were obtained by counting a thousand cells on each slide of a biological replicate and expressing them as a percentage of cells in interphase, mitotic phases and apoptosis.

I. Materials

Haematoxylin, eosin, ethanol, Entellem® fixative, xylol were purchased from Merck (Darmstadt, Germany). Bouin's fixative was bought from Sigma-Aldrich (Ltd) (Clubview, South Africa).

II. Methods

Exponentially growing SNO cells were seeded at 250 000 cells per well in 6-well plates on heat-sterilized coverslips. After a 24 hours incubation period at 37°C, cells were exposed to 2-MeOE2bisMATE. Cells were fixed in Bouin's fixative for 30 minutes. The fixative was discarded and 70% ethanol was added to the cells which were on coverslips, then incubated for 20 minutes, then rinsed in tap water and subsequently left for 20 minutes in Mayer's Hemalum. After rinsing with running tap water for 2 minutes, coverslips were washed with 70% ethanol before being subjected to 1% eosin for 2 minutes. This was followed by rinsing twice for 5 minutes with 70% ethanol, 96% ethanol, 100% ethanol and xylol respectively. Coverslips were then mounted with resin and left to dry before they were evaluated with a Zeiss Axiovert MRs microscope (Zeiss, Göttingen, Germany).

2.4.2.3. Transmission electron microscopy

Transmission Electron microscopy (TEM) is a technique which allows imaging of internal cell structures with a resolution power of about 0.1-0.4 nm [192]. The latter was used to study the effects induced by 2-MeOE2bisMATE on SNO cells' internal structures' morphology.

I. Materials

Glutaraldehyde, aqueous osmium tetroxide, quetol, aqueous uranyl acetate, Reynold's lead citrate were purchased from Merck (Darmstadt, Germany) by the Electron Microscopy Unit (Pretoria, South Africa).

II. Methods

Exponentially growing SNO cells were seeded at 500 000 cells per 25cm² flask. To allow for cell attachment, cells were incubated at 37°C for a period of 24 hours. Thereafter, the

medium was discarded and the cells were exposed to 2-MeOE2bisMATE, and the other cells were exposed to the controls. The experiment was terminated by trypsinizing the cells, fixing them in 2.5% glutaraldehyde in 0.075M phosphate buffer (pH 7.4) and then washing them with 0.075M phosphate buffer. The cells were then be fixed in 0.25% aqueous osmium solution and rinsed with increasing concentrations of ethanol (30%, 50%, 70%, 90%, and 100%) and embedded in Quetol resin. Ultra-thin sections were prepared with a microtome and thereafter they were mounted on a copper grid. Samples were contrasted with 4% uranyl acetate and Reynolds' lead citrate and viewed with a Multi-purpose Philips 301 TEM (Electron Microscopy Unit, Pretoria, South Africa).

2.4.2.4. Confocal-alpha (α)-tubulin assay

Tubulin polymerization dynamics within the cell are critical for the process of mitosis and are frequently targeted by agents that induce mitotic arrest. Since the parental molecule of 2-MeOE2bisMATE has been shown to be a tubulin poison, the α -tubulin detection assay was utilized to determine the effects of 2-MeOE2bisMATE on tubulin morphology of SNO cells [193].

I. Materials

Alpha-tubulin antibody, alexafluor 488 and 4',6-diamidino-2-phenylindole (DAPI) were purchased from BIOCROM biotech (Pty) Ltd. (Clubview, South Africa).

II. Methods

Exponentially growing SNO cells were seeded at 250 000 cells per well in 6-well plates on coverslips. After 24 hours of attachment, cells were exposed to 2-MeOE2bisMATE and to appropriate controls for a period of 24 hours. The experiment was then terminated by fixing the cells in 10% formalin (containing 2mM EGTA in phosphate buffered saline (PBS)) for 10 minutes and then permeabilizing them in ice-cold 97% methanol (containing 2mM EGTA), which was dissolved by adding a few drops of 1mM sodium hydroxide at -20°C for 10 minutes. After 10 minutes of incubation, the coverslips were washed in PBS (5 minutes) between successive 1 hour incubations with each of the following: mouse monoclonal antibody against human α -tubulin (Clone 2-28-33; 1:1000), biotin-conjugated anti-mouse IgG

(Fab-specific, developed in goat) in FITC-conjugate diluent as secondary antibody (1:15) and ExtrAvidin-FITC conjugates (1:200 in FITC-conjugate diluent). Following three 5 minute washes with PBS, the coverslips were stained with 4',6-Diamidino-2-Phenylindole (DAPI, a nucleic stain) that produces blue fluorescence and were mounted with a glycerol-based mounting fluid and Cells were then examined with a ZEISS, LSM 510 Meta confocal microscope at the Electron Microscopy unit at the University of Pretoria (Pretoria, South Africa).

2.4.3. Determination of possible types of cell deaths induced

2.4.3.1. Fluorescent microscopy - triple staining technique

A triple fluorescent dye staining method was used to study the type(s) of cell death (apoptosis, autophagy) induced after exposure of SNO cells to 2-MeOE2bisMATE. Hoechst 33342 (HO) is a fluorescent dye that can enter intact cell membranes of viable cells and cells undergoing apoptosis, and it stains the cell nuclei blue. Acridine orange (AO) is a fluorescent compound (green) that serves as a tracer for acidic vesicular organelles such as vacuoles and lysosomes. Cells undergoing autophagy will have an increased affinity for AO staining when compared to viable cells. This is because cells undergoing autophagy have an increased lysosomal activity compared to viable cells. Propidium iodide (PI) is a red fluorescent dye that is unable to penetrate an intact cell membrane; thus it stains the nuclei of cells that have lost their membrane integrity owing to necrotic processes [194].

I. Materials

Acridine orange, bisbenzimidazole (Hoechst 33342) and propidium iodide were bought from Sigma-Aldrich (Ltd) (Clubview, South Africa).

II. Methods

SNO cells were seeded according to the same procedure describe for light microscopy. Cells which were exposed to actinomycin D served as positive control for apoptosis, while starved cells were included to serve as a positive control for autophagy. 0.5ml HO solution (3.5µg/ml in PBS) was added to the medium to give a final concentration of 0.9µM and cells were

incubated for a period of 30 minutes at 37°C. After 25 minutes into incubation, 0.5ml of AO solution (4µg/ml in PBS) was added to the medium to provide a final concentration of 1µg/ml and 0.5ml of PI solution (40µg/ml in PBS) was also be added to the medium to give a final concentration of 12µM and incubated for another 5 minutes at 37°C. The medium was discarded and the cells were rinsed twice with PBS. Samples were examined with a Zeiss inverted Axiovert CFL40 microscope and Zeiss Axiovert MRm monochrome camera (Zeiss, Göttingen, Germany). Zeiss Filter 2 was used for HO-stained cells (blue emission), Zeiss Filter 9 was used for AO-stained cells (green emission) and Zeiss filter 15 was used for PI-stained cells (red emission). In order to prevent fluorescent dye quenching; all procedures were performed with plates and reagents covered with foil.

2.4.3.2. Flow cytometry - cell cycle progression

The cell cycle is an essential functional parameter that can be used to assess cellular metabolism, physiology and pathology. This technique takes advantage of the different DNA concentrations found in cycling cells, which allows quantifying the distribution of cycling cells along the various phases of the cell cycle (G_0/G_1 , S, G_2 , and M) [195]. With flow cytometry, cell cycle distribution can be analyzed rapidly based on the DNA content of individual cells. Since PI binds stoichiometrically to DNA, and cells at different stages of their cell cycle will have different amounts of DNA, discrimination of these subpopulations of cells based on fluorescence intensity is possible. G_2/M phase cells have twice the amount of DNA of G_1 phase cells, and S phase cells possess variable amounts of DNA as they progress through S between G_1 and G_2 [195]. Because PI also stains double-stranded RNA, the latter is removed by the addition of RNase A to the staining solution [196]. Flow cytometry was used to identify the distribution of SNO cells during the various phases of the cell cycle after exposure to 2-MeOE2bisMATE. Four distinct phases can be recognized in a proliferating cell population: the G_1 , S (DNA synthesis phase), G_2 and M phase (mitosis). An increase in the number of cells in the sub- G_1 phase indicates the presence of apoptosis [197].

I. Materials

Propidium iodide and RNase A were bought from Sigma-Aldrich (Ltd) (Clubview, South Africa). Ethanol was purchased from Merck (Darmstadt, Germany).

II. Methods

SNO cells were seeded at 500 000 per 25cm² flask. Cells were incubated for a period of 24 hours to allow for attachment, subsequently, the medium was discarded and cells were exposed to 2-MeOE2bisMATE and appropriate controls were included as defined previously. After 24 hours of incubation, cells were trypsinized and resuspended in 1ml of growth medium. Cells with a density of 500 000 were centrifuged for 5 minutes at 300×g. The supernatant was discarded and cells were resuspended in 200µl of ice-cold PBS containing 0.1% FCS. In order to avoid cell clumping, 4ml of ice-cold 70% ethanol was added in a drop wise manner while vortexing. Samples were stored at 4°C for 24 hours and cells were subsequently pelleted by centrifuging at 300×g for 5 minutes. The supernatant was removed and the cells were resuspended in 1ml of PBS containing 40µg/ml PI and 100µg/ml RNase A. The solution was incubated for 45 minutes in an incubator (5% CO₂, 37°C). The fluorescence of PI (measuring relative DNA content per cell) was measured with a fluorescence activated cell sorting (FACS) FC500 System flow cytometer (Beckman Coulter South Africa (Pty) Ltd.) equipped with an air-cooled argon laser excited at 488nm. Data from no less than 30 000 cells were analyzed with CXP software (Beckman Coulter South Africa (Pty) Ltd). For accuracy, the data from cell debris and clumps of two or more cells were excluded from analysis. Cell cycle distributions were calculated with Cyflogic 1.2.1 (Perttu Terho & Cyflo Ltd) by assigning relative DNA content per cell to sub-G₁, G₁, S and G₂/M fractions. Data obtained from the fluorescence channel for red monomers (FL3 Lin) were represented as histograms on the x-axis.

2.4.3.3. Flow cytometry - apoptosis detecting study (annexin V-FITC)

Phosphatidylserine (PS) is a phospholipid which is predominantly located on the inner surface of the plasma membrane, facing the cytosol. Cells undergoing apoptosis lose their phospholipid asymmetry of the plasma membrane and expose PS by translocating it to the outer layer of the plasma membrane. This occurs in the early phases of apoptosis during which the cell membrane remains intact. Annexin V is a phospholipid-binding protein and it has been proven to be a useful tool in detecting apoptotic cells since it preferentially binds to negatively charged phospholipids like PS in the presence of calcium. By conjugating fluorescein isothiocyanate (FITC) to Annexin V it is possible to identify and quantify

apoptotic cells by flow cytometry [198-199]. The simultaneous staining with PI allows for adequate detection of necrotic cells among the annexin-V positive group of cells.

I. Materials

Annexin V- FITC kit was bought from BIOCOM biotech Pty (Ltd) (Clubview, South Africa).

II. Methods

Exponentially growing SNO cells were seeded at 500 000 cells per 25cm² flask. Cells were incubated for 24 hours to allow for attachment, the medium was discarded and the cells were exposed to either 2-MeOE2bisMATE or previously defined controls. After exposure, the cells were trypsinized, 500 000 cells were resuspended in 1ml of 1x Binding Buffer and then centrifuged at 300×g for 10 minutes. The supernatant was removed and the cells were resuspended in 100µl of the 1x Binding Buffer. Subsequently, 10µl of Annexin V-FITC was added and incubated for 15 minutes in the dark at room temperature. After incubation, cells were washed with 1ml of the 1x Binding Buffer and then centrifuged at 300×g for 10 minutes. The supernatant was carefully pipetted off and the cells were resuspended in 500µl of the 1x Binding Buffer solution. Prior to analysis, 12.5µl of the PI was added and mixed into the solution. PI fluorescence and annexin V-FITC fluorescence were measured with a FACS FC500 System flow cytometer (Beckman Coulter South Africa (Pty) Ltd) equipped with an air-cooled argon laser excited at 488nm. Data from at least 30 000 cells were analysed with CXP software(Beckman Coulter South Africa (Pty) Ltd. Information gained was analyzed using Cyflogic 1.2.1 software, data from fluorescence channel for green monomers (F11 Log) and fluorescence channel for red monomers (F13 Log) were represented as dot plots on the y- and x-axis, respectively.

2.4.3.4. Flow cytometry – mitocapture mitochondrial assay

One of the earliest intracellular events that occur following the induction of apoptosis is the disruption of the mitochondrial transmembrane potential. 5,5',6,6'tetrachloro-1,1',3,3'tetraethylbenzimidazolylcarbocyanine iodide is a fluorescent lipophilic cationic reagent that can be used to detect the loss of the mitochondrial membrane potential; therefore the mitotracker assay allows distinguishing between apoptotic

cells and viable cells based on changes in the mitochondrial membrane potential. In normal cells, the dye will concentrate in the mitochondrial matrix which will give off a bright red fluoresce colour, whereas in cells with a reduced mitochondrial membrane potential, such as apoptotic cells, the dye will remain in the cytoplasm and the cells will fluoresce a green colour [200].

I. Materials

MitoCapture™ Mitochondrial apoptosis detection kit was bought from BIOCOM biotech Pty (Ltd) (Clubview, South Africa).

II. Methods

Exponentially growing SNO cells were seeded at 500 000 cells per 25cm² flask. After 24 hours of attachment, the medium was discarded and cells were exposed to 2-MeOE2bisMATE. Cells were subsequently trypsinized and centrifuged at 13 000xg for 5 minutes. Cells (500 000 per 25cm²) were resuspended in 500µl of the diluted MitoCapture solution, then incubated for 20 minutes in an incubator (5% CO₂, 37°C) and centrifuged at 500xg. The supernatant was discarded, cells were resuspended in 500µl of pre-warmed incubation buffer and samples were analysed using a flow cytometer (fluorescence channel for green monomers (F11 Log) (Beckman Coulter South Africa (Pty) Ltd). Generated data was analysed with Cyflogic 1.2.1 software.

2.4.3.5. Spectrophotometry- caspase 6 & 8 calorimetric assays

Caspases are proteases which play a significant role in the apoptotic pathway. The activation of caspase 8, an intracellular cysteine protease, plays an essential role in death receptor mediated apoptosis. Once activated, caspase 8 cleaves Bid or activates effector caspase such as caspase 3 or caspase 6 [201].

I. Materials

Caspase 6 colorimetric and (FLICE)/Caspase 8 colorimetric kits were bought from BIOCOM biotech Pty (Ltd) (Clubview, South Africa). BCA protein assay was purchased from Thermo Scientific (Johannesburg, South Africa).

II. Methods

Caspase 6 & 8 calorimetric assays were conducted to observe whether or not 2-MeOE2bisMATE has an effect on the caspase 6 activity of SNO cells. Exponentially growing SNO cells were seeded at 1000 000 cells per 25cm² flask. After a 24 hours incubation period at 37°C, cells were exposed to 2-MeOE2bisMATE. Cells were trypsinized and then centrifuged at 3 000 rpm for 3 minutes. Pellets were then resuspended in 50 µl of cell lysis buffer and incubated on ice for 10 minutes. After incubation the cells were centrifuged at 14 000 rpm for 1 minute. After determining the protein concentration using the BCA protein assay (Thermo Scientific, Johannesburg, SA), the supernatant was transferred into 50µl of 2X reaction buffer containing 10mM dithiothreitol (DTT) and 5µl of 4mM VEID-*p*NA substrate (for caspase 6), IETD-*p*NA substrate (for caspase 8) was added to the supernatants, and the reaction mixtures were incubated at 37°C for 2 hours in the dark. The absorbances were determined at 405nm using an EL_x800 Universal Microplate Reader available from Bio-Tek Instruments Inc. (Vermont, United States of America).

2.4.3.6. Flow cytometry - autophagy detection: anti-LC3B

Autophagy is a process where cytoplasmic materials are degraded through the lysosomal machinery and it is a form of programmed cell death. The LC3 antibody detection method was utilized to determine whether 2-MeOE2bisMATE induces autophagy in SNO cells. LC3 is a soluble protein that is found in mammalian tissues and in cultured cells. LC3 exists in two forms, LC3-I and its proteolytic derivative LC3-II. LC3-I is located in the cytoplasm whereas LC3-II binds to autophagosomes. The induction of autophagy stimulates the conversion of LC3-I to LC3-II and the upregulation of LC3 expression. Therefore, lysosomal turnover of the autophagosomal marker LC3-II reveals autophagic activity. Identification of LC3 by immunofluorescence is a reliable method for monitoring autophagy [202].

I. Materials

Formaldehyde, methanol, triton-X100, propidium iodide and bovine serum albumin (BSA) were purchased from Sigma-Aldrich (Ltd) (Clubview, South Africa). Rabbit polyclonal anti-LC3B conjugated to DyLight 488 was purchased from BIOCROM biotech Pty (Ltd) (Clubview, South Africa).

II. Methods

Exponentially growing SNO cells were seeded at 500 000 cells per 25cm² flask. After 24 hours of attachment, the medium was discarded and the cells were exposed to 2-MeOE2bisMATE. After incubation the cells were trypsinized and washed with cold PBS. Cells were fixed with 0.01% formaldehyde in PBS for 10 minutes, pelleted and then resuspended in 200µl PBS. To further fix and permeabilize the cells, 1ml of ice-cold methanol (-20°C) was added to the solution in a dropwise manner. Cells were then pelleted and washed twice with cold PBS. After washing, the cells were pelleted and 0.5ml of the primary antibody cocktail was added and then incubated for 2 hours at 4°C in the dark. Following 2 hours of incubation, the cells were washed trice with a wash buffer (PBS/0.05% Triton/1%BSA) and then analyzed with CXP software (Beckman Coulter South Africa (Pty) Ltd). Data was analyzed using Cyflogic 1.2.1 software; data from fluorescence channel for green monomers (FL1 Log) was represented as histogram on the x-axis.

2.4.3.7. Flow cytometry - cyto-ID autophagy detection assay

Cyto-ID Autophagy Detection Kit measures autophagic vacuoles using a novel dye that selectively labels autophagic vacuoles. This method allows for staining of pre-autophagosomes, autophagosomes, and autolysosome, thus offering a rapid and quantitative approach for detecting autophagy [203].

I. Materials

Cyto-ID Green autophagy detection assay kit was purchased from BIOCOM biotech Pty (Ltd) (Clubview, South Africa).

II. Methods

SNO cells were seeded into 25cm² flasks at a density of 500 000 each. After 24 hours of attachment, the cells were exposed to 2-MeOE2bisMATE and to appropriate controls for 24 hours. Following compound treatment, the cells were washed once in PBS and resuspended in a dilution of Cyto-ID Green autophagy detection reagent and incubated at room temperature for 30 minutes. Thereafter, the cells were analyzed using CXP software

(Beckman Coulter South Africa (Pty) Ltd). Cyto-ID Green autophagy reagent was measured in the fluorescent channel (F11 Log) using Cyflogic 1.2.1 software.

2.5. Logistics

Experiments were conducted in the cell culture laboratory of the Department of Physiology at the University of Pretoria. All techniques defined were standardized at the Department of Physiology at the University of Pretoria. Transmission electron microscope and confocal microscope were performed at the Electron Microscopy Unit of the University of Pretoria. Flow cytometry was conducted at the Department of Pharmacology (University of Pretoria).

2.6. Statistical analysis

Cell number and viability determination, cell cycle progression analysis, the apoptosis detection assay (annexin V-FITC, caspase 6 & 8 calorimetric assays), mitocapture mitochondrial assay and autophagy detection analysis (anti-LC3B & cyto-ID) assays were analyzed quantitatively. PlasDIC, TEM, α -tubulin assay and triple staining were analyzed qualitatively. Haematoxylin and eosin staining results were analyzed both quantitatively (mitotic indices) and qualitatively. The ANOVA students' *t*-test was used to determine the analytical variation in experimental procedures and biological variations within each experiment. A *P*-value of <0.05 was regarded as statistically significant. Means are presented in bar charts, with T-bars referring to standard deviations. For flow cytometric data no less than 30 000 events were counted for each sample and three independent experiments were conducted and data produced was analysed using Cyflogic 1.2.1 (Perttu Terho & Cyflo Ltd).

Chapter 3

Results

3.1. Cell number and viability assays

3.1.1. Crystal violet staining

The crystal violet assay is a method that is used to spectrophotometrically determine the number of cells in a specific sample by measuring the dye uptake by the DNA. This assay was conducted to determine the effects of 2-MeOE2bisMATE on the proliferation of SNO cells. Cell numbers were expressed as a percent of cells relative to the control (cells propagated in growth medium).

Cells exposed to 0.2-1µM of 2-MeOE2bisMATE for 24, 48 and 72 hours were compared to the cells propagated in growth medium and the vehicle-treated cells. Concentrations and times of exposure were selected based on previous studies which proved that it is within this range that 2-MeOE2bisMATE is most efficient as an antiproliferative agent [179, 186]. The 50% growth inhibitory (GI₅₀) effect of 2-MeOE2bisMATE on SNO cells was calculated according to the National Cancer Institute [204]. GI₅₀ is the concentration of test drug that inhibits the growth of cells by 50%. The following equation was used:

$$100 \times (T - T_0) / (C - T_0) = 50$$

T is the optical density of the test well after the 24, 48 or 72 hour drug exposure; T₀ is the optical density at time zero and C is the control optical density.

From growth studies results it is clear that 2-MeOE2bisMATE inhibits the growth of SNO cells after 24 hours. Although inhibition of cell growth is present in concentrations lower than 0.4µM of the 2-MeOE2bisMATE, the degree of inhibition is not statistically significant (Figure 3.1). A statistically significant reduction in cell growth by 74% was observed in cells exposed to 0.4µM 2-MeOE2bisMATE (*P*-value <0.05). Cells treated with 0.5µM and 0.6µM of 2-MeOE2bisMATE respectively demonstrated a slight decrease in cell growth, while those treated with 0.7-1µM of 2-MeOE2bisMATE decreased cell growth to approximately the

same extend as those that were treated with 0.4 μ M of 2-MeOE2bisMATE (Figure 3.1). The concentration of 0.4 μ M of 2-MeOE2bisMATE revealed a significant growth inhibition of 40% in SNO cells after 24 hours of exposure (Figure 3.2).

Compared with vehicle treated cells, the proliferation of SNO cells was greatly affected after 48 and 72 hours of exposure with 2-MeOE2bisMATE. 0.4 μ M of 2-MeOE2bisMATE inhibited cell proliferation by 36.5% and 35% in SNO cells after 48 and 72 hours, respectively (Figure 3.3 and Figure 3.5). The growth-inhibitory action of 2-MeOE2bisMATE was dose-dependent within the range examined. 2-MeOE2bisMATE (0.4 μ M) resulted in growth inhibition of 4% in SNO cells after 48 and 72 hours (Figure 3.4 & Figure 3.6).

A concentration of 0.4 μ M of 2-MeOE2bisMATE and an exposure time of 24 hours were selected as the optimal time and dose, given that these conditions significantly inhibited cell growth (Figure 3.1 & Figure 3.2). Hence, all succeeding studies were conducted using 0.4 μ M of 2-MeOE2bisMATE with an exposure period of 24 hours.

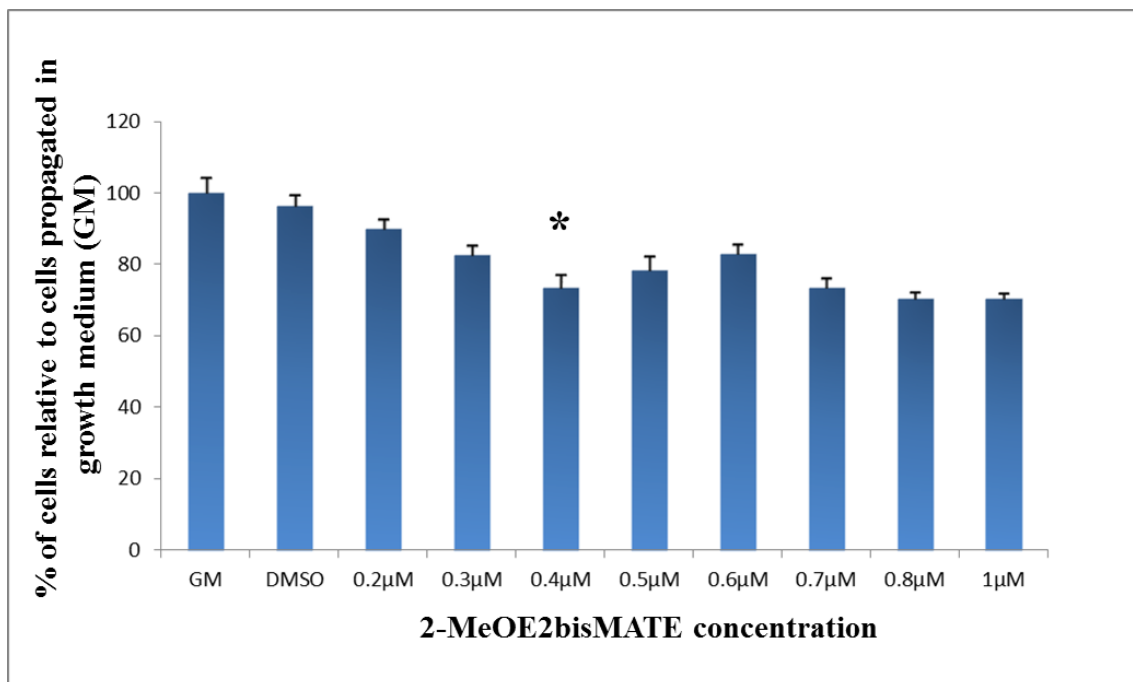


Figure 3.1. SNO cell numbers expressed as a % of cells relative to the growth medium (GM) control (cells propagated in growth medium only) after being exposed to 2-MeOE2bisMATE (0.2-1µM) and vehicle (DMSO) for 24 hours. A significant inhibition of cell growth was observed after a 24 hours exposure period to 0.4µM 2-MeOE2bisMATE (74%). An * indicates a *P*-value < 0.05. Bar indicates SD.

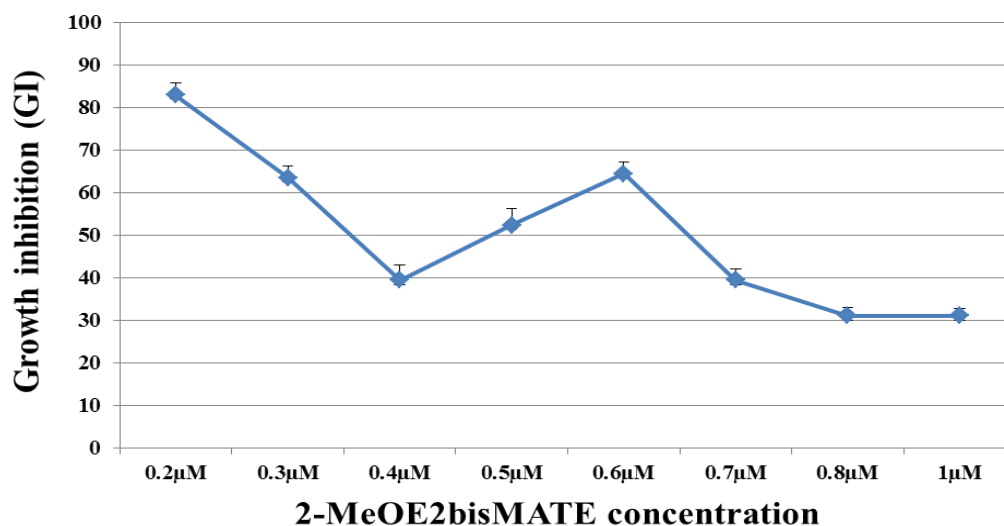


Figure 3.2. Growth inhibitory effects of 2-MeOE2bisMATE (0.2-1µM) on SNO cells after 24 hours of exposure. GI of 40% was observed at 0.4 µM of 2-MeOE2bisMATE.

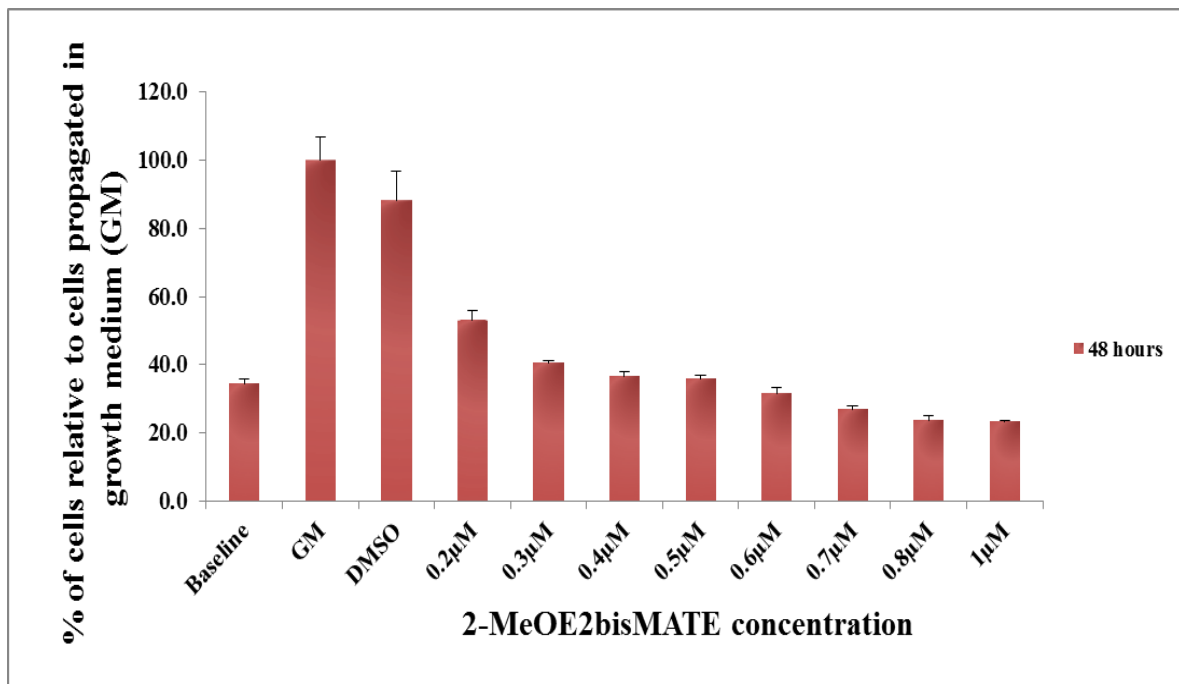


Figure 3.3. Effects of 2-MeOE2bisMATE (0.2-1.0µM) on the proliferation of SNO cell after 48 hours of exposure. Cell numbers were expressed as a % of cells relative to the growth medium (GM) control (cells propagated in growth medium only). 2-MeOE2bisMATE significantly decreased the proliferation of SNO cells. Bar indicates SD.

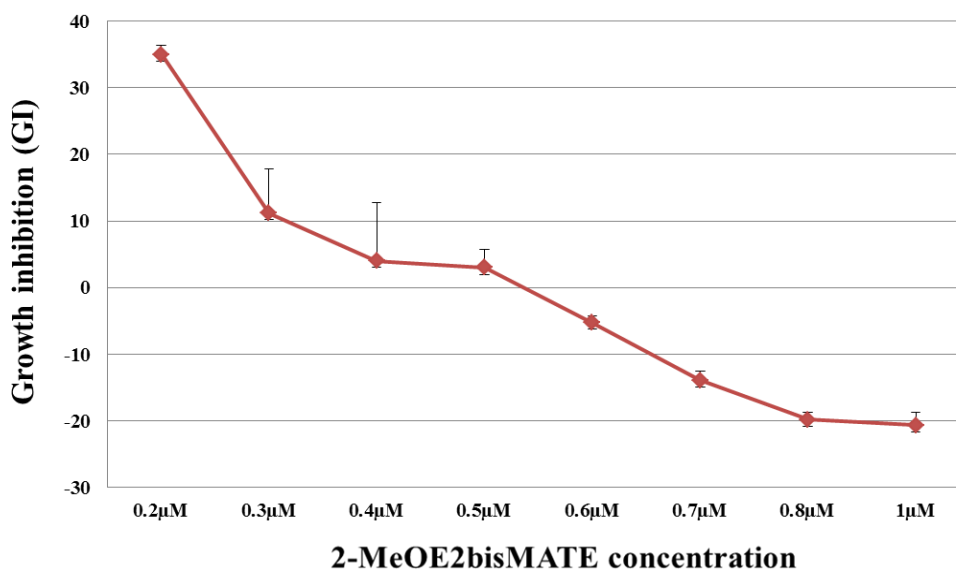


Figure 3.4. Growth inhibitory effects of 0.2-1µM of 2-MeOE2bisMATE on SNO cells after 48 hours of exposure. There was a drastic decline in the GI values of SNO cells treated with 2-MeOE2bisMATE.

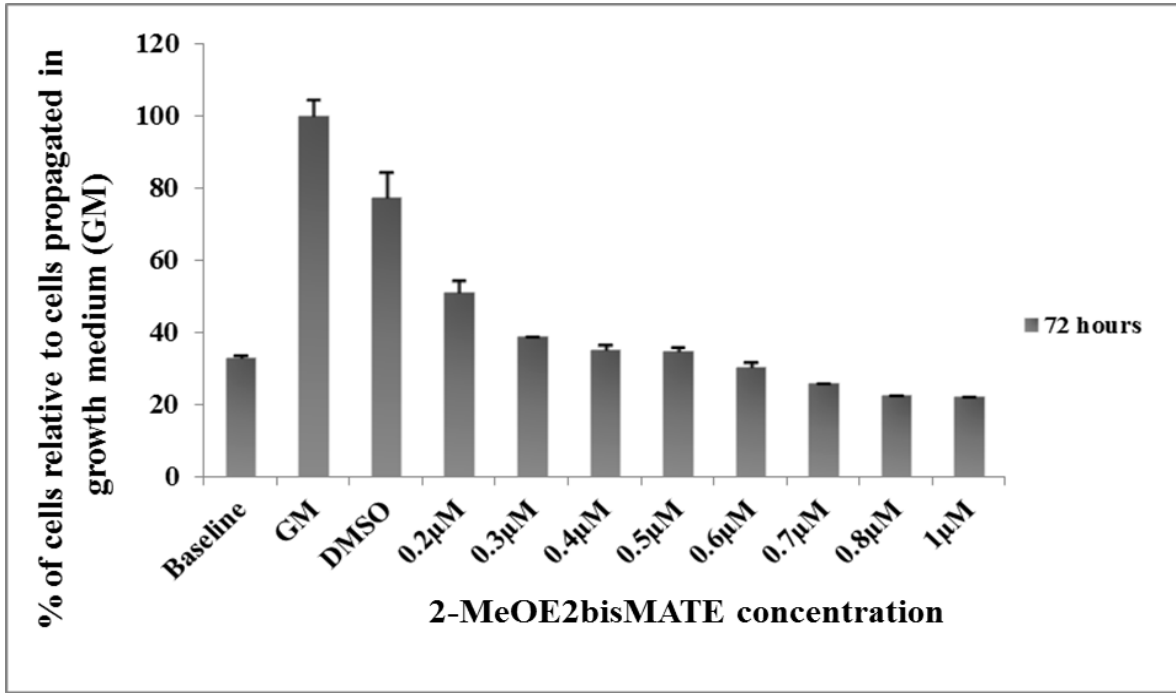


Figure 3.5. Crystal violet staining results following 72 hours of exposure of the 2-MeOE2bisMATE to SNO cell line. 2-MeOE2bisMATE treatment resulted in decreased cell numbers. Bar indicates SD.

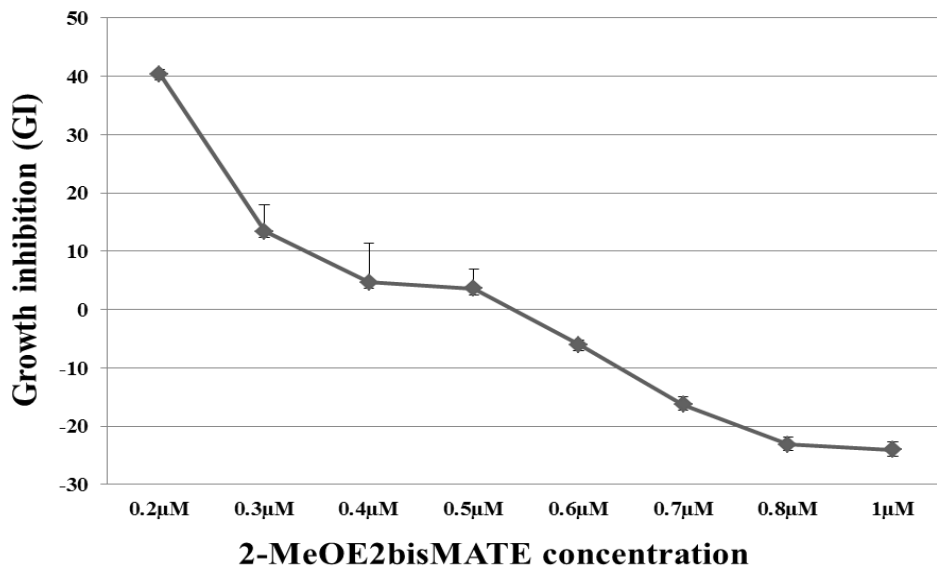


Figure 3.6. Growth inhibitory values of SNO cells after 72 hours of exposure. 2-MeOE2bisMATE caused a significant decline in GI values of SNO cells.

3.1.2. Lactate dehydrogenase assay

Intracellular LDH release, as a result of plasma membrane damage was evaluated as it is a commonly used method for testing of cell membrane integrity and as measurement of the cytotoxicity of a drug. The LDH released in the culture medium was measured by means of spectrophotometry. The low and high controls were included as specified in the manufacturer's instructions. The low control refers to cells propagated in growth medium only, while the high control refers to cells propagated in growth medium with cell lysis solution added to the cells 15 minutes prior to termination. The results of LDH release by SNO cells after 24 hours of exposure to 0.4 μ M of 2-MeOE2bisMATE demonstrated that there was a slight increase (statistically insignificant) in the LDH released compared to the vehicle-treated cells. Therefore, 2-MeOE2bisMATE was not cytotoxic to the cells. LDH activity was represented by the absorbance at 450 nm with a reference absorbance of 630 nm.

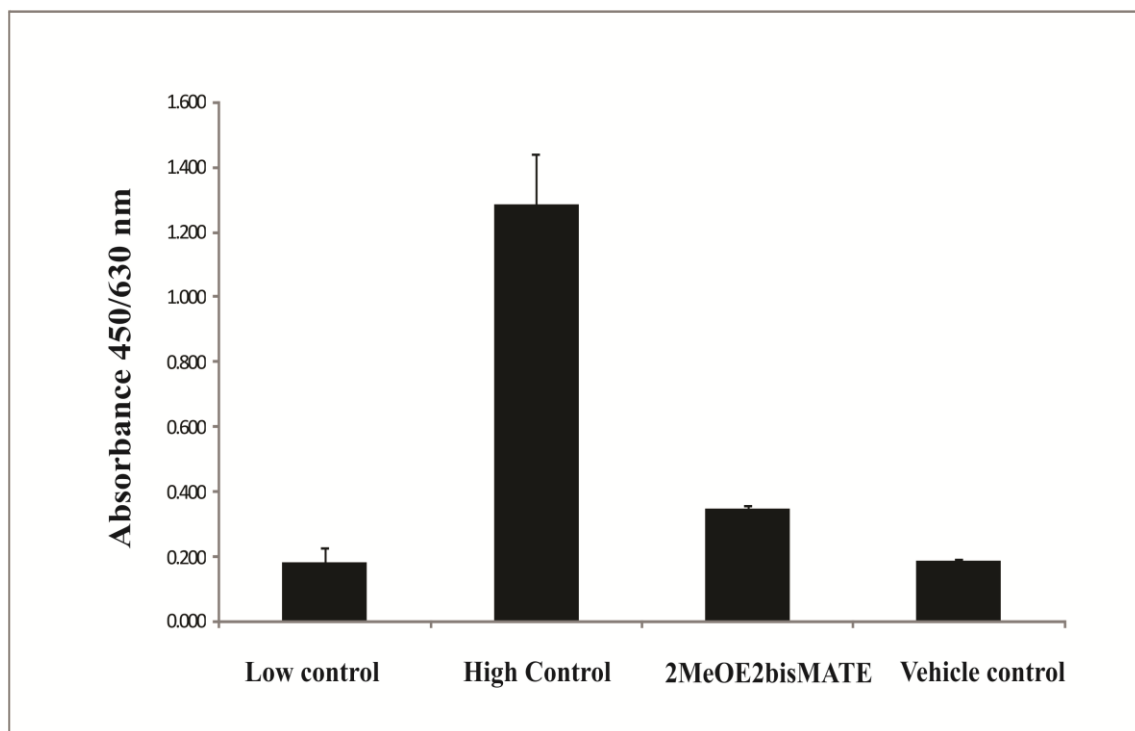


Figure 3.7. Analysis of LDH release in SNO cells treated with vehicle or 2-MeOE2bisMATE after 24 hours of exposure. There was a statistically insignificant LDH that was released by the 2-MeOE2bisMATE-treated cells compared to the vehicle-treated cells.

3.2. Morphology studies

3.2.1. Polarization-optical differential interference contrast

PlasDIC was used to visualize the effect of 0.4 μ M of 2-MeOE2bisMATE on the morphology of SNO cells after 24 hours of exposure. Following treatment, significant morphological and density alterations were noticeable in 2-MeOE2bisMATE-treated-SNO cells when compared to cells propagated in growth medium and to vehicle-treated cells (Figure 3.8 A&B & Figure 3.9A). Features of apoptosis (shrunken cells, membrane blebbing and apoptotic bodies) and cells blocked in metaphase were observed in 2-MeOE2bisMATE-treated-SNO cells (Figure 3.9A).

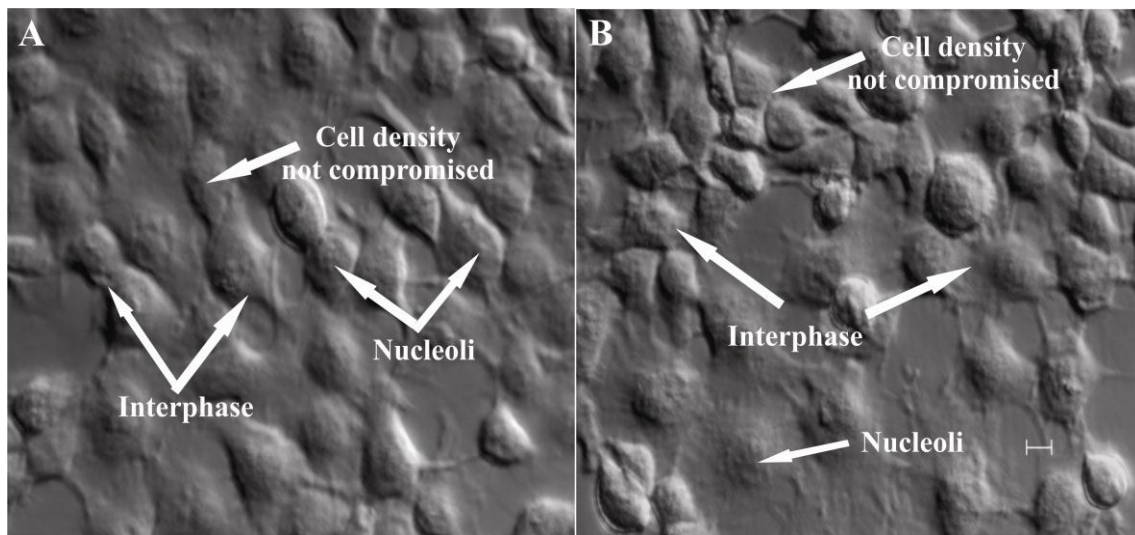


Figure 3.8. PlasDIC images of SNO cells propagated in growth medium (A) and vehicle-treated control (B) after an exposure period of 24 hours. Many cells were in interphase and cell density was not compromised (scale bar indicates 10 μ m).

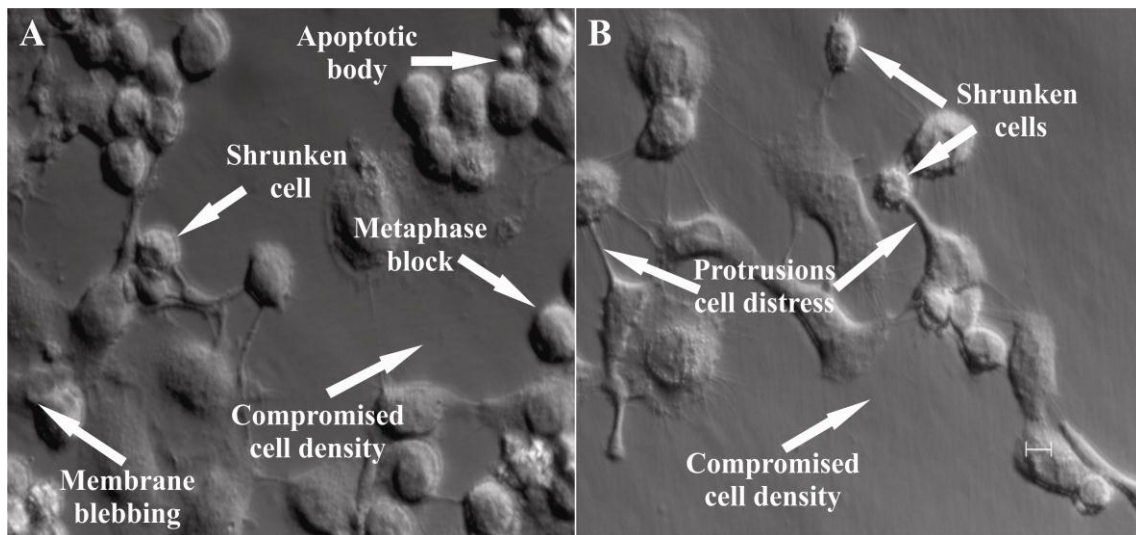


Figure 3.9. PlasDIC images of SNO cells 0.4 μ M 2-MeOE2bisMATE-treated cells (A) and actinomycin D-treated cells (B) after an exposure period of 24 hours. SNO cells treated with 2-MeOE2bisMATE revealed cells blocked in metaphase (round cells), as well as the presence of apoptotic bodies.

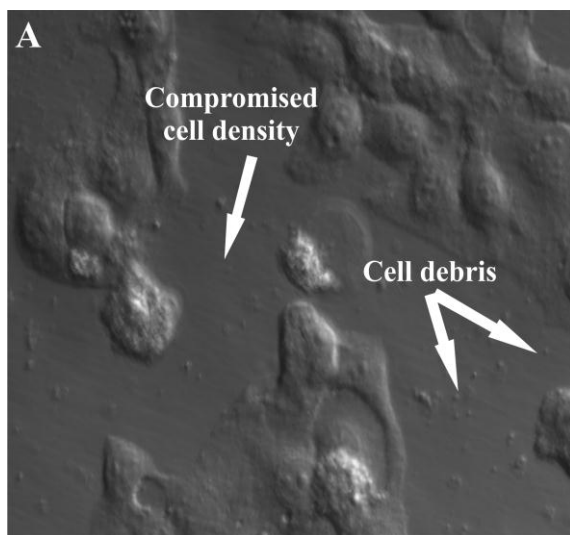


Figure 3.10. PlasDIC image of SNO cells with induced starvation (A) after 24 hours of exposure. Decreased cell density as well as cellular debris was observed.

3.2.2. Light microscopy - haematoxylin & eosin staining

Haematoxylin and eosin cell staining were conducted in order to reveal the morphological changes of the nuclear and cytoplasmic components of the SNO cells after 24 hours of exposure to 0.4 μ M of 2-MeOE2bisMATE (Figure 3.12 and Figure 3.14) by means of a light microscopy. After exposure to 2-MeOE2bisMATE, cells revealed apoptotic features namely

shrunken cells, hypercondensed chromatin, membrane blebbing and presence of apoptotic bodies. A large number of cells were also blocked in metaphase (Figure 3.12 and Figure 3.14) and the number of cells was decreased. The SNO control showed interphase cells and normal cell division including a cell in telophase after 24 hours of exposure (Figure 3.11 and Figure 3.13).

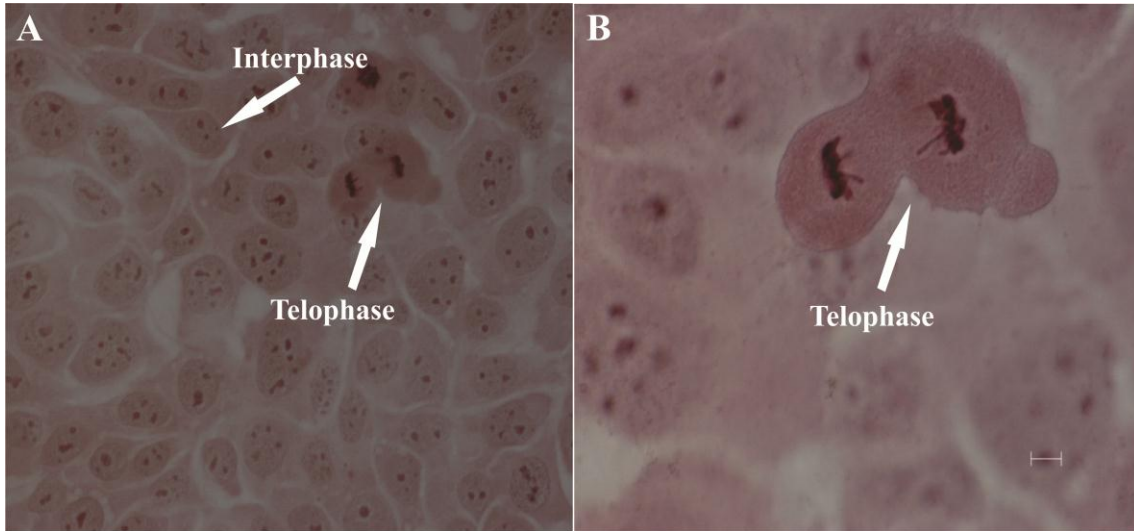


Figure 3.11. Haematoxylin and eosin staining of SNO cells propagated in growth medium after 24 hours at 40x (A), and 100x magnification (B). Cells showed normal cell division including a cell in telophase. Interphase cells as well as a dense population were also observed. Scale bar indicates 10 μ m.

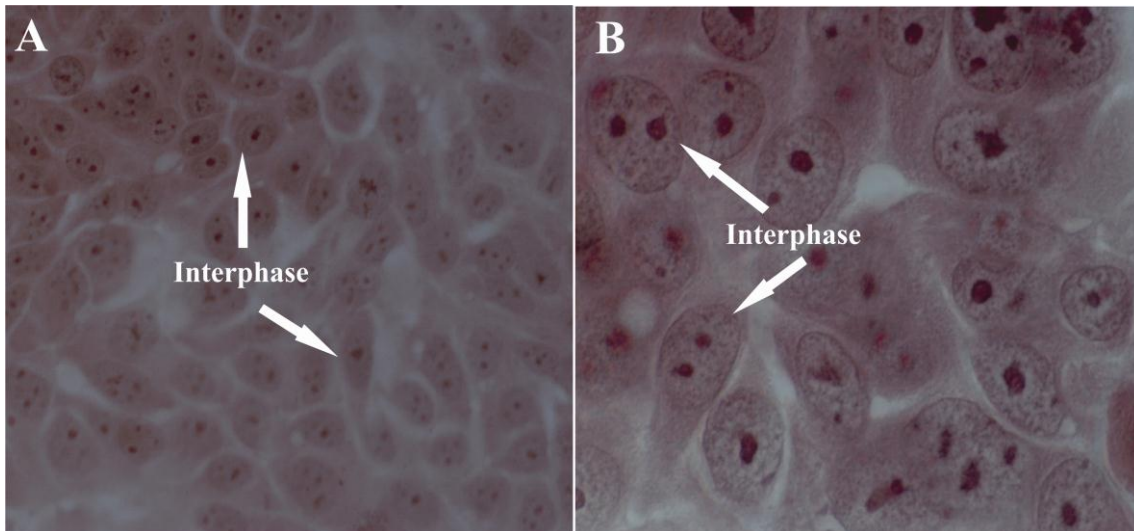


Figure 3.12. Haematoxylin and eosin staining of vehicle-treated cells after 24 hours of exposure at 40x (A), and 100x magnification (B). Results revealed cells in interphase and a dense population.

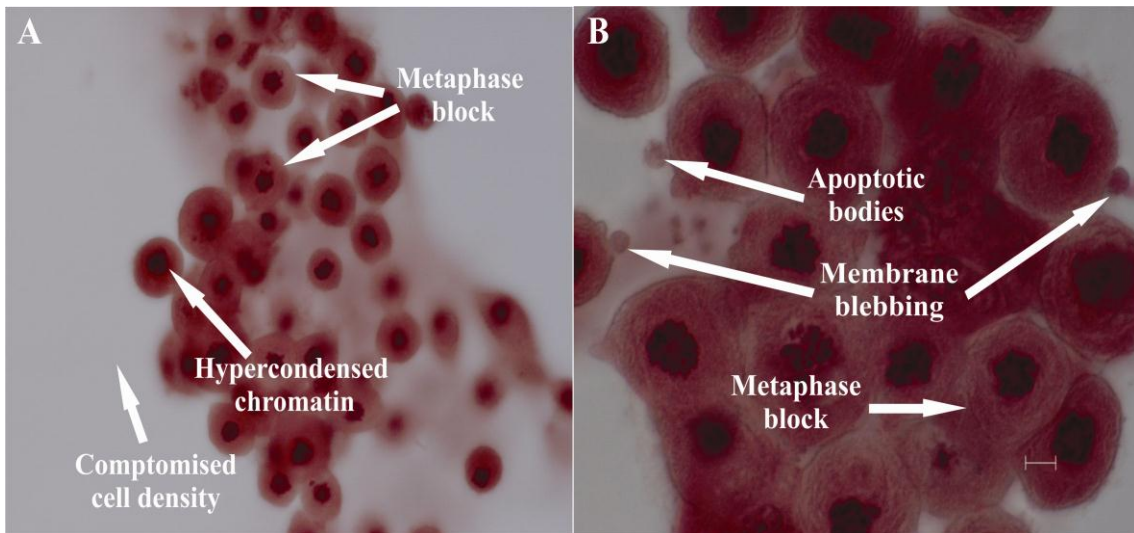


Figure 3.13. Haematoxylin and eosin staining of SNO cells exposed to $0.4\mu\text{M}$ 2-MeOE2bisMATE at 40x (A) and 100x magnification (B) following 24 hours of exposure. Significant numbers of rounded cells, chromatin condensation and presence of apoptotic bodies were seen after treatment with 2-MeOE2bisMATE. The density of the cells was also compromised.

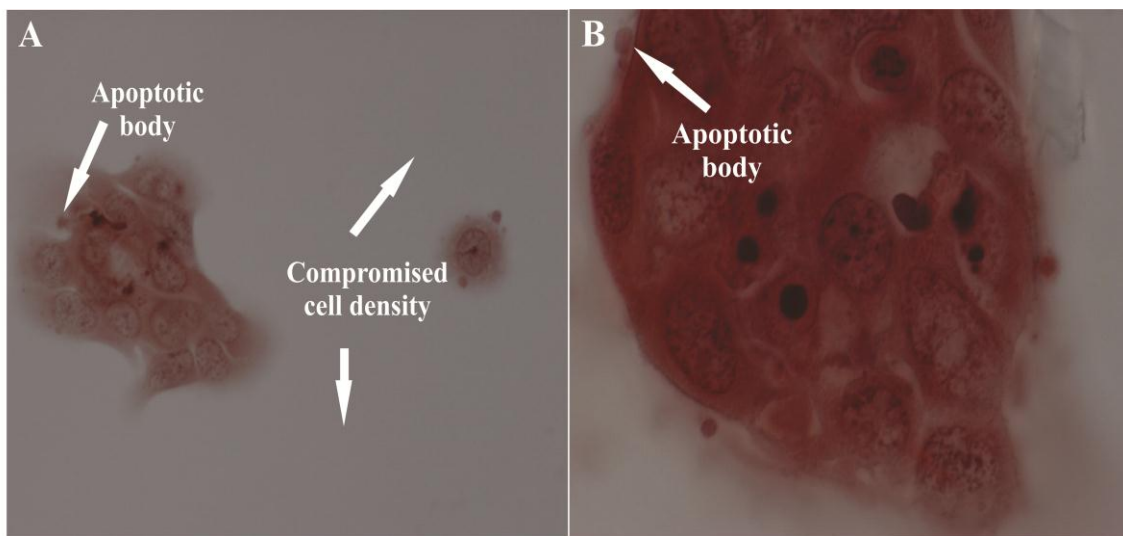


Figure 3.14. Haematoxylin and eosin staining of actinomycin D-treated cells at 40x (A) and 100x (B) after 24 hours of treatment. (Magnification: 100x, scale bar indicates $10\mu\text{m}$). Actinomycin D-treated-SNO cells showed the presence of apoptotic bodies and a compromised cell density.

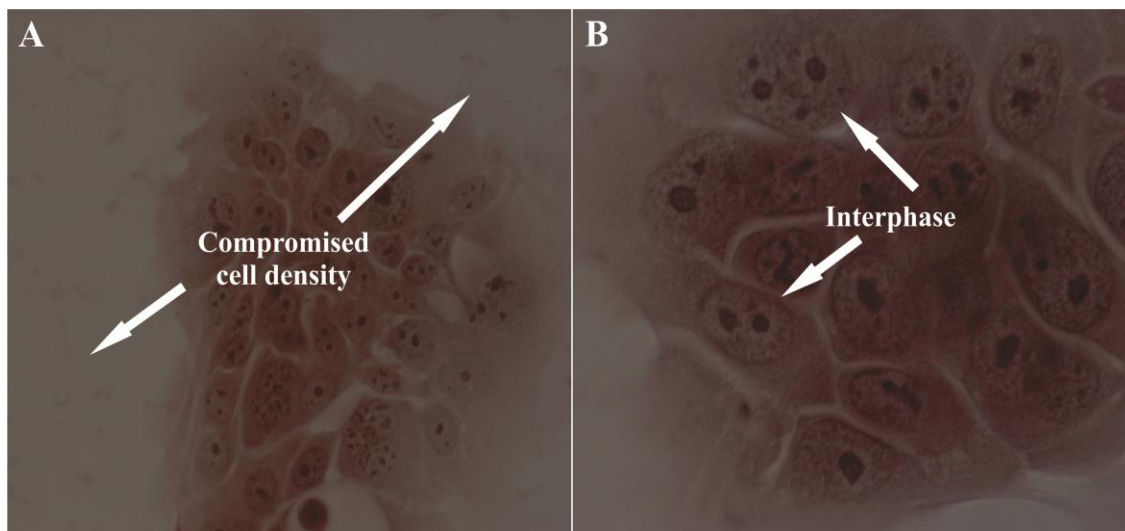


Figure 3.15. Haematoxylin and eosin staining of starved cells at 40x (A) and 100x (B) following 24 hours of treatment. Cells showed a compromised cell density.

3.2.3. Transmission electron microscopy

TEM was conducted in order to determine the influence of 2-MeOE2bisMATE on cell morphology. Results showed an increase in the presence of apoptotic bodies and autophagy vacuoles (autophagosomes) in SNO cells that were exposed to 0.4 μ M of 2-MeOE2bisMATE when compared to vehicle-treated SNO cells (Figure 3.16 & Figure 3.17). 2-MeOE2bisMATE-treated cells had increased cell membrane processes (indicative of cellular stress) and were shrunken in size.

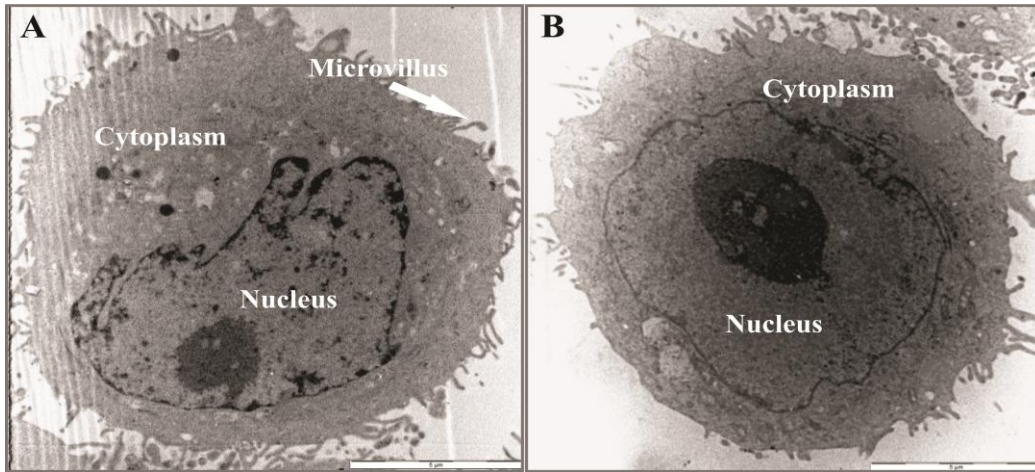


Figure 3.16. Transmission electron microscopy (TEM; images 6000x magnification) of SNO cells propagated in growth medium (A) and vehicle-treated control (B) following 24 hours of exposure. Cells showed no sign of distress.

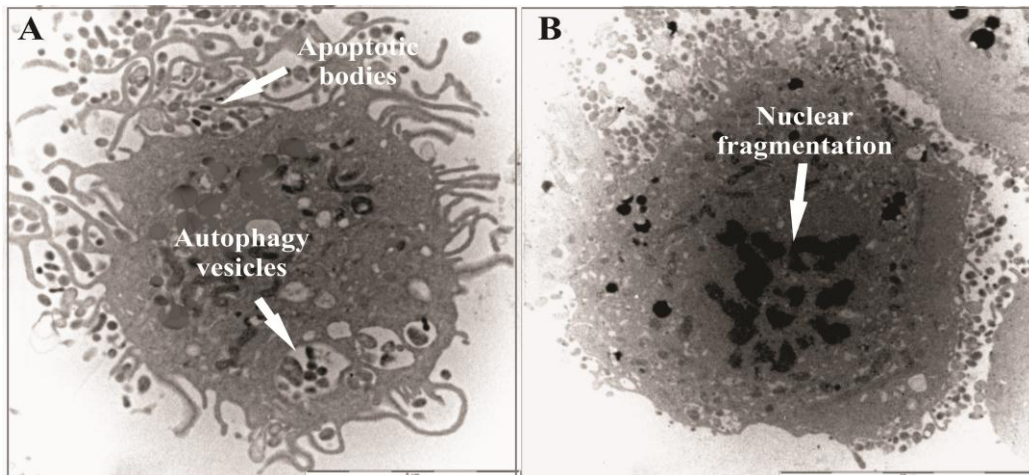


Figure 3.17. Transmission electron microscopy images (6000x magnification) of SNO cells treated with 0.4 μ M 2-MeOE2bisMATE (A&B) after 24 hours of exposure. 2-MeOE2bisMATE exposed cells revealed significant changes with the characteristics of apoptosis (condensed or fragmented nuclei, apoptotic bodies) and autophagy (autophagosomes) being observed.

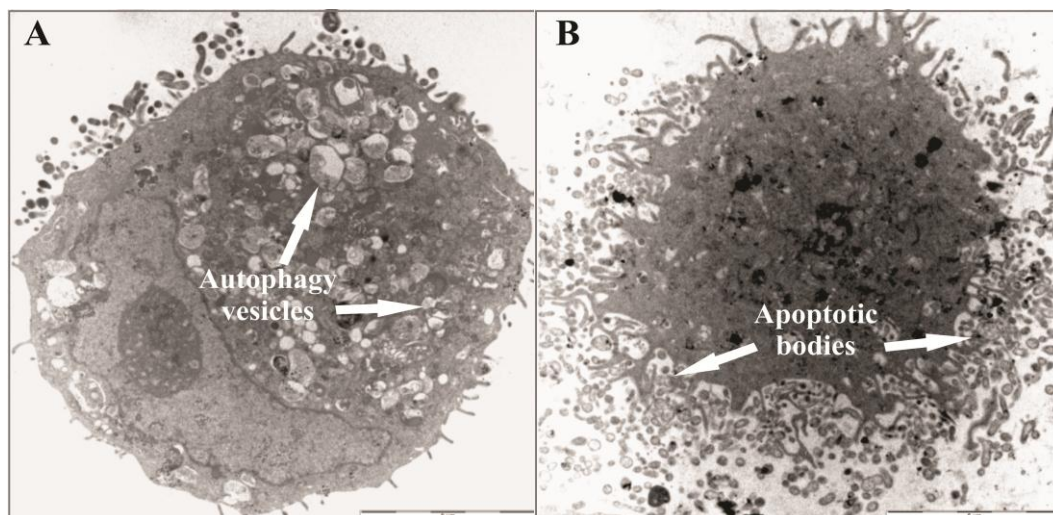


Figure 3.18. Transmission electron microscopy images (6000x magnification) of tamoxifen-treated (A) and actinomycin D-treated cells (B) after 24 hours of treatment. Features of autophagy and apoptosis were observed respectively.

3.2.4. Confocal-alpha (α)-tubulin assay

To determine whether the observed antitumour effect of 0.4 μ M 2-MeOE2bisMATE on SNO cells may be a consequence of alterations in microtubule structure, the morphology of tubulin networks were examined by immunofluorescence staining using an antibody against α -tubulin. The vehicle-treated cells and cells propagated in the growth medium showed intact and well-extended microtubules (Figure 3.19A & B); whereas 2-MeOE2bisMATE treated cells showed complete loss of microtubule network (Figure 3.20).

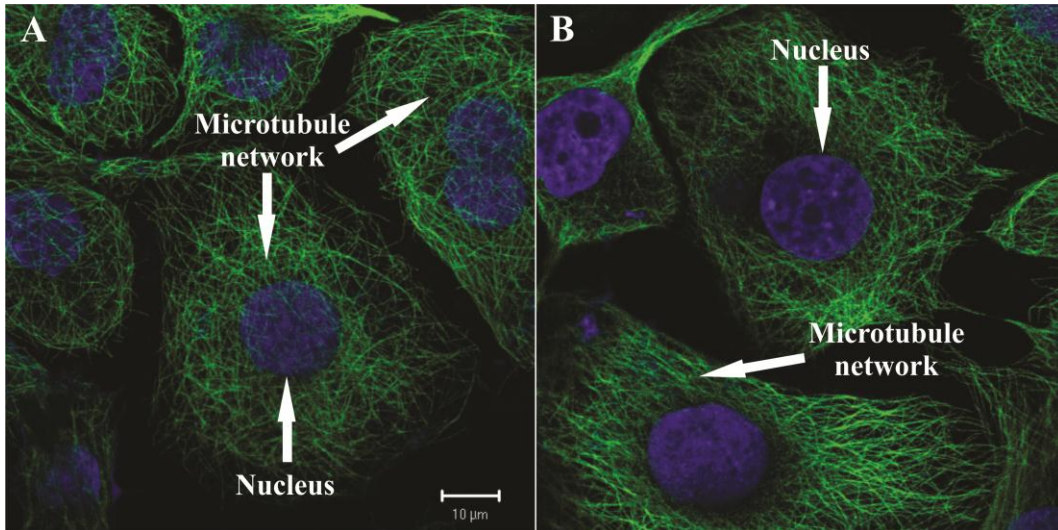


Figure 3.19. Immunofluorescence with anti- α -tubulin antibodies and DAPI in cells propagated in growth medium (A) and in vehicle (B) after exposure for a period of 24 hours. Vehicle-treated cells and cells propagated in the growth medium showed intact and intact microtubules (scale bar indicates 10 μ m).

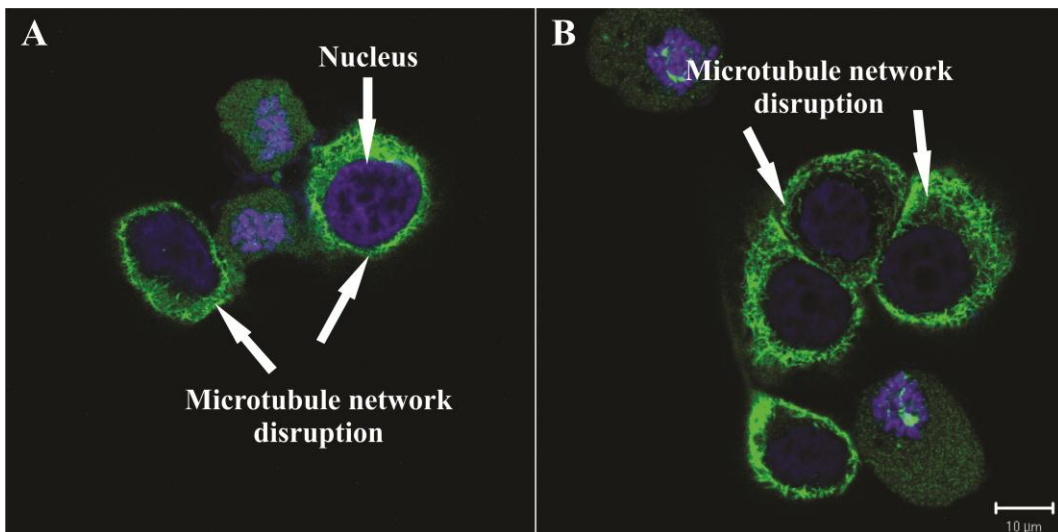


Figure 3.20. Immunofluorescence with anti- α -tubulin antibodies and DAPI in cells treated with 0.4 μ M 2-MeOE2bisMATE. 2-MeOE2bisMATE-treated cells revealed a complete loss of microtubule network (scale bar indicates 10 μ m).

3.3. Determination of possible types of cell deaths induced

3.3.1. Fluorescent microscopy - triple staining technique

Triple staining was used to distinguish between viable, apoptotic, autophagic and necrotic/oncotic cells after 24 hours of exposure to 0.4 μ M 2-MeOE2bisMATE. AO stains lysosomes and vacuoles of cells green, therefore undergoing autophagy will have increased tendency for AO when compared to viable cells. HO is a fluorescent dye that can penetrate intact cell membranes of viable cells and cells undergoing apoptosis and stains the nucleus blue. PI stains cells with compromised membrane integrity (necrotic/oncotic processes) and provides a red fluorescence. Results showed an increased tendency for AO in both 2-MeOE2bisMATE-treated SNO cells and starved cells (Figure 3.22A, Figure 3.23A) when compared to the vehicle control (Figure 3.21). Features of apoptosis such as the presence of apoptotic bodies were observed in both 2-MeOE2bisMATE-treated and actinomycin D-treated cells.

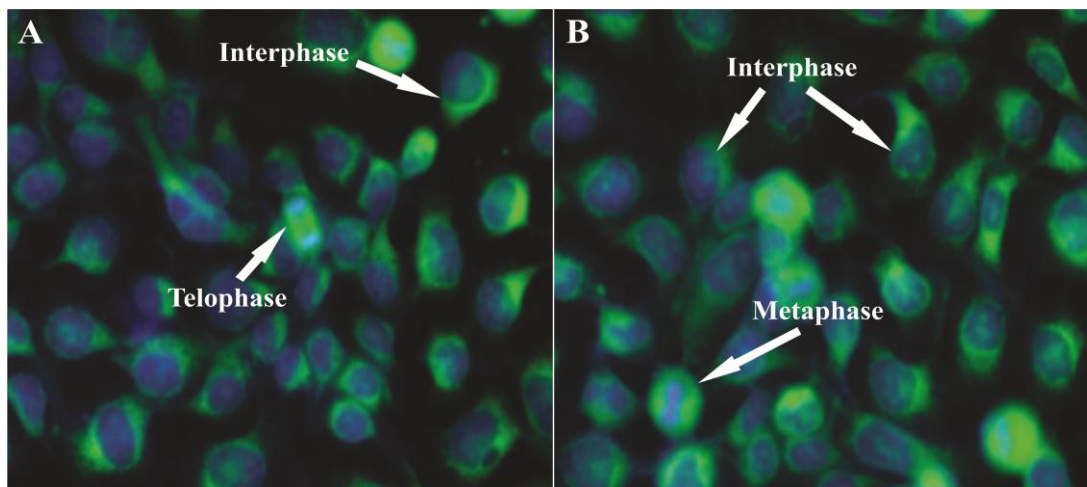


Figure 3.21. Triple-stained SNO cells propagated in growth medium (A), and vehicle-treated control cells (B). Cells were confluent and showed normal cell division including a cell in telophase and in metaphase.

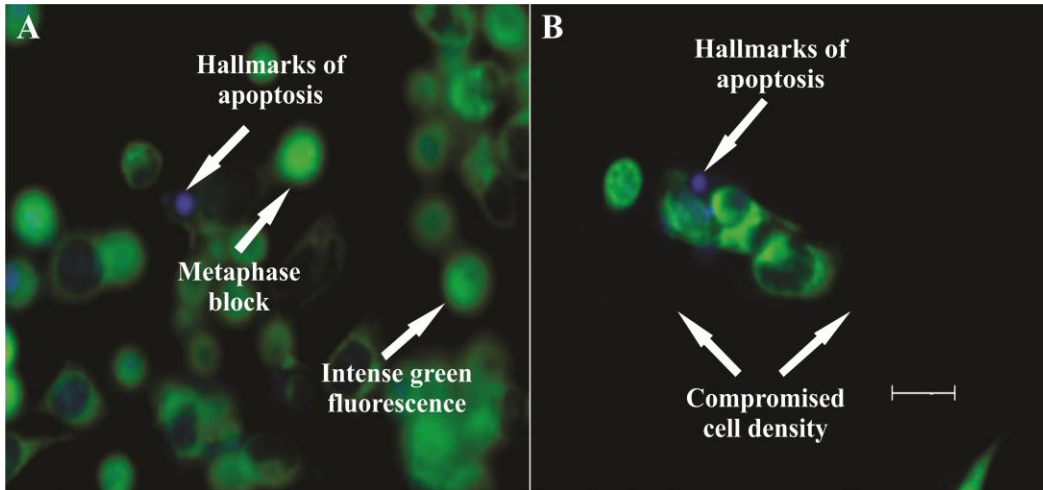


Figure 3.22. Triple-stained images of 0.4µM 2-MeOE2bisMATE-treated cells (A) and actinomycin D-treated cells (B). The latter served as a positive control for apoptosis. 2-MeOE2bisMATE-SNO-treated cells revealed an extensive green fluorescence suggesting autophagy was induced by 2-MeOE2bisMATE. 2-MeOE2bisMATE-treated cells were rounded in appearance due to a metaphase block and showed hallmarks of apoptosis (magnification 400x, scale bar indicates 10 µm).

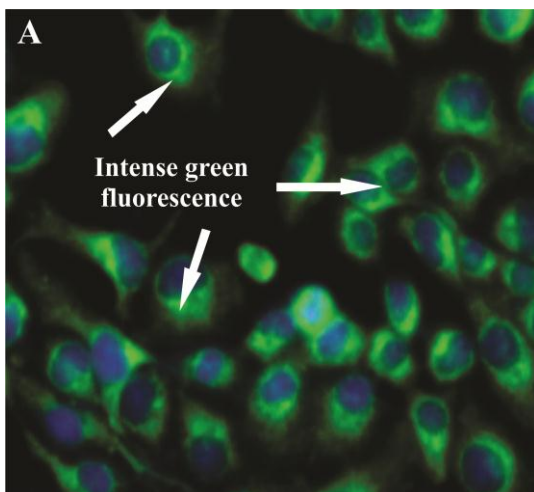


Figure 3.23. Triple-stained images of starved cells (A). The latter served as a positive control for autophagy. Intense green staining was observed in these cells.

3.3.2. Flow cytometry - cell cycle progression

Flow cytometry was used to analyze the effects of 2-MeOE2bisMATE on cell cycle progression. DNA content analyses showed a statistically significant increase in the number of cells in the G₂/M phase (76%) and those in sub-G₁ phase (4%) when compared to vehicle-

treated cells present in G₂/M (26%) and sub-G₁ (0.6%) (Figure 3.24 and Figure 3.25). The increase in G₂/M and sub-G₁ indicates metaphase block and the presence of apoptosis, respectively. These flow cytometry results suggest that 2-MeOE2bisMATE inhibits the growth of SNO cells *in vitro* by mechanisms involving G₂/M cell cycle arrest and apoptosis.

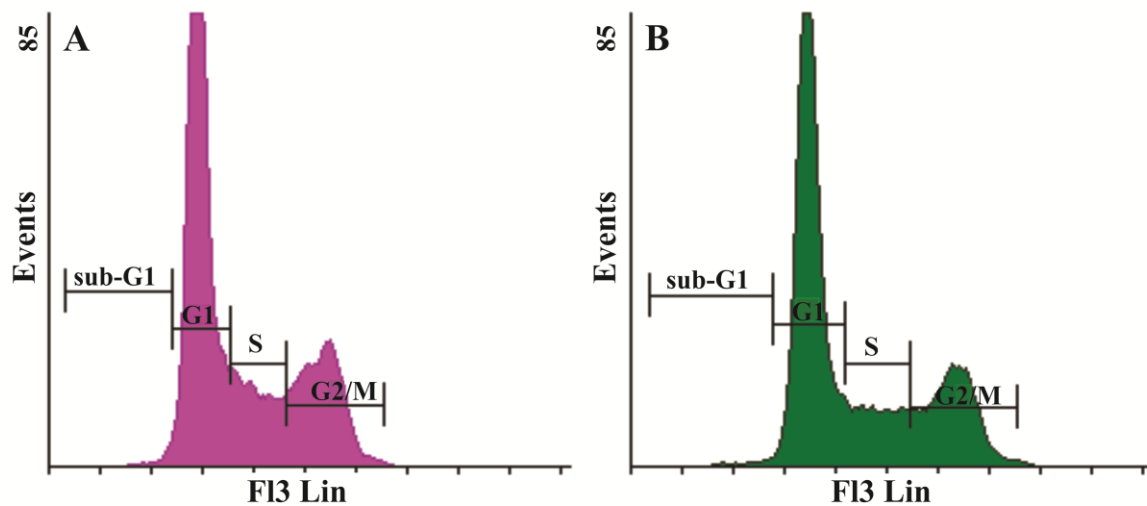


Figure 3.24. Cell cycle distribution histograms of cells propagated in growth medium (A) and of vehicle-treated cells (B) after 24 hours. The % of cells in sub-G₁, G₁, S and G₂/M phase of the cell cycle are displayed.

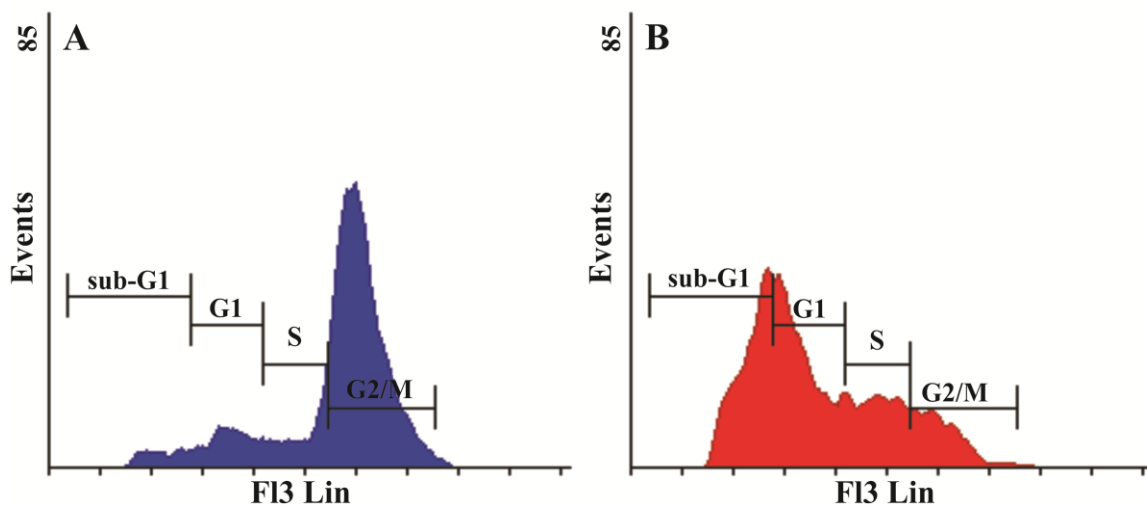


Figure 3.25. Cell cycle distribution histograms following 24 hours exposure to 0.4µM 2-MeOE2bisMATE (A) and actinomycin D (B). A statistically significant increase in the number of cells in G₂/M and sub-G₁ were observed in 2-MeOE2bis-MATE treated cells when compared to vehicle-treated cells.

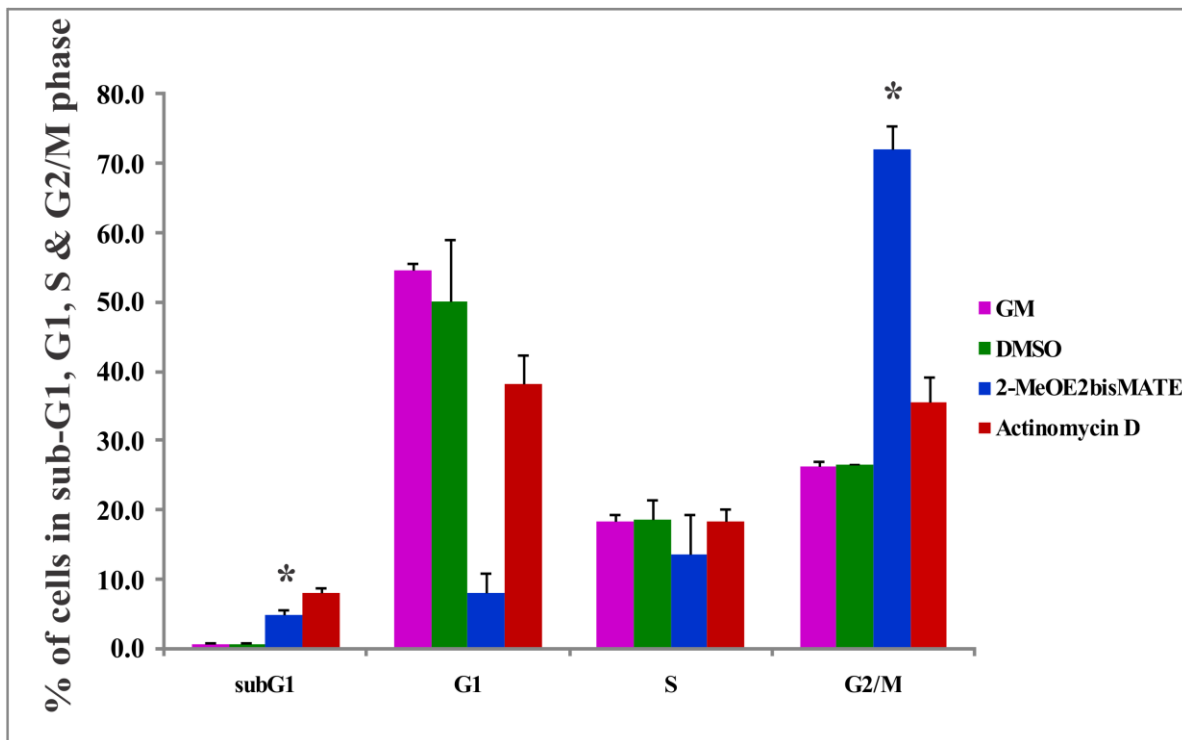


Figure 3.26. Percentage of cells in sub-G₁, G₁, S and G₂/M phases. GM represents cells that were propagated in growth medium. A statistically significant increase in the numbers of cells present in the sub-G₁ and G₂/M phase was observed in 2-MeOE2bisMATE-treated cells when compared with the controls. An * indicates a *P*-value < 0.05.

Table 3.1. Percentage of cells in sub-G₁, G₁, S and G₂/M phases as determined by Cyflogic 1.2.1 (Perttu Terho & Cyflo Ltd).

Cell cycle phase	GM	DMSO	2-MeOE2bisMATE	Actinomycin D
sub-G ₁	0.5	0.6	4	7.9
G ₁	54.5	50.5	6.33	38.2
S	18.3	19.5	13.6	18.4
G ₂ /M	26.3	26.4	76.04	35.5

3.3.3. Flow cytometry- apoptosis detection analysis (annexin V-FITC)

Apoptosis induction by 2-MeOE2bisMATE in SNO cells was confirmed by an annexin V-FITC assay. During the early phases of apoptosis, cells lose their phospholipid asymmetry of the plasma membrane and expose PS by translocating it to the outer layer of the plasma membrane. Annexin V (phospholipid-binding protein) preferentially binds to the negatively charged phospholipids like PS in the presence of calcium. By conjugating FITC to Annexin V, apoptotic cells were identified and quantified by flow cytometry. When compared to the vehicle-treated cells, 2-MeOE2bisMATE-exposed cells showed an increase in the number of cells present in early and late stages of apoptosis (16.8% and 13.9% respectively) (Figure 3.27 & Figure 3.28).

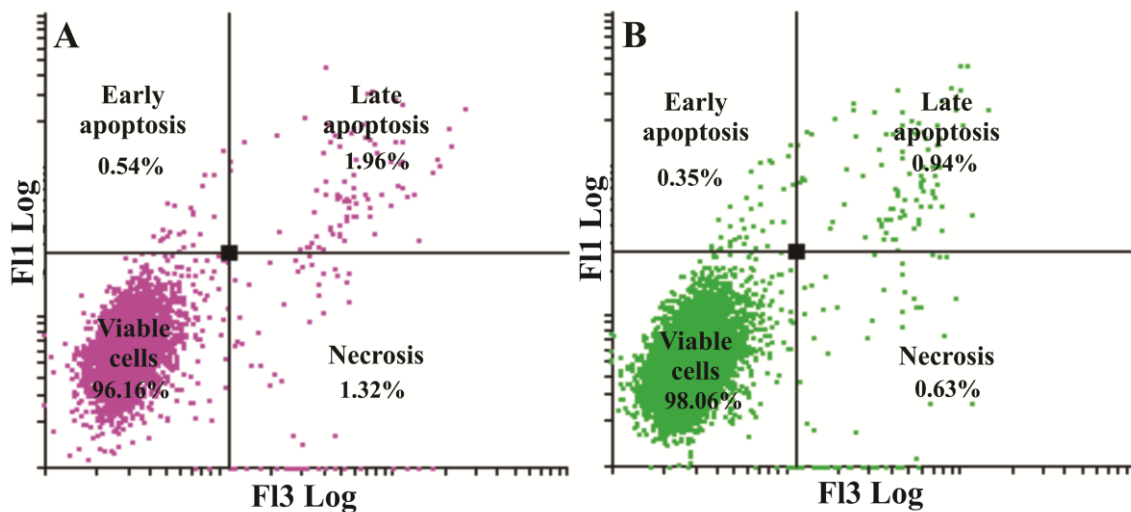


Figure 3.27. PI (FL3 Log) versus Annexin V (FL1 Log) dot-plot of cells propagated in the growth medium (A) and of vehicle-treated cells (B). An increase in the number of viable cells was observed.

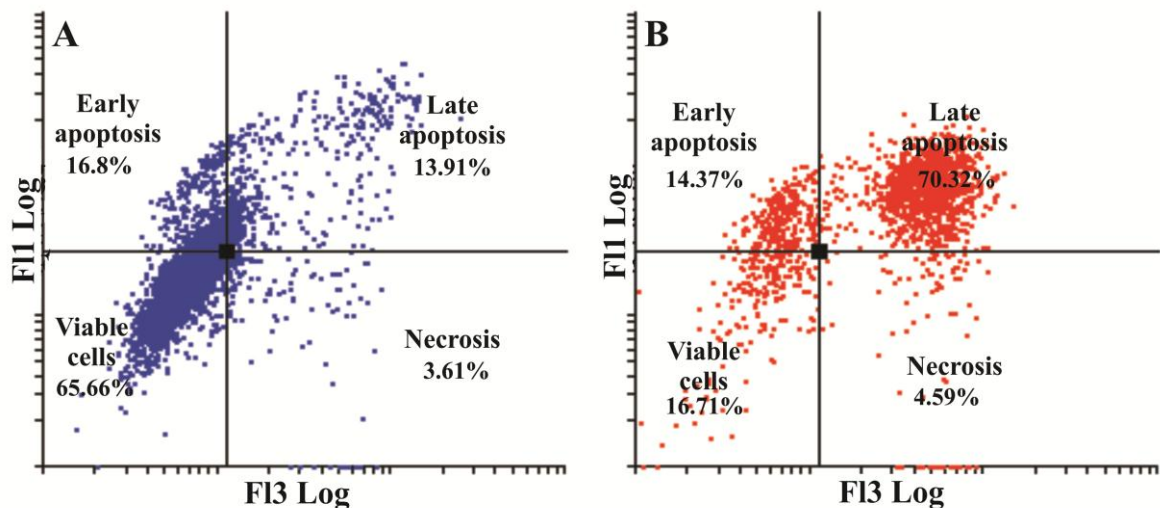


Figure 3.28. PI (FL3 Log) versus Annexin V (FL1 Log) histogram of 0.4 μ M 2-MeOE2bisMATE-treated SNO cells (A) and actinomycin D-treated cells after 24 hours of exposure. Data revealed that 65.6% of the 2-MeOE2bisMATE-treated SNO cells were viable, 16.8% were present in early apoptosis, 13.9% in late apoptosis, and 3.6% in necrosis.

3.3.4. Flow cytometry - mitocapture mitochondrial assay

To test whether alterations of mitochondrial membrane potential is involved in 2-MeOE2bisMATE -induced apoptosis, changes in mitochondrial membrane potential were studied. Exposure of SNO cells to 2-MeOE2bisMATE resulted in an increase in mean fluorescence intensity, as seen by a 1.47-fold shift to the right on the histogram observed in 2-MeOE2bisMATE-treated cells when compared to the vehicle-treated control (Figure 3.29). These data suggest that a mechanism through 2-MeOE2bisMATE which induces apoptosis in SNO cells is through loss of mitochondrial membrane potential.

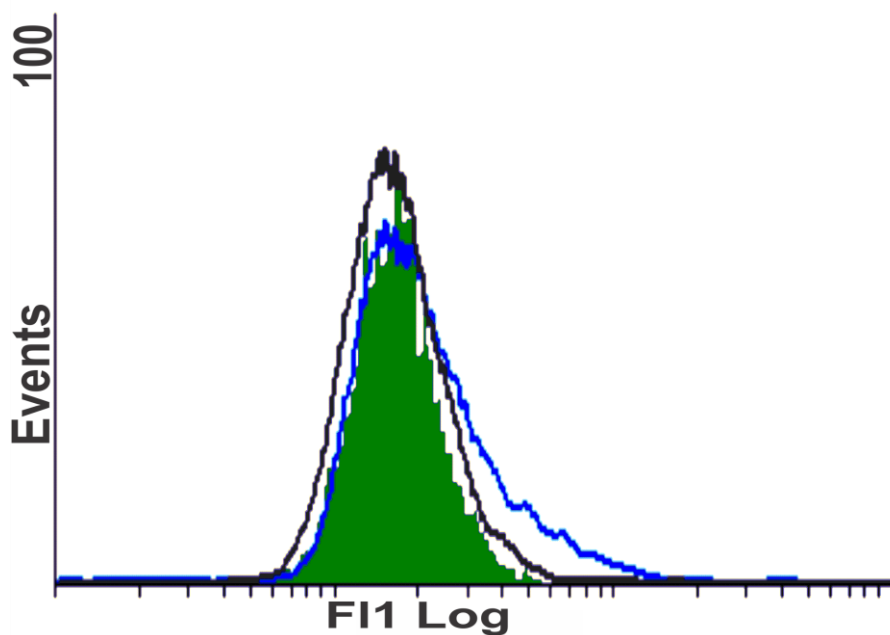


Figure 3.29. Histogram of mean fluorescence intensity of 2-MeOE2bisMATE-treated cells (blue) overlaid on the vehicle-treated (green) and 2ME2-treated cells (black). An increase in the number of cells with reduced mitochondrial potential in cells treated with 2-MeOE2bisMATE was observed compared to the vehicle-treated control cells.

3.3.5. Spectrophotometry- caspase 6 & 8 calorimetric assays

To further understand the mechanism of action by which 2-MeOEbisMATE induces apoptosis in SNO cells, caspase 6 and 8 calorimetric assays were conducted. Figure 3.30 & Figure 3.31 represents caspase 6 and caspase 8 activity ratios of 2-MeOEbisMATE-treated and actinomycin D-treated cells compared to vehicle-treated cells. The activity of executioner caspase (caspase 6) was statistically significantly increased in 2-MeOEbisMATE-treated cells when compared to the vehicle-treated cells (Figure 3.30). Activity of initiator caspase (caspase 8) was statistically insignificantly increased in 2-MeOEbisMATE-treated cells when compared to the vehicle-treated cells (Figure 3.31).

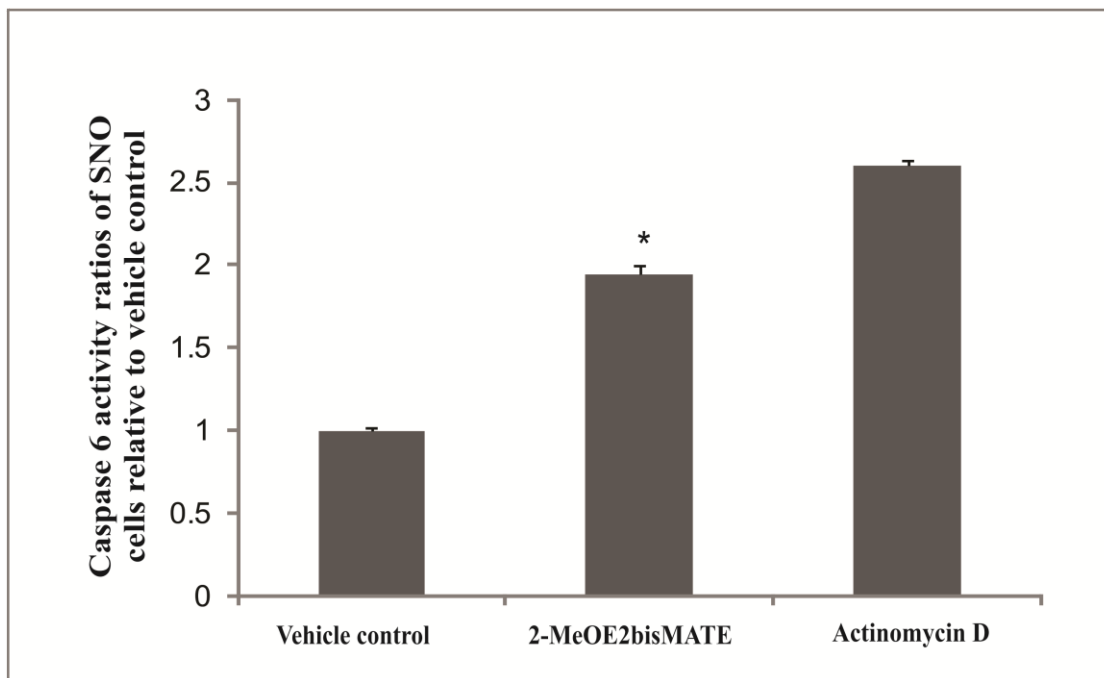


Figure 3.30. Caspase 6 activity ratios of 0.4 μ M 2-MeOEbisMATE-treated and actinomycin D-treated cells compared to vehicle-treated cells following 24 hours of exposure. Activity of caspase 6 was increased in 2-MeOEbisMATE-treated cells compared to the vehicle-treated cells. An * indicates a P -value < 0.05.

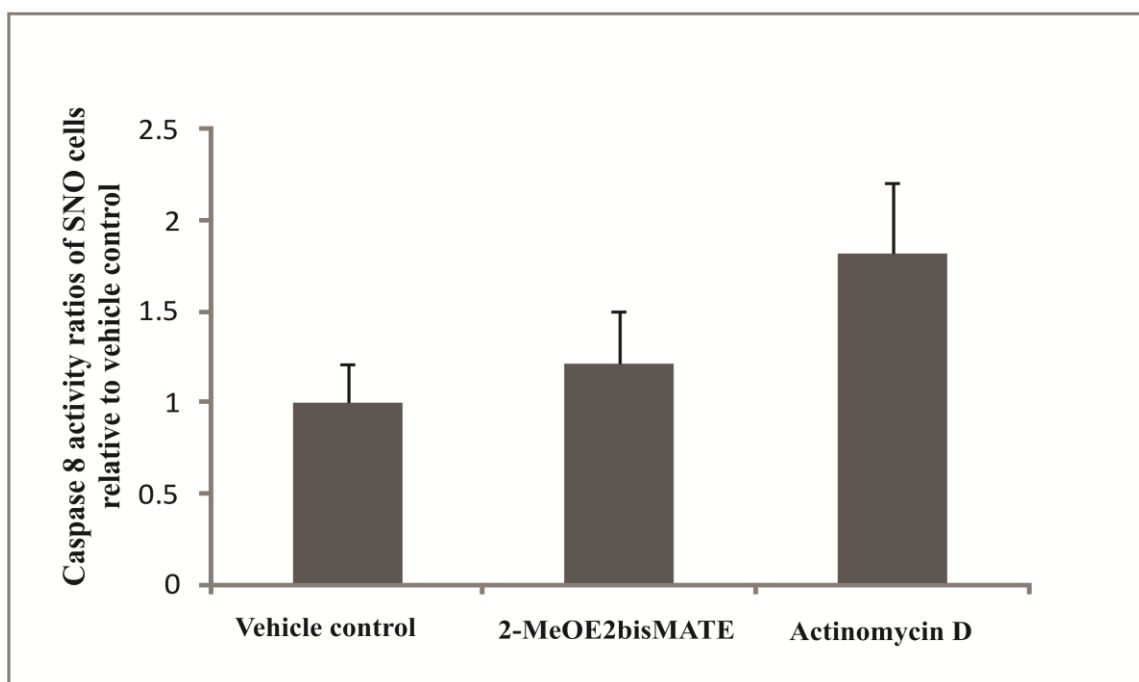


Figure 3.31. Caspase 8 activity ratios of 0.4 μ M 2-MeOEbisMATE-treated and actinomycin D-treated cells compared to vehicle-treated cells. Activity of caspase 8 was statistically insignificantly increased in 2-MeOEbisMATE-treated cells compared to vehicle-treated cells.

3.3.6. Flow cytometry - autophagy detection analysis (anti-LC3B)

To further contribute to autophagy detection a conjugated rabbit polyclonal anti-LC3B antibody assay was performed. An increase in mean fluorescence intensity (shift to the right) of 1.1-fold was observed in 2-MeOE2bisMATE-treated cells when compared to the vehicle-treated control, but the increase was not statistically significant (Figure 3.32).

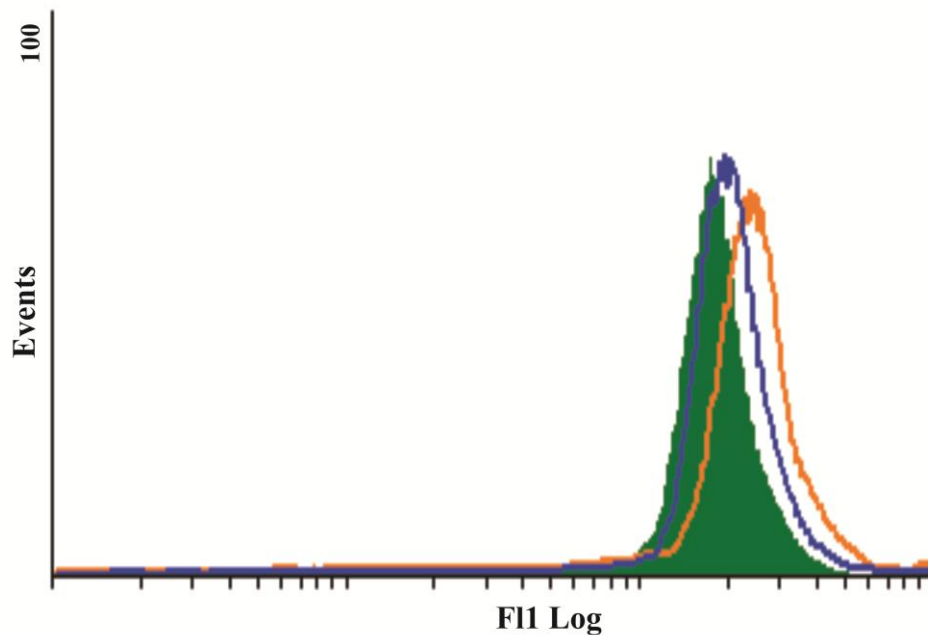


Figure 3.32. LC3 Histogram of mean fluorescence intensity of 2-MeOE2bisMATE-treated cells (blue) overlaid on the vehicle-treated control cells (green) in SNO cells after 24 hours of exposure. There was a statistically insignificant increase in LC3 levels in cells treated with 2-MeOE2bisMATE when compared to the vehicle-treated control cells. The orange histogram represents the positive control (tamoxifen-treated cells).

3.3.7. Flow cytometry - autophagy detection analysis Cyto-ID autophagy assay

To test for the presence of autophagy vesicles in 2-MeOE2bisMATE-treated SNO cells, the cyto-ID autophagy detection assay was conducted. Tamoxifen was used as a positive control agent known for induction of autophagy. The exposure of SNO cells to 2-MeOE2bisMATE resulted in an increase in the presence of autophagosomes, as demonstrated by the shift to the right on the histogram, when compared to the vehicle-treated control (Figure 3.33). These results indicated an increase of 1.17-fold in mean fluorescence intensity of

2-MeOE2bisMATE-treated cells when compared to the vehicle-treated control however; it was statistically insignificant (Figure 3.33).

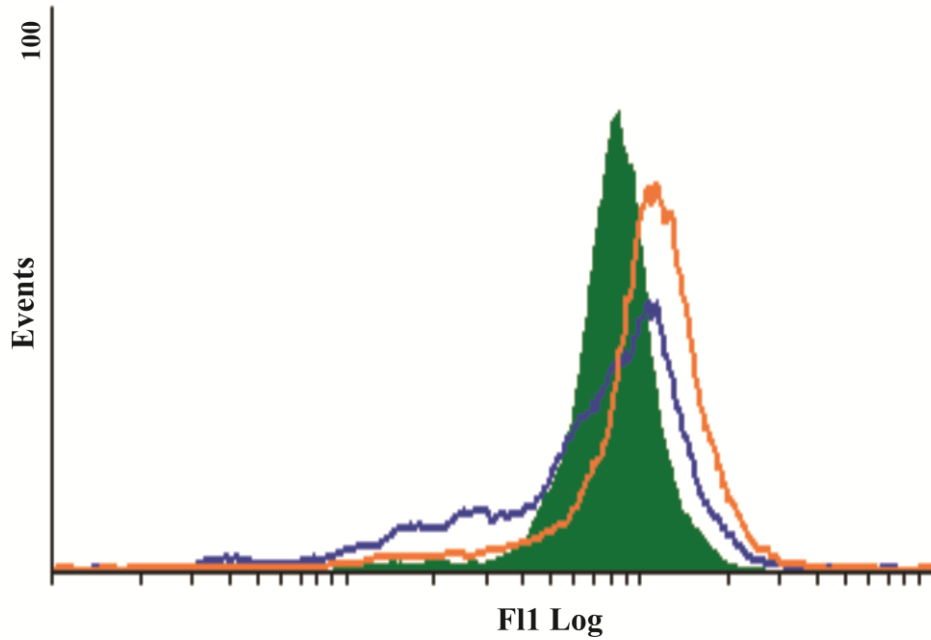


Figure 3.33. Cyto-ID Histogram of 2-MeOE2bisMATE-treated cells (blue) overlaid on the vehicle-treated control cells (green) in SNO cells after 24 hours of exposure. A statistically insignificant increase in the mean fluorescence intensity of 2-MeOE2bisMATE-treated cells was observed when compared to the vehicle-treated control. The orange histogram represents the positive control (tamoxifen-treated cells).

Chapter 4

Discussion

Compounds that target and disrupt microtubule function are at present one of the most successful groups of chemotherapeutic compounds that are used to treat cancer [43, 44]. These compounds inhibit normal progression of mitosis thus resulting in the inhibition of the hyperproliferation of cancer cells [46]. Several microtubule-targeting compounds have been identified, these include compounds such as paclitaxel, docetaxel, colchicine and 2ME2 [19, 20]. It has been demonstrated that 2ME2 to exert both *in vitro* and *in vivo* antiproliferative activity in various cancer cell lines [138-142]. However, 2ME2 undergoes rapid metabolic breakdown, thus several analogues of 2ME2 were developed in recent years in an attempt to create compounds with improved anticancer potency and oral bioavailability [173, 176, 183].

2-MeOE2bisMATE is a 2ME2 analogue and currently being studied as a potential anticancer drug. 2-MeOE2bisMATE has antiproliferative effects and it is a more potent inhibitor of cell proliferation when compared to 2ME2 [164]. The exact mechanism of action of 2-MeOE2bisMATE still remains to be determined and it appears to vary according to the cell type. In this study the *in vitro* effects of 2-MeOE2bisMATE on cell growth, morphology, cell cycle progression and its possible induction of different types of cell deaths in oesophageal carcinoma cells were evaluated. Squamous cell carcinoma of the oesophagus presents a major health problem both internationally and in South Africa; it is categorized as the 8th most frequent cancer in the world [3, 4]. The development of chemotherapeutic compounds that have a high potency and increased efficacy against this malignancy is therefore of utmost importance.

Crystal violet staining was conducted to study the anti-proliferative effects of 0.2-1 μ M of 2-MeOE2bisMATE on SNO cells after an exposure periods of 24, 48 and 72 hours. Concentrations and times of exposure were chosen based on previous research and studies conducted in our laboratory [172, 174, 178, 186]. Research demonstrated that a concentration of 0.4 μ M of 2-MeOE2bisMATE causes 50% growth inhibition (IG₅₀) in the breast cancer cell line (MCF-7) [172, 174, 178, 186]. Day *et al.* (2009) found that 2-MeOE2bisMATE caused significant inhibition of MCF-7 and MCF-7_{MR} (an MCF-7 derivative resistant to

mitoxantrone) at a concentration of 0.24 μ M and 1.53 μ M, respectively [205]. Another study showed that 0.5 μ M of 2-MeOE2bisMATE inhibited growth of breast cancer cells (CAL51) in a dose dependent manner [206]. After 24 hours of exposure, a concentration of 0.4 μ M of 2-MeOE2bisMATE revealed significant growth inhibition of SNO cells.

Since spectrophotometry studies suggests that 2-MeOE2bisMATE has anti-proliferative effects on SNO cells, the LDH assay was conducted to study the cytotoxic effects of 2-MeOE2bisMATE in SNO cells. LDH is a stable cytosolic enzyme that becomes released in the early stage of necrosis, but only in the late stage of apoptosis [189]. 2-MeOE2bisMATE had a minimal effect on LDH release, which shows that 2-MeOE2bisMATE does not severely affect the integrity of the SNO cell's plasma membrane. Similar results were observed in another study which was conducted in our laboratory using non-tumorigenic breast cancer cell line [179]. Thus, these results suggest that 2-MeOE2bisMATE does not cause induction of necrosis.

Morphological studies were conducted by means of PlasDIC, light microscopy and TEM to evaluate the mechanism/s by which 2-MeOE2bisMATE may inhibit cell growth of oesophageal carcinoma SNO cells. PlasDIC and light microscopy revealed features of apoptosis such as shrunken cells, hypercondensed chromatin, membrane blebbing and apoptotic bodies in SNO cells that were exposed to 0.4 μ M of 2-MeOE2bisMATE and the cells' densities was also compromised. Similarly, Raobaikady *et al.* (2003) and Day *et al.* (2003) found that there was a significant increase in the number of rounded, shrunken and detached cancer cells after treatment with 2-MeOE2bisMATE [174, 176]. Apoptotic-like cells were observed in 2-MeOE2bisMATE-treated MCF-7_{DOX} and MCF-7_{WT} cell lines [195]. These results were consistent with those of a study which was conducted Day *et al.* (2009) using ovarian cancer cell line (A2780wt), the results revealed that 1 μ M of 2-MeOE2bisMATE resulted in the cells to detach and to be round in appearance and in showing features of apoptosis after an exposure period of 72 hours [205].

TEM was used to view the internal cellular structures of the SNO cells after exposure to 2-MeOE2bisMATE. Results showed significant morphological changes that were characteristic of both apoptosis (condensed and fragmented nuclei, apoptotic bodies) and autophagy (intracellular vacuoles). Since TEM results suggested that 2-MeOE2bisMATE

induced cell death by both apoptosis and autophagy in SNO cells, triple staining studies were used to distinguish between viable, apoptotic, autophagic and oncotic/necrotic cells. Results showed an increased affinity for AO in both 2-MeOE2bisMATE-treated SNO cells and starved cells when compared to the negative controls. An increase in the number of acidic intracellular lysosomes proposes the involvement of autophagic processes.

Since previous studies conducted on the source molecule of 2-MeOE2bisMATE, namely 2ME2, reported that 2ME2 interacts with microtubules, which may result in the destruction of the tubulin network with subsequent cell cycle arrest, the α -tubulin detection assay was utilized to determine the effects of 2-MeOE2bisMATE on the tubulin structure of SNO cells. In this study, it was shown that 2-MeOE2bisMATE disrupts the microtubule structure of SNO cells. Immunofluorescence staining results of this study revealed that 2-MeOE2bisMATE does have an effect on the morphology of microtubules in oesophageal carcinoma cells. This finding was consistent with previous studies that demonstrated that 2ME2 disrupts microtubule structures of colon cancer (HCT116) and breast cancer (MCF-7) cell lines [143, 207, 208]. Thus, the newly derivatives and 2ME2 share the same intracellular target molecule, namely tubulin.

To further investigate the mechanism of action of 2-MeOE2bisMATE in SNO cells, flow cytometry studies were conducted to investigate the effects of 2-MeOE2bisMATE on cell cycle progression. Results demonstrated that the treatment of SNO cells with 2-MeOE2bisMATE caused an increase in cells in sub- G_1 as well as G_2/M phases, indicative of the presence of apoptosis and metaphase block, respectively. The annexin V-FITC further confirmed the induction of apoptosis by 2-MeOE2bisMATE. There was an increase in the number of cells in early apoptosis (16.8%) and late apoptosis (13.9%) in 2-MeOE2bisMATE-treated cells when compared to the vehicle-treated cells.

Our findings were compatible with a previous report which showed that $1\mu\text{M}$ of 2-MeOE2bisMATE caused an increase in the number of prostate cells and ovarian cells in the G_2/M and sub- G_1 phases within 24 hours of exposure to the drug [176]. Similarly, $1\mu\text{M}$ of 2-MeOE2bisMATE caused an increase in the G_2/M peak of MCF-7 and MCF-7_{MR} cell lines [173]. Data collected in our laboratory demonstrated that the exposure of a non-tumorigenic breast cancer cell line (MCF-12A) and a tumorigenic breast cancer cell line (MCF-7) to

2-MeOE2bisMATE resulted in an increase in the number of cells in apoptosis [172]. Ho *et al.* (2003) revealed that 24 hours of exposure of adult human dermal fibroblasts to 0.1 μ M 2-MeOE2bisMATE induced G₂/M arrest. However, the treatment of human umbilical vein endothelial cells (HUVECs) with 2-MeOE2bisMATE for 24 hours did not induce cell cycle arrest [209]. Therefore 2-MeOE2bisMATE seems to have variable effects in different cell types.

Since 2-MeOE2bisMATE induces apoptosis in SNO cells, its effects on mitochondrial membrane potential and caspase 6 and 8 activities were evaluated. It is postulated that a decrease in membrane potential results in the opening of the mitochondrial permeability transition pore (PTP), which may lead to the release of pro-apoptotic proteins such as cyt *c*, leading to intrinsic pathway of apoptosis [210, 211]. The extrinsic pathway on the other hand, involves receptor binding to ligand, followed by activation of initiator caspases. Caspase 8, one of the initiator caspases involved in the extrinsic pathway. Caspase 6 is one of the executioner caspases and it is involved in both the extrinsic and intrinsic pathways of apoptosis. Thus, data from these assays would provide information of whether the intrinsic and/or the extrinsic pathway are implicated in 2-MeOE2bisMATE-induced apoptosis in this study.

Data of mitochondrial membrane potential revealed an increase in the number of 2-MeOE2bisMATE-treated cells that were undergoing a reduction in their mitochondrial membrane potential compared to the vehicle control. Foster *et al.* (2008) demonstrated that 500nM of 2-MeOE2bisMATE caused depolarization of the inner mitochondrial membrane potential in MDA-MB-231 and HUVECs after 72 hours of exposure [175]. The caspase 6 results showed a statistically significant increase within SNO cells that were exposed to 2-MeOE2bisMATE, however, the caspase 8 activity results showed a statistically insignificant increase in caspase 8 activity in 2-MeOE2bisMATE-treated cells. Wood *et al.* (2004) established no effect of 2-MeOE2bisMATE on caspase 8 activation in CAL51 breast cancer cell line [206].

Our data suggests that mitochondria are involved in the process of 2-MeOE2bisMATE-induced apoptosis as it was shown in studies using 2ME2 [210-213]. Since the caspase 8 activity was not significantly increased, it seems that the intrinsic pathway of the apoptotic

arising from mitochondria may be a potential pathway underlying 2-MeOE2bisMATE-induced apoptosis in the current study.

Results obtained using TEM, as well as fluorescence microscopy (triple staining) revealed that autophagy is one of the types of cell death induced by 2-MeOE2bisMATE. Cyto-ID autophagy detection and the conjugated rabbit polyclonal anti-LC3 antibody assays were conducted to further confirm our previous results of autophagy induction in SNO cells by 2-MeOE2bisMATE. These assays revealed an increase in the presence of autophagosomes and in the LC3 levels, respectively; however the results were not statistically significant. To date, the only studies that showed the induction of autophagy in cancer cells by 2-MeOE2bisMATE were that of Visagie *et al.* (2011) and Vorster *et al.* (2010), which were conducted in our laboratory [178, 179]. Visagie *et al.* (2011) demonstrated that 0.4 μ M of 2-MeOE2bisMATE induced a statistically significant increase in LC3 levels in MCF-7 breast cancer cells after 48 hours of exposure [178]. Thus 2-MeOE2bisMATE appears to have variable effects in the different cell types.

Various studies have shown induction of both apoptosis and autophagy by 2ME2 [214-216] Lorin *et al.* (2009) demonstrated that 2ME2 induces both apoptosis and autophagy of ewing sarcoma cells, similarly Azad *et al.* (2009) demonstrated that treatment of human tumorigenic breast epithelial cell line (MCF-7), human glioblastoma astrocytoma epithelial-like cell line (U87), human cervical adenocarcinoma cells (HeLa), and transformed human embryonic kidney cells (HEK293) with 2ME2 induced both types of cell deaths [214, 215]. Data from currently available literature has demonstrated the induction of apoptosis by 2-MeOE2bisMATE however, only a small number of studies have revealed the induction of both apoptosis and autophagy by 2-MeOE2bisMATE. The occurrence of both apoptosis and autophagy suggests that there is a crosstalk between these two types of cell death.

Studies on cell death have demonstrated that there are some common signaling pathways between apoptosis and autophagy [217-219]. These include signaling pathways such as PI3k/AKT, regulatory genes such as p53 and p19ARF, as well as some of the basic machinery that execute the cell death programs (such as Atg5, Bcl-2) [220, 221]. It has been shown that Bcl-2 and Bcl-xL, the anti-apoptosis proteins, bind to Beclin 1 thus resulting in the inhibiting Beclin 1-mediated autophagy [222, 223]. Therefore, stimuli that lead to the

activation or suppression of these genes or signaling pathways can influence both apoptosis and autophagy [220]. Treatment of murine fibrosarcoma L929 cells with *Polygonatum cyrtonema* lectin, a mannose/sialic acid-binding lectin induced both apoptosis and autophagy by blocking Ras/Raf and PI3K/Akt signaling pathways [224]. Similarly, arsenic trioxide treatment of T-lymphocytic leukemia induced both apoptosis and autophagy by targeting proteins such as Beclin 1 and Bax and both processes contributed to cell death and complete tumor reduction [225].

This *in vitro* study revealed that 2-MeOE2bisMATE acts as an anticancer agent in SNO cells. The proposed mechanisms of action for 2-MeOE2bisMATE's anticancer effect in SNO cells is the disruption of microtubules which inhibits progression of the cell cycle, consequently leading to the induction of cell death by both apoptosis and autophagy. Apoptosis induction was demonstrated by morphological and cell cycle progression studies, as well as the following targets in the apoptotic pathway: exposure of phosphatidylserine on the outer plasma membrane, reduction in mitochondrial membrane potential and an increase in the activity of caspase 6 (Figure 4.1). Autophagy induction was revealed by an increase in lysosomal activity. An increase in the presence of autophagosomes and in the LC3 levels was observed in 2-MeOE2bisMATE-treated cells, though the latter results were not statistically significant.

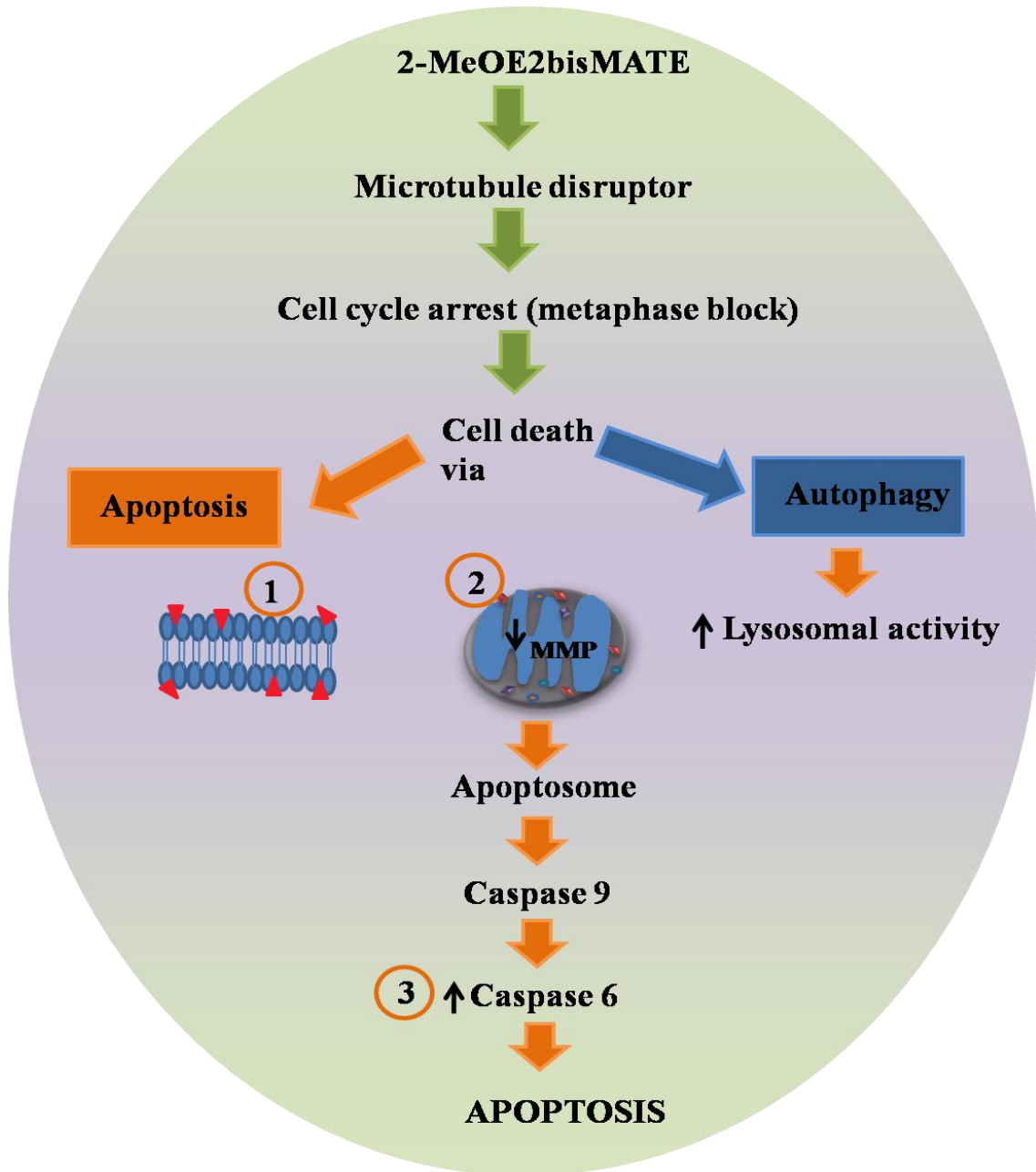


Figure 4.1. Proposed mechanism of action of 2-MeOE2bisMATE in oesophageal carcinoma cells. 2-MeOE2bisMATE disrupted the microtubule network and induced a metaphase block. The presence of PS on the outer plasma membrane (▲.), reduced mitochondrial membrane potential (2.) and an increase in caspase 6 activity (3.) were observed confirming apoptosis as a means of cell death in SNO cells. Autophagy induction was indicated by an increase in lysosomal activity.

Chapter 5

Conclusion

The objective of this *in vitro* study was to determine the influence of 2-MeOE2bisMATE on cell growth, morphology, cell cycle progression, as well as its potential to induce certain types of cell death in an oesophageal carcinoma (SNO) cell line. Data revealed that 0.4 μ M of 2-MeOE2bisMATE significantly inhibited cell growth, induced disruption of microtubules and increased the number of cells that were in G₂/M as well as in sub-G₁ phases after 24 hours of exposure. In addition, cell death by both apoptosis and autophagy was induced in 2-MeOE2bisMATE-treated cells. These activities have not been studied in oesophageal carcinoma cells up to date, thus contributing towards the understanding of the action mechanism of 2-MeOE2bisMATE in oesophageal carcinoma cells.

Future studies will be conducted to further elucidate the action mechanism of 2-MeOE2bisMATE within SNO cells. Since both apoptosis and autophagy were revealed as the types of cell death that are induced by 2-MeOE2bisMATE in SNO cells, other molecular targets within these types of cell deaths will be studied. These studies will add collective knowledge to the proposed biochemical map of 2-MeOE2bisMATE's mechanism of action in SNO cells. The identification of 2-MeOE2bisMATE as a potential anticancer drug warrants it as a possible candidate for the discovery of targets for cancer therapies that will aid in the design of antiproliferative- and microtubule disrupting agents against oesophageal cancer.

References

1. Zhao Y, Wang R, Fan D. The molecular mechanisms of oesophageal cancer. *Exp Clin Sci J.* 2006;5:79-92.
2. Dlamini Z, Bhoola K. Oesophageal cancer in African blacks of Kwazulu natal, South Africa: an epidemiological brief. *Ethn Dis.* 2005;15:786-789.
3. Melhado RE, Alderson D, Tucker O. The Changing Face of Oesophageal Cancer. *Cancers.* 2010;2:1379-1404.
4. Hendricks D, Parker MI. Oesophageal Cancer in Africa. *Life.* 2002;53:263-268.
5. Jemal A, Bray F, Center MM, Ferlay J, Ward E, Forman D. Global Cancer Statistics. *Cancer J Clin.* 2011;61:69-90.
6. Sumeruk R, Segal I, Te Winkel W, Van der merwe CF. Oesophageal cancer in three regions of South Africa. *SAMJ.* 1992;81:91-93.
7. Du Plessis L, Dietzsch E, Van Gele M, Van Roy N, Van Helden P, Parker MI. Mapping of Novel Regions of DNA Gain and Loss by Comparative Genomic Hybridization in Oesophageal Carcinoma in the Black and Colored Populations of South Africa. *Cancer Res.* 1999;59:1877-1883.
8. Wakhisi J, Patel K, Buziba N, Rotich J. Oesophageal cancer in north rift valley of western Kenya. *Afr H Sci.* 2005;5(2):157-163.
9. Sydenham EW, Thiel PG, Marasas WFO, Shephard GS, Van Schalkwyk DJ, Koch KR. Natural Occurrence of Some *Fusarium* Mycotoxins in Corn from Low and High Oesophageal Cancer Prevalence Areas of the Transkei, Southern Africa. *J Agric Food Chem.* 1990;38:1900-1903.
10. Van Rensburg SJ, Bradshaw ES, Bradshaw D, Rose EF. Oesophageal cancer in Zulu men, South Africa: A case-control study. *Br J Cancer.* 1985;51:399-405.
11. Wang X, Tian X, Liu F, Zhao Y, Sun M, Chen D. Detection of HPV DNA in oesophageal cancer specimens from different regions and ethnic groups: a descriptive study. *BMC Cancer.* 2010;10:19-26.
12. Essack M, Radovanovic A, Schaefer U, Schmeier S, Seshadri SV, Christoffels A, et al. DDEC: Dragon database of genes implicated in oesophageal cancer. *BMC Cancer.* 2009;9:219-225.
13. Mkele, G. Rational selection of cancer chemotherapy. *SAPJ.* 2010:32-34.

14. N'Da DD. Synthesis of methotrexate and ferrocene conjugates as potential anticancer agents [thesis]. University of Witwatersrand; 2004.
15. American Cancer Society. Surgery. Accessed at www.cancer.gov/cancertopics/factsheet/Therapy/surgery on July 21, 2010.
16. American Cancer Society. Radiation therapy principles. Accessed at [www.cancer.gov/cancertopics/factsheet/Therapy/radiation therapy](http://www.cancer.gov/cancertopics/factsheet/Therapy/radiation%20therapy) on July 21, 2010.
17. American Cancer Society. Chemotherapy. Accessed at www.cancer.gov/cancertopics/factsheet/Therapy/chemotherapy, 2010.
18. Motoori M, Yano M, Yasuda T, Miyata H, Peng YF, Yamasaki M, et al. Chemotherapy-induced toxicities and treatment efficacy in advanced oesophageal cancer treated with neoadjuvant chemotherapy followed by surgery. *Esophagus*. 2011;8:81-87.
19. Zhou J, Giannakakou P. Targeting Microtubules for Cancer Chemotherapy. *Curr Med Chem Anti-Canc Agents*. 2005;5:65-71.
20. Mooberry SL, Weiderhold KN, Dakshanamurthy S, Hamel E, Banner EJ, Kharlamova A, et al. Identification and Characterization of a New Tubulin-Binding Tetrasubstituted Brominated Pyrrole. *Mol Pharmacol*. 2007;72:132-140.
21. McGrogan BT, Gilmartin B, Carney DN, McCann A. Taxanes, microtubules and chemoresistant breast cancer. *Biochim Biophys Acta*. 2008;1785:96-132.
22. Risinger AL, Giles FJ, Mooberry SL. Microtubule Dynamics as a Target in Oncology. *Cancer Treat Rev*. 2009;35(3):255-261.
23. Schafer KA. The Cell Cycle: A Review. *Vet Pathol*. 1998;35:461-478.
24. Tessema M, Lehmann U, Kreipe H. Cell cycle and no end. *Virchows Arch*. 2004;444:313-323.
25. Garrett MD. Cell cycle control and cancer. *Curr Sci*. 2001;81(5):515-522.
26. Tyson JJ, Csikasz-Nagy A, Novak B. The dynamics of cell cycle regulation. *Bio Essays*. 2002;24:1095-1109.
27. Wesierska-gadek J, Maurer M, Zulehner N, Komina O. Whether to target single or multiple CDKs for Therapy? That is the Question. *J Cell Physiol*. 2011;226:341-349.
28. Collins K, Jacks T, Pavletich NP. The cell cycle and cancer. *Proc Natl Acad Sci USA*. 1997;94:2776-2778.
29. Vermeulen K, Van Bockstaele DR, Berneman ZN. The cell cycle: a review of regulation, deregulation and therapeutic targets in cancer. *Cell Prolif*. 2003;36:131-149.

30. Herrup K, Yang Y. Cell cycle regulation in the postmitotic neuron: oxymoron or new biology? *Nature*. 2007;8:368-378.
31. Johnson DG, Walker CL. Cyclins and cell cycle checkpoints *Annu. Rev. Pharmacol. Toxicol.* 1999;39:295-312.
32. Blagosklonny MV, AB Pardee. The Restriction Point of the Cell Cycle. *Cell Cycle*. 2002;1(2):103-110.
33. Ford HL, Pardee AB. Cancer and the Cell Cycle. *J Cell Biochem Suppl.* 1999;32/33:166-172.
34. Besson A, Dowdy SF, Roberts JM. CDK Inhibitors: Cell Cycle Regulators and Beyond. *Dev Cell*. 2008;14:159-169.
35. Wikman H, Kettunen E. regulation of the G1/S phase of the cellcycle and alterations in the RB pathway in human lung cancer. *Expert Rev Anticancer Ther.* 2006;6(4):515-530.
36. Sun J, Kong D. DNA replication origins, ORC/DNA interaction, and assembly of pre-replication complex in eukaryotes. *Acta Biochim Biophys Sin.* 2010;42:433-439.
37. Woo RA, Poon RYC. Cyclin-dependent kinases and S phase control in mammalian cells. *Cell Cycle*. 2003;2(4):316-324.
38. Masai H, Matsumoto S, You Z, Yoshizawa-Sugata N, Oda M. Eukaryotic Chromosome DNA Replication: Where, When, and How? *Annu Rev Biochem.* 2010;79:89-130.
39. Porter ACG. Preventing DNA over-replication: a Cdk perspective. *Cell Div.* 2008;3:3.
40. Malumbres M. Physiological relevance of cell cycle kinases. *Physiol Rev.* 2011;91:973-1007.
41. Nigg EA. Mitotic kinases as regulators of cell division and its checkpoints. *Mol Cell Biol.* 2001;2:21-32.
42. Jordan A, Hadfield JA, Lawrence NJ, McGown AT. Tubulin as a Target for Anticancer Drugs: Agents Which Interact with the Mitotic Spindle. *Med Res Rev.* 1998;18(4):259-296.
43. Pasquier E, Kavallaris M. Microtubules: A Dynamic Target in Cancer Therapy. *Life.* 2008;60(3):165-170.
44. McGrogan BT, Gilmartin B, Carney DN, McCann A. Taxanes, microtubules and chemoresistant breast cancer. *Biochim Biophys Acta.* 2008;1785:96-132.

45. Das A, Chakrabarty S, Choudhury D, Chakrabarti G. 1,4-Benzoquinone (PBQ) Induced Toxicity in Lung Epithelial Cells Is Mediated by the Disruption of the Microtubule Network and Activation of Caspase-3. *Chem Res Toxicol.* 2010;23:1054-1066.
46. Schmidt M, Bastians H. Mitotic drug targets and the development of novel anti-mitotic anticancer drugs. *Drug Resist Updat.* 2007;10:162-181.
47. Rieder CL, Salmon ED. Motile kinetochore and polar ejection forces dictate chromosome position on the vertebrate mitotic spindle. *J Cell Biol.* 1994;124:223-233.
48. Peters J-M. The anaphase promoting complex/cyclosome: a machine designed to destroy. *Nature.* 2006;7:643-657.
49. Reinhardt HC, Hasskamp P, Schmedding I, Morandell S, van Vugt M, Wang X. DNA Damage Activates a Spatially Distinct Late Cytoplasmic Cell-Cycle Checkpoint Network Controlled by MK2-Mediated RNA Stabilization. *Mol Cell.* 2010;40:34-49.
50. DiPaola RS. To Arrest or Not To G2-M Cell-Cycle Arrest. *Clin Cancer Res.* 2002;8:3311-3314.
51. Luch A. Cell Cycle Control and Cell Division: Implications for Chemically Induced Carcinogenesis. *Chembiochem.* 2002;3:506-516.
52. Ricci MS, Zong W-X. Chemotherapeutic Approaches for Targeting Cell Death Pathways. *Oncologist.* 2006;11:342-357.
53. Kroemer G, Galluzzi L, Brenner C. Mitochondrial membrane permeabilization in cell death. *Physiol Rev.* 2007;87:99-163.
54. Galluzzi L, Maiuri MC, Vitale I, Zischka H, Castedo M, Zitvogel L, Kroemer G. Cell death modalities: classification and pathophysiological implications. *Cell Death Differ.* 2007;14:1237-1266.
55. Kroemer G, El-Deiry WS, Golstein P, Peter ME, Vaux D, Vandenabeele P, et al. Classification of cell death: recommendations of the Nomenclature Committee on Cell Death. *Cell Death Differ.* 2005;12:1463-1467.
56. Majno G, Joris I. Apoptosis, Oncosis, and Necrosis An Overview of Cell Death. *Am J Pathol.* 1995;146:3-15.
57. Trump BE, Berezsky IK, Chang SH, Phelps PC. The Pathways of Cell Death: Oncosis, Apoptosis, and Necrosis. *Toxicol Pathol.* 1997;25:82-89.
58. Folmer F, Jaspars M, Dicato M, Diederich M. Marine cytotoxins: callers for the various dances of death. *Gastroenter Hepatol.* 2009;2:S34-S50.

59. Van Cruchten S, Van den Broeck W. Morphological and Biochemical Aspects of Apoptosis, Oncosis and Necrosis. *Anat Histol Embryol.* 2002;31:214-223.
60. Hotchkiss RS, Andreas Strasser A, McDunn JE, Swanson PE. Cell Death. *N Engl J Med.* 2009;361:1570-1583.
61. Guimarães CA, Linden R. Programmed cell death Apoptosis and alternative deathstyles. *Eur J Biochem.* 2004;271,1638-1650.
62. Hitomi J, Christofferson DE, Ng A, Yao J, Degterev A, Xavier RJ, Yuan J. Identification of a Molecular Signaling Network that Regulates a Cellular Necrotic Cell Death Pathway. *Cell.* 2008;135:1311-1323.
63. Dunai Z, Bauer PI, Mihalik R. Necroptosis: Biochemical, Physiological and Pathological Aspects. *Pathol Oncol Res.* 2011;17:791-800.
64. Sun Y, Peng Z-L. Programmed cell death and cancer. *Postgrad Med J.* 2009;85:134-140.
65. Tsujimoto Y, Shimizu S. Another way to die: autophagic programmed cell death. *Cell Death Differ.* 2005;12:1528-1534.
66. Qin J, Ye N, Liu X, Lin B. Microfluidic devices for the analysis of apoptosis. *Electrophoresis.* 2005;26:3780-3788.
67. Schultz DR, Harrington WJ. Apoptosis: Programmed Cell Death at a Molecular Level. *Sem Arth Rheum.* 2003;32(6): 345-369.
68. Ghobrial IM, Witzig TE, Adjei AA. Targeting apoptotic pathways in cancer therapy. *CA Cancer J Clin.* 2005; 55:178-194.
69. Plati J, Octavian Bucurab O, Khosravi-Far R. Apoptotic cell signaling in cancer progression and therapy. *Integr Biol.* 2011;3:279-296.
70. Zuzarte-Luis V, Hurlle JM. Programmed cell death in the developing limb. *Int J Dev Biol.* 2002;46(7):871-876.
71. Degterev A, Boyce M, Yuan J. A decade of caspases. *Oncogene.* 2003;22(53):8543-8567.
72. Seon-Yong J, Dai-Wu S. The role of mitochondria in apoptosis. *BMB rep.* 2008;41(1):11-22.
73. Fulda S, Debatin KM. Extrinsic versus intrinsic apoptosis pathways in anticancer chemotherapy. *Oncogene.* 2006;25:4798-4811.

74. Huppertz B, Frank H-G, Kaufmann P. The apoptosis cascade- morphological and immunohistochemical methods for its visualization *Anat Embryol.* 1999;200:1-18.
75. De Bruin EC, Medema JP. Apoptosis and non-apoptotic deaths in cancer development and treatment response. *Cancer Treatment Rev.* 2008;34:737-749.
76. Fink SL, Cookson BT. Apoptosis, Pyroptosis, and Necrosis: Mechanistic Description of Dead and Dying Eukaryotic Cells. *Infect Immun.* 2005;73(4):1907-1916.
77. Cohen GM. Caspases: the executioners of apoptosis. *Biochem J.* 1997;326:1-16.
78. Cain K, Bratton SB, Cohen GM. The Apaf-1 apoptosome: a large caspase-activating complex. *Biochimie.* 2002;84:203-214.
79. Inoue S, Browne G, Melino G, Cohen GM. Ordering of caspases in cells undergoing apoptosis by the intrinsic pathway. *Cell Death Differ.* 2009;16:1053-1061.
80. Wang C, Youle RJ. The Role of Mitochondria in Apoptosis. *Annu Rev Genet.* 2009;43:95-118.
81. Zhang X, Chen Y, Larry W Jenkins LW, Kochanek PM, Clark RSB. Bench-to-bedside review: Apoptosis/programmed cell death triggered by traumatic brain injury. *Critical Care.* 2005;9:66-75.
82. Elmore S. Apoptosis: A Review of Programmed Cell Death. *Toxicol Pathol.* 2007;35(4):495-516.
83. Gewies A. Introduction to apoptosis. *ApoReview.* 2003:1-26.
84. Lavrik IN. Systems biology of apoptosis signaling networks. *Curr Opin Biotechnol.* 2010;21:551-555.
85. Chen M, Wang J. Initiator caspases in apoptosis signaling pathways. *Apoptosis.* 2002;7:313-319.
86. Mayer B, Oberbauer R. Mitochondrial Regulation of Apoptosis. *News Physiol Sci.* 2003;18:89-94.
87. Debatin K-M. Apoptosis pathways in cancer and cancer therapy. *Cancer Immunol Immunother.* 2004;53:153-159.
88. Li H, Zhu H, Xu CJ, Yuan J. Cleavage of BID by caspase 8 mediates the mitochondrial damage in the Fas pathway of apoptosis. *Cell.* 1998;94:491-501.
89. Luo X, Budihardjo I, Zou H, Slaughter C, Wang X. Bid, a Bcl2 interacting protein, mediates cytochrome c release from mitochondria in response to activation of cell surface death receptors. *Cell.* 1998;94:481-490.

90. Barišić K, Petrik J, Rumora L. Biochemistry of apoptotic cell death. *Acta Pharm.* 2003;53:151-164.
91. Spencer SL, Sorger PK. Measuring and Modeling Apoptosis in Single Cells. *Cell.* 2011;144:926-939.
92. Levine B, Sinha S, Kroemer G. Bcl-2 family members: Dual regulators of apoptosis and autophagy. *Autophagy.* 2008;4(5):600-606.
93. Igney FH, Krammer PH. Death and anti-death: tumour resistance to apoptosis. *Nature.* 2002;2:277-288.
94. Fan T-J, Han L-H, Cong R-S, Liang J. Caspase Family Proteases and Apoptosis. *Acta Biochim Biophys Sin.* 2005;37(11):719-727.
95. Sayers TJ. Targeting the extrinsic apoptosis signaling pathway for cancer therapy. *Cancer Immunol Immunother.* 2011;60:1173-1180.
96. Rasheva VI, Domingos PM. Cellular responses to endoplasmic reticulum stress and apoptosis. *Apoptosis.* 2009;14:996-1007.
97. Szegezdi E, Fitzgerald U, Samali A. Caspase 12 and ER-stress-mediated apoptosis the story so far. *Ann NY Acad Sci.* 2003;1010:186-194.
98. Xu C, Bailly-Maitre B, Reed JC. Endoplasmic reticulum stress: cell life and death decisions. *J Clin Invest.* 2005;115:2656-2664.
99. Arnoult D, Gaume B, Karbowski M, Sharpe JC, Cecconi F, Youle RJ. Mitochondrial release of AIF and EndoG requires caspase activation downstream of Bax/Bak-mediated permeabilization. *EMBO.* 2003;22(17):4385-4399.
100. Lambert C, Apel K, Biesalski HK, Frank J. 2-methoxyestradiol induces caspase-independent, mitochondria-centered apoptosis in ds-sarcoma cells. *Int J Cancer.* 2004;108:493-501.
101. Chwieralski CE, Welte T, Buhling F. Cathepsin-regulated apoptosis. *Apoptosis.* 2006;11:143-149.
102. Tan Y, Dourdin N, Wu C, De Veyra T, Elce JS, Greer PA. Ubiquitous Calpains Promote Caspase-12 and JNK Activation during Endoplasmic Reticulum Stress-induced Apoptosis. *J Biol Chem.* 2006;281(23):16016-16024.
103. Wolf BB, Goldstein JC, Stennicke HR, Beere H, Amarante-Mendes GP, Salvesen GS. Calpain Functions in a Caspase-Independent Manner to Promote Apoptosis-Like Events During Platelet Activation. *Blood.* 1999;94(5):1683-1692.

104. Nakagawa T, Yuan J. Cross-talk between Two Cysteine Protease Families: Activation of Caspase-12 by Calpain in Apoptosis. *J Cell Biol.* 2000;150 (4):887-894.
105. Orrenius S, Zhivotovsky B, Nicotera P. Regulation of cell death: the calcium–apoptosis link. *Mol Cell Biol.* 2003;4:552-565.
106. Cullen SP, M Brunet M, SJ Martin SJ. Granzymes in cancer and immunity. *Cell Death Differ.* 2010;17:616-623.
107. Chen G, Shi L, Litchfield DW, Greenberg AH. Rescue from Granzyme B-induced Apoptosis by Kinase. *J Exp Med.* 1995;181:2295-2300.
108. Cuervo AM. Autophagy: in sickness and in health. *Trends Cell Biol.* 2004;14(2):70-77.
109. Levine B, Yuan J. Autophagy in cell death: an innocent convict?. *J Clin Invest.* 2005;115:2679-2688.
110. Codogno P, Meijer AJ. Autophagy and signaling: their role in cell survival and cell death. *Cell Death Differ.* 2005;12:1509-1518.
111. Mizushima N. Autophagy: process and function. *Genes Dev.* 2007;21:2861-2873.
112. Mizushima N, Levine B, Cuervo AM, Klionsky DJ. Autophagy fights disease through cellular self-digestion. *Nature.* 2008;451(7182):1069-1075.
113. Klionsky DJ, Emr SD. Autophagy as a Regulated Pathway of Cellular Degradation. *Science.* 2000;290:1717-1721.
114. Levine B. Autophagy and cancer. *Nature.* 2007;446:745-747.
115. Kimmelman AC. The dynamic nature of autophagy in cancer. *Genes Dev.* 2011;25:1999-2010.
116. Yang ZJ, Chee CE, Huang S, Sinicrope FA. The Role of Autophagy in Cancer: Therapeutic Implications. *Mol Cancer Ther.* 2011;10(9):1533-1541.
117. Jung CH, Ro S-H, Cao J, Otto NM, Kim D-H. mTOR regulation of autophagy. *FEBS Lett.* 2010;584(7):1287-1295.
118. Mehrpour M, Audrey Esclatine A, Isabelle Beau1 I, Patrice Codogno P. Overview of macroautophagy regulation in mammalian cells. *Cell Res.* 2010;20:748-762.
119. Jung CH, Jun CB, Ro S-H, Kim Y-M, Otto NM, Cao J. ULK-Atg13-FIP200 complexes mediate mTOR signaling to the autophagy machinery. *Mol Biol Cell.* 2009;20(7):1992-2003.

120. Chan EY, Kir S, Tooze SA. siRNA screening of the kinome identifies ULK1 as a multidomain modulator of autophagy. *J Biol Chem.* 2007;282:25464-25474.
121. Yang Z, Klionsky DJ. Mammalian autophagy: core molecular machinery and signaling regulation. *Curr Opin Cell Biol.* 2010;22:124-131.
122. Dikic I, Johansen T, Kirkin V. Selective Autophagy in Cancer Development and Therapy. *Cancer Res.* 2010;70:3431-3434.
123. Klionsky DJ, Cuervo AM, Seglen PO. Methods for Monitoring Autophagy from Yeast to Human. *Autophagy.* 2007;3(3):181-206.
124. Li W-w, Li J, Bao J-k. Microautophagy: lesser-known self-eating. *Cell Mol Life Sci.*
125. Arias E, Cuervo AM. Chaperone-mediated autophagy in protein quality control. *Curr Opin Cell Biol.* 2011;23:184-189.
126. Cuervo AM. Chaperone-mediated autophagy: selectivity pays off. *Tr Endocr Met.* 2009;21(3):142-150.
127. Orenstein SJ, Cuervo AM. Chaperone-mediated autophagy: Molecular mechanisms and physiological relevance. *Sem Cell Dev Biol.* 2010;21:719-726.
128. Bandyopadhyay U, Sridhar S, Kaushik S, Kiffin R, Cuervo AM. Identification of Regulators of Chaperone-Mediated Autophagy. *Mol Cell.* 2010;39:535-547.
129. Kon M, Cuervo AM. Chaperone-mediated autophagy in health and disease. *FEBS Lett.* 2010;584:1399-1404.
130. Agarraberes F. An intralysosomal hsp70 is required for a selective pathway of lysosomal protein degradation. *J Cell Biol.* 1997;137:825-834.
131. Kuiper GG, Carlson B, Grandien K, Enmak E, Haggblad J, Nilsson S et al. Comparison of the ligand binding specificity and transcript tissue distribution of estrogen receptors α and β . *Endocrinol.* 1997;138:863-870.
132. A Joubert A, Van Zyl H, Laurens J, Lottering M-L. C2- and C4-position 17 β -estradiol metabolites and their relation to breast cancer. *Biocell.* 2009;33(3):137-140.
133. Parl FF, Dawling S, Roodi N, Philip S, Croke PS. Estrogen Metabolism and Breast Cancer A Risk Model. *Ster Enz Can Ann NY Acad Sci.* 2009; 1155:68-75.
134. Yager JD. Endogenous estrogens as carcinogens through metabolic activation. *J Natl Cancer Inst Monogr.* 2000;27:67-73.
135. Clemons M, Goss P. Estrogen and the risk of breast cancer. *N Engl J Med.* 2001;344(4):276-285.

136. Van Zijl C, Lottering ML, Steffens F, Joubert A. In vitro effects of 2-methoxyestradiol on MCF-12A and MCF-7 cell growth, morphology and mitotic spindle formation. *Cell Biochem Funct.* 2008;26(5):632-642.
137. Mueck AO, Seeger H, Lippert TH. Estradiol metabolism and malignant disease. *Maturitas.* 2002;43:1-10.
138. Pribluda VS, Gubish ER, LaVallee TM, Treston A, Swartz GM, Green SJ. 2-Methoxyestradiol: An endogenous anti-angiogenic and anti-proliferative drug candidate. *Cancer Metastasis Rev.* 2000;19:173-179.
139. Fotsis T, Zhang Y, Pepper MS. The endogenous oestrogen metabolite 2-methoxyoestradiol inhibits angiogenesis and suppresses tumour growth. *Nature.* 1994;368:237-239.
140. Bhati R, Gokmen-Polar Y, Sledge GW, Fan C, Nakshatri H, Ketelsen D, Borchers CH, Dial MJ, Patterson C, Klauber-DeMore N. 2-Methoxyestradiol inhibits the anaphase-promoting complex and protein translation in human breast cancer cells. *Cancer Res.* 2007;67:702-708.
141. Dingli D, Timm M, Russell SJ, Witzing TE, Rajkumar SV. Promising preclinical activity of 2-methoxyestradiol in multiple myeloma. *Clin Cancer Res.* 2002;8:3948-3954.
142. Fukui M, Zhu BT. Mechanism of 2-methoxyestradiol-induced apoptosis and growth arrest in human breast cancer cells, *Mol Carcinog.* 2009;48(1):66-78.
143. Van Zijl C, Lottering ML, Steffens F, Joubert A. In vitro effects of 2-methoxyestradiol on MCF-12A and MCF-7 cell growth, morphology and mitotic spindle formation, *Cell Biochem Funct.* 2008;26(5):632-642.
144. Thaver V, Lottering M, Van Papendorp D, Joubert A. *In vitro* effects of 2-methoxyestradiol on cell numbers, morphology, cell cycle progression, and apoptosis induction in oesophageal carcinoma cells. *Cell Biochem Funct.* 2009;24(4):205-210.
145. LaVallee TM, Zhan XH, Herbstritt CJ, Kough EC, Green SJ, Pribluda VS. 2-Methoxyestradiol Inhibits Proliferation and Induces Apoptosis Independently of Estrogen Receptors α and β . *Cancer Res.* 2002;62:3691-3697.
146. Szekanecza Z, Besenyeia T, Paragh G, Kochc AE. New insights in synovial angiogenesis. *Joint Bone Spine.* 2010;77(1):13-19.
147. Dubey RK, Jackson EK. Potential vascular actions of 2-methoxyestradiol. *Trends Endocrinol Metab.* 2009;20(8):374-379.

148. Mabeesh NJ, Escuin D, LaVallee TM, Pribluda VS, Swartz GM, Johnson MS, Willard MT, Zhong H, Simons JW, Giannakakou P. 2ME2 inhibits tumor growth and angiogenesis by disrupting microtubules and dysregulating HIF. *Cancer Cell*. 2003;3(4):363-375.
149. Bãrdos J, Ashcroft M. Negative and positive regulation of HIF-1: A complex network. *Biochim Biophys Acta*. 2005;1755:107-120.
150. Wassberg E. Angiostatic treatment of neuroblastoma. *Ups J Med Sci*. 1999;104:1-24.
151. D'Amato R, Lin CM, Flynn E, Folkman J, Hamel E. 2-Methoxyestradiol, an endogenous mammalian metabolite, inhibits tubulin polymerisation by interacting at the colchicine site. *Proc Natl Acad Sci U S A*. 1994;91:3964-3968.
152. Bhati R, Gökmen-Polar Y, Sledge GW, Fan C, Nakshatri H, Ketelsen D, et al. 2-Methoxyestradiol inhibits the anaphase-promoting complex and protein translation in human breast cancer cells. *Cancer Res*. 2007;67:702-708.
153. Kamath K, Okouneva T, Larson G, Panda D, Wilson L, Jordan MA. 2-Methoxyestradiol suppresses microtubule dynamics and arrests mitosis without depolymerising microtubules. *Mol Cancer Ther*. 2006;5:2225-2233.
154. Stander BA, Marais S, Vorster CJJ, Joubert AM. In vitro effects of 2-methoxyestradiol on morphology, cell cycle progression, cell death and gene expression changes in the tumorigenic MCF-7 breast epithelial cell line. *J Steroid Biochem Mol Biol*. 2010;119:149-160.
155. Seegers JC, Lottering ML, Grobler CJS. The mammalian metabolite 2-methoxyestradiol affects p53 levels and apoptosis induction in transformed cells but not normal cells. *J Steroid Biochem Mol Biol*. 1997;62:253-267.
156. Mukhopadhyay T, Roth JA. Induction of apoptosis in human lung cancer cells after wild-type p53 activation by methoxyestradiol. *Oncogene*. 1997;14:379-384.
157. Zacharia LC, Jackson EK, Gillespie DG, Dubey RK. Increased 2-methoxyestradiol production in human coronary versus aortic vascular cells. *Hypertension*. 2001;37:658-62.
158. Schumacher G, Kataoka M, Roth JA, Mukhopadhyay T. Potent antitumor activity of 2-methoxyestradiol in human pancreatic cancer cell lines. *Clin Cancer Res*. 1999;5:493-499.

159. La Valee TM, Zhan XH, Johnson MS, Herbstritt CJ, Swartz G, Williams MS, et al. 2-Methoxyestradiol upregulates death receptor 5 and induces apoptosis through activation of the extrinsic pathway. *Cancer Res.* 2003;63:468-475.
160. Dahut WL, Lakani NJ, Gulley JL, Arlen PM, Kohn EC, Kotz H, et al. Phase I clinical trial of oral 2-methoxyestradiol, an antiangiogenic agent, in patients with solid tumors. *Cancer Biol Ther.* 2006;5:271-280.
161. Sweeney C, Liu G, Yiannoutsos C, Kolesar J, Horvath D, Staab MJ, et al. A Phase II Multicenter Randomized Double-Blind Safety Trial Assessing the Pharmacokinetics Pharmacodynamics and Efficacy of Oral 2-Methoxyestradiol Capsules in Hormone-Refractory Prostate Cancer. *Clin Cancer Res.* 2005;11:6625-6633.
162. James J, Murry DJ, Treston AM, Storniolo AM, Sledge GW, Sidor C, et al. Phase I Safety, Pharmacokinetic and Pharmacodynamic Studies of 2-Methoxyestradiol Alone or in Combination with Docetaxel in Patients with Locally Recurrent or Metastatic Breast Cancer. *Invest New Drugs.* 2006;25:41-48.
163. Tevaarwerk AJ, Holen KD, Alberti DB, Sidor C, Arnott J, Quon C, et al. Phase I trial of 2-methoxyestradiol NanoCrystal dispersion in advanced solid malignancies, *Clin Cancer Res.* 2009;15(4):1460-1465.
164. Ireson CR, Chander SK, Purohit A, Perera S, Newman SP, Parish D, et al. Pharmacokinetics and efficacy of 2-methoxyestradiol and 2-methoxyestradiol-bis-sulphamate in vivo in rodents. *Br J Cancer.* 2004;90:932-937.
165. Klauber N, Parangi S, Flynn E, Hamel E, D'Amato RJ. Inhibition of Angiogenesis and Breast Cancer in Mice by the Microtubule Inhibitors 2-Methoxyestradiol and Taxol. *Cancer Res.* 1997;57:81-86.
166. Newman SP, Ireson CR, Tutill HJ, Day JM, Parsons MFC, Leese MP, et al. The Role of 17 β -Hydroxysteroid Dehydrogenases in Modulating the Activity of 2-Methoxyestradiol in Breast Cancer Cells. *Cancer Res.* 2006;66(1):324-330.
167. Sano T, Hirasawa G, Takeyama J, Darnel AD, Suzuki T, Moriya T, et al. 17 β -Hydroxysteroid dehydrogenase type 2 expression and enzyme activity in the human gastrointestinal tract. *Clinical Sci.* 2001;101(5):485-491.
168. Purohit A, Woo LWL, Chander SK, Newman SP, Ireson C, Ho Y, Grasso A, et al. Non-steroidal and steroidal sulfamates: new drugs for cancer therapy. *Mol Cell Endocrinol.* 2001;171:129-135.

169. Harrison MR, Hahn NM, Pili R, Oh WK, Hammers H, Sweeney C, et al. A phase II study of 2-methoxyestradiol (2ME2) NanoCrystal (R) dispersion(NCD)in patients with taxane-refractory, metastatic castrate-resistant prostate cancer (CRPC). *Invest New Drugs*. 2010;29(6):1465-1474.
170. Purohit A, Woo LWL, Chander SK, Newman SP, Ireson C, Ho Y, et al. Steroid sulphatase inhibitors for breast cancer therapy. *J Steroid Biochem Mol Biol*. 2003;86:423-432.
171. Tagg SLC, Foster PA, Leese MP, Potter BVL, Reed MJ, Purohit A, et al. 2-Methoxyoestradiol-3,17-*O,O*-bis-sulphamate and 2-deoxy-D-glucose in combination: a potential treatment for breast and prostate cancer. *British J Cancer*. 2008;99:1842-1848.
172. Vorster CJ, Joubert AM. In vitro effects of 2-methoxyestradiol-bis-sulphamate on cell numbers, morphology and cell cycle dynamics in the MCF-7 breast adenocarcinoma cell line. *Biocell*. 2010;34(2):71-79.
173. Suzuki RN, Newman SP, Purohit A, Leese MP, Potter BVL, Reed MJ. Growth inhibition of multi-drug-resistant breast cancer cells by 2-methoxyoestradiol-bis-sulphamate and 2-ethyloestradiol-bis-sulphamate. *J Steroid Biochem Mol Biol*. 2003;84:269-278.
174. Raobaikady B, Purohit A, Chander SK, Woo LWL, Leese MP, Potter BVL, et al. Inhibition of MCF-7 breast cancer cell proliferation and in vivo steroid sulphatase activity by 2-methoxyoestradiol-bis-sulphamate. *J Steroid Biochem Mol Biol*. 2003;84:351-358.
175. Foster PA, Ho YT, Newman SP, Kasprzyk PG, Leese MP, Potter BVL, et al. 2-MeOE2bisMATE and 2-EtE2bisMATE induce cell cycle arrest and apoptosis in breast cancer xenografts as shown by a novel ex vivo technique. *Breast Cancer Res Treat*. 2008;111:251-260.
176. Day JM, Newman SP, Comminos A, Solomon C, Purohit A, Leese MP, et al. The effects of 2-substituted oestrogen sulphamates on the growth of prostate and ovarian cancer cells. *J Steroid Biochem Mol Biol*. 2003;84:317-325.
177. Newman SP, Foster PA, Stengel C, Day JM, Ho YT, Leese MP, et al. STX140 is efficacious in vitro and in vivo in taxane-resistant breast carcinoma cells. *Clin Cancer Res*. 2008;14:597-606.

178. Visagie MH, Joubert AM. 2-Methoxyestradiol-bis-sulfamate induces apoptosis and autophagy in a tumorigenic breast epithelial cell line. *Mol Cell Biochem.* 2011;357(1-2):343-352.
179. Visagie MH, Joubert AM. The in vitro effects of 2-methoxyestradiol-bis-sulphamate on cell numbers, membrane integrity and cell morphology, and the possible induction of apoptosis and autophagy in a non-tumorigenic breast epithelial cell line. *Cell Mol Bio Lett.* 2010;15(4):564-581.
180. Chander S, Foster P, Leese M, Woo LWL, Leese MP, Potter BVL et al., In vivo inhibition of angiogenesis by sulphamoylated derivatives of 2-methoxyoestradiol. *Br J Cancer.* 2007;96:1368-1376.
181. Raobaikady B, Reed MJ, Leese MP. Inhibition of MDA-MB-231 cell cycle progression and cell proliferation by C-2-substituted oestradiol mono- and bis-3-O-sulphamates. *Int J Cancer.* 2005;117:150-159.
182. Jourdan F, Leese MP, Dohle W, Hamel E, Ferrandis E, Newman SP, et al. Synthesis, Antitubulin, and Antiproliferative SAR of Analogues of 2-Methoxyestradiol-3,17-O,O-bis-sulfamate. *J Med Chem.* 2010;53:2942-2951.
183. Stander A, Joubert F, Joubert A. Docking, Synthesis, and in vitro Evaluation of Antimitotic Estrone Analogs. *Chem Biol Drug Des.* 2011;77:173-181.
184. Supuran CT, Scozzafava A. Carbonic anhydrases as targets for medicinal chemistry. *Bioorg Med Chem.* 2007;15:4336-4350.
185. Strober W. Trypan Blue Exclusion Test of Cell Viability. *Current Prot Immunol.* 2001;A3B1-A3B2.
186. Utsumi T, Leese MP, Chander SK, Gaukroger K, Purohit A, Newman SP, et al. The effects of 2-methoxyoestrogen sulphamates on the in vitro and in vivo proliferation of breast cancer cells. *J Steroid Biochem Mol Biol.* 2005;94:219-227.
187. Gillies RJ, Didier N, Denton M. Determination of cell number in monolayer cultures. *Anal Biochem.* 1989;159:109-113.
188. Kueng W, Silber E, Eppenberger U. Quantification of cells cultured on 96 well plates. *Anal Biochem.* 1989;182:16-19.
189. Fotakis G. and Timbrell, JA. In vitro cytotoxicity assays: Comparison of LDH, neutral red, MTT and protein assay in hepatoma cell lines following exposure to cadmium chloride. *Toxicol Lett.* 2006;160:171-177.

190. Wehner E. PlasDIC, an Innovative Relief Contrast for Routine Observation in Cell Biology. *GIT Imag Microsc.* 2003;4:23-24.
191. Thompson SW. Selected Histochemical and histopathological methods. Thomas Publ. 1966:377-378.
192. Krysko DV, Vanden Berghe T, D'Herde K, Vandenabeele P. Apoptosis and necrosis: Detection, discrimination and phagocytosis. *Methods.* 2008;44:205-221.
193. Hait W, Rubin E, Alli E, Goodin S. Tubulin targeting agents. *Updat Cancer Ther.* 2007;2:1-18.
194. Rowland SC, Jacobson JD, Patton WC, King A, Chan PJ. Dual fluorescence analysis of DNA apoptosis in sperm. *Am J Obstet Gynecol.* 2003;188(5):1156-1157.
195. Darzynkiewicz Z, Halicka HD, Zhao H. Analysis of Cellular DNA Content by Flow and Laser Scanning Cytometry. *Adv Exp Med Biol.* 2010;676:137-147.
196. Pozarowski P, Darzynkiewicz Z. Analysis of Cell Cycle by Flow Cytometry. *Meth Mol Biol.* 2004;281:301-311.
197. Kar S, Wang M, Carr BL. 2-Methoxyestradiol inhibits hepatocellular carcinoma cell growth by inhibiting Cdc25 and inducing cell cycle arrest and apoptosis. *Cancer Chemother Pharmacol.* 2008;62:831-840.
198. Koopman, G, Reutelingsperger CP, Kuijten GAM, Keehnen RMJ, Pals ST, van Oers MHJ. Annexin V for flow cytometric detection of phosphatidylserine expression on B cells undergoing apoptosis. *Blood.* 1994;84:1415-1421.
199. Vermes I, Haanen C, Steffens-Nakken H, Reutelingsperger C. A novel assay for apoptosis - flow cytometric detection of phosphatidylserine expression on early apoptotic cells using fluorescein labelled Annexin V. *J Immunol Methods.* 1995;184:39-40.
200. Ly JD, Grubb DR, Lawen A. The mitochondrial membrane potential ($\Delta\psi_m$) in apoptosis; an update. *Apoptosis.* 2003;8:115-128.
201. Fan T-J, Han L-H, Cong R-S, Liang J. Caspase Family Proteases and Apoptosis. *Acta Biochim Biophys Sin.* 2005;37(11):719-727.
202. Mizushima N, Yoshimori T, Levine B. Methods in Mammalian Autophagy Research. *Cell.* 2010;140(3):313-326.
203. Warenius HM, Kilburn JD, Essex JW, Maurer RI, Blaydes P, Agarwala U. Selective anticancer activity of a hexapeptide with sequence homology to a non-kinase domain of cyclin dependent kinase. *Mol Cancer.* 2011;10:72.

204. Boyd MR, Paul KD. Some Practical Considerations and Applications of the National Cancer Institute In Vitro Anticancer Drug Discovery Screen. *Drug Dev Res.* 1995;34:91-109.
205. Day JM, Foster PA, Tutill HJ, Newman SP, Ho YT, Leese MP, et al. BCRP expression does not result in resistance to STX140 in vivo, despite the increased expression of BCRP in A2780 cells in vitro after long-term STX140 exposure. *Br J Cancer.* 2009;100:476-486.
206. Wood L, Leese MP, Mouzakiti A, Purohit A, Potter BVL, Reed MJ, et al. 2-MeOE2bisMATE induces caspase-dependent apoptosis in CAL51 breast cancer cells and overcomes resistance to TRAIL via cooperative activation of caspases. *Apoptosis.* 2004;9:323-332.
207. Chua YS, Chua YL, Hagen T. Structure Activity Analysis of 2-Methoxyestradiol Analogues Reveals Targeting of Microtubules as the Major Mechanism of Antiproliferative and Proapoptotic Activity. *Mol Cancer Ther.* 2010;9:224-235.
208. Shen J-B, Pappano AJ. An Estrogen Metabolite, 2-Methoxyestradiol, Disrupts Cardiac Microtubules and Unmasks Muscarinic Inhibition of Calcium Current. *JPET.* 2008;325:507-512.
209. Ho YT, Newman SP, Purohit A, Leese MP, Potter BVL, Reed MJ. The effects of 2-methoxy oestrogens and their sulphamoylated derivatives in conjunction with TNF- α on endothelial and fibroblast cell growth, morphology and apoptosis. *J Steroid Biochem Mol Biol.* 2003;86:189-196.
210. Dobos J, Timar J, Bocsi J, Burian Z, Nagy K, Barna G, et al. In vitro and in vivo antitumor effect of 2-methoxyestradiol on human melanoma. *Int J Cancer.* 2004;112:771-776.
211. Ghosh R, Ganapathy M, Alworth WL, Chan DC, Kumar AP. Combination of 2-methoxyestradiol (2ME2) and eugenol for apoptosis induction synergistically in androgen independent prostate cancer cells. *J Steroid Biochem Mol Biol.* 2009;113:25-35.
212. Chang YF, Hsu YC, Hung HF, Lee HJ, Lui WY, Chi, CW et al. Quercetin induces oxidative stress and potentiates the apoptotic action of 2-methoxyestradiol in human hepatoma cells. *Nutr Cancer.* 2009;61:735-745.

213. Zhang X, Huang H, Xu Z, Zhan R. 2-Methoxyestradiol blocks cell-cycle progression at the G₂/M phase and induces apoptosis in human acute T lymphoblastic leukemia CEM cells. *Acta Biochim Biophys Sin.* 2010;42:615-622.
214. Lorin S, Borges A, Dos Santos LR, Souque`re S, Pierron G, Ryan KM. c-Jun NH₂-Terminal Kinase Activation Is Essential for DRAM-Dependent Induction of Autophagy and Apoptosis in 2-Methoxyestradiol-Treated Ewing Sarcoma Cells. *Cancer Res.* 2009;69(17):6924-6931.
215. Azad MB, Chen Y, Gibson SB. Regulation of autophagy by reactive oxygen species (ROS): Implications for Cancer Progression and Treatment. *Ant Red Signaling.* 2009;11(4):777-790.
216. Parks M, Tillhon M, Donà F, Prosperi E, Scovassi AI. 2-Methoxyestradiol: New perspectives in colon carcinoma treatment. *Mol Cell Endocrinol.* 2011;331:119-128.
217. Basciani S, Vona R, Matarrese P, Ascione B, Mariani S, Cauda R et al. Imatinib interferes with survival of multi drug resistant Kaposi's sarcoma cells. *FEBS Lett.* 2007;581:5897-5903.
218. Yang W, Monroe J, Zhang Y, George D, Bremer E, Li H. Proteasome inhibition induces both pro- and anti-cell death pathways in prostate cancer cells. *Cancer Lett.* 2006;243:217-227.
219. Yokoyama T, Miyazawa K, Naito M, Toyotake J, Tauchi T, Itoh M et al. Vitamin K₂ induces autophagy and apoptosis simultaneously in leukemia cells. *Autophagy.* 2008;4:629-640.
220. Eisenberg-Lerner A, Bialik S, Simon H-U, Kimchi A. Life and death partners: apoptosis, autophagy and the cross-talk between them. *Cell Death Diff.* 2009;16:966-975.
221. Maiuri MC, Ciriollo A, Kroemer G. Crosstalk between apoptosis and autophagy within the Beclin 1 interactome. *EMBO J.* 2010;29:515-516.
222. Zhou F, Yang Y, Xing D. Bcl-2 and Bcl-xL play important roles in the crosstalk between autophagy and apoptosis. *FEBS J.* 2011;278:403-413.
223. Fimia GM, Piacentini M. Regulation of autophagy in mammals and its interplay with apoptosis. *Cell Mol Life Sci.* 2010;67:1581-1588.
224. Liu B, Wu JM, Li J, Li WW, Liu JJ, Bao JK. Polygonatum cyrtonema lectin induces cell apoptosis and autophagy via blocking Ras-Raf and PI3K-Akt signaling pathways. *Biochem.* 2010;92:1934-1938.

225. Qian W, Liu J, Jin J, Ni W, Xu W. Arsenic trioxide induces not only apoptosis but also autophagic cell death in leukemia cell lines via up-regulation of Beclin-1. *Leuk Res.* 2007;31:329-339.